CR-183974

CONTRACT NO. NAS8-37777

VOLUME III
THIOKOL CORPORATION
SPACE OPERATIONS

HYBRID PROPULSION TECHNOLOGY PROGRAM PHASE I

FINAL REPORT

GENERAL DYNAMICS
SPACE SYSTEMS DIVISION

CONTRACT NO. NAS8-37777

VOLUME III
THIOKOL CORPORATION
SPACE OPERATIONS

HYBRID PROPULSION TECHNOLOGY
PROGRAM PHASE I

FINAL REPORT

1 DECEMBER 1989

GENERAL DYNAMICS
SPACE SYSTEMS DIVISION

PREFACE

This volume is part of a four-volume set that describes the work performed from 6 March to 30 November 1989 under contract NAS8- 37777 entitled, "The Hybrid Propulsion Technology Program Phase I." The study was directed by Mr. Ben Shackelford of the NASA/Marshall Space Flight Center. Listed below are major sections from the four volumes that comprise this Final Report.

Volume I—Executive Summary

Volume II—General Dynamics Final Report

- Conept Definition
- Technology Acquisition Plans
- Large Subscale Motor System Technology Demonstration Plan

Volume III—Thiokol Corporation Final Report

- Trade Studies and Analyses
- Technology Acquisition
- Large Subscale Motor Demonstration

Volume IV—Rockwell International Corporation Final Report

- Concept Evaluation
- Technology Identification
- Technology Acquisition Plan

CONTENTS

FIGURES

FIGURES (cont)

FIGURES (cont)

TABLES

ABBREVIATIONS, ACRONYMS, AND SYMBOLS

<	less than
>	greater than
ΔV	delta velocity
ADP	Automated Design Program
Al	aluminum
AN	ammonium nitrate
AP	ammonium perchlorate
ASRM	advanced solid rocket motor
AT	aminotetrazole
ATJ	graphite material
ave	average
avg	average
B&P	bid and proposal
BP	boiling point
C	centigrade
C-C	carbon-carbon
C*	characteristic velocity
CAT	catazine
cc	cubic centimeter
CCP	carbon-cloth phenolic
CFD	computational fluid dynamics
Cl	chloride
CMA	charring material ablation
CP	center perforated
DCDA	dicyandiamide
deg	degree
Delrin	polyformaldehyde
dia	diameter
DSC	differential scanning calorimeter
EPDM	ethylene propylene diene monomer
F	fahrenheit
F	fluorine
f/s	foot/second
fps	feet per second
ft	foot
FY	fiscal year
g	gram
GAP	glycidyl azide polymer
GD	General Dynamics
GOX	gaseous oxygen
GRE	graphite epoxy
H	hydrogen
HAN	hydroxylamine nitrate
HCl	hydrogen chloride
HDPE	high density polyethylene
HF	hydrogen fluoride
HMX	cyclotetramethylene tetranitramine
HN	hydrazine mononitrate
HPT	Hybrid Propulsion Technology
HRB	hybrid rocket booster
HT	hydroxyl-terminated polybutadiene
HTPB	hydroxyl-terminated polybutadiene
in.	inch
ips	inch per second
IRFNA	inhibited red fuming nitric acid
I_{sp}	specific impulse
IUS	inertial upper stage
K	thousand
K	kelvin
kcal	kilocalorie

L/D	length to diameter
L/Dh	length to hydraulic diameter
LAH	$LiAlH_4$
lb	pound
lbf	pound-force
lbm	pound-mass
LCC	life cycle cost
Li	lithium
LITVC	liquid injection thrust vector control
LOX	liquid oxygen
M	million
max	maximum
MEOP	maximum expected operating pressure
Mg	magnesium
MNASA	modified NASA (motor)
N	nitrogen
NASA	National Aeronautics and Space Administration
NDE	nondestructive evaluation
No.	number
NOx	nitrogen oxide
O	oxygen
O/F	oxidizer-to-fuel (ratio)
OD	outside diameter
OX	oxygen
PAN	polyacrylonitrile
PBAN	polybutadiene acrylonitrile
PE	polyethylene
PEG	polyethylene glycol
PG	pyrolytic graphite
PK	Peacekeeper
PMMA	polymethyl methacrylate
polyTHF	polytetrahydrylfuran
PPG	polypropylene glycol
ppm	parts per million
psi	pound per square inch
psia	pound per square inch, absolute
psig	pound per square inch gage
PTHF	polymethyl methacrylate
R_b	burn rate
RDX	trimethylene trinitranmine
RSRM	redesigned solid rocket motor
s	second
S/A	safe/arm
SCP	silica-cloth phenolic
sec	second
SICBM	small intercontinental ballistic missile
sq in.	square inch
SRB	solid rocket booster
SRM	solid rocket motor
SSSL	supersonic splitline
TGA	thermogravimetric analysis
TPE	thermoplastic elastomer
TPH	Thiokol propellant H series
TVC	thrust vector control
UFAP	ultrafine ammonium perchlorate
vac	vacuum
W	tungsten
Zn	zinc

1.0 INTRODUCTION

Recently, renewed emphasis has been placed on improvements in safety, reliability, cost, and environmental impacts in the nation's launch vehicle systems. This emphasis has led NASA to initiate a new look at hybrid propulsion systems. The Hybrid Propulsion Technology (HPT) program, Contract NAS8-37777, was conducted by General Dynamics, Thiokol Corporation, and Rocketdyne. The team provided for technical expertise in solid propulsion, liquid propulsion, and propulsion systems integration. Thiokol's responsibility as part of this program was to address hybrid technology that related to elements of solid rocket motor (SRM) propulsion.

The hybrid rocket motor has inherent characteristics that specifically address safety, reliability, cost, and environmental concerns. Simplicity of the inert fuel grain and oxidizer feed system offers the potential for greatly enhanced flight safety and reliability. Due to the nature of combustion in a hybrid motor, performance is insensitive to fuel grain defects such as cracks, voids, and unbonds that could be catastrophic in a conventional SRM. In the event of a system malfunction, shutdown of this oxidizer feed system extinguishes the motor. Additionally, explosive mixing of fuel and oxidizer components is not possible as with a conventional liquid rocket motor.

SRMs have historically proven to provide a significant cost advantage over liquid engines. By similarity, the hybrid motor retains this cost advantage with the added benefit of low-cost liquid oxidizers (oxygen cost is $.08 per pound).

During combustion of an SRM, large quantities of hydrogen chloride (HCl) are produced. Several approaches to eliminating HCl in solid rocket exhaust are being taken by Thiokol. One approach replaces ammonium perchlorate (AP) with ammonium nitrate (AN) and another approach uses sodium nitrate to form sodium chloride rather than HCl in the exhaust. All of these techniques degrade propellant energy. As currently formulated, the SRM propellant for the space shuttle (TP-H1148) delivers a theoretical specific impulse (I_{sp}) of 278 sec at vacuum conditions. The best sodium-scavenged clean propellant delivers an I_{sp} of 258 sec. In contrast, a hybrid motor using a liquid oxygen (LOX) oxidizer and hydroxyl-terminated polybutadiene (HTPB) as a fuel delivers a theoretical I_{sp} of 316 sec with zero HCl in the exhaust plume. A hybrid can meet demanding performance requirements without the production of environmentally damaging exhaust products.

2.0 SUMMARY

Three candidate hybrid propulsion concepts were identified, optimized, evaluated, and refined through an iterative process that continually forced improvement to the systems with respect to safety, reliability, cost, and performance criteria. A full-scale booster meeting advanced SRM (ASRM) thrust-time constraints and a booster application for one-quarter ASRM thrust were evaluated. Trade studies and analyses were performed for each of the motor elements related to SRM technology. Based on trade study results, the optimum hybrid propulsion concept for both full- and one-quarter-sized systems was defined. Further refinements and definition of the selected concepts identified shortcomings in state-of-the-art technology. Plans to resolve these technology shortcomings, Phase II, and demonstrate the selected concept in a large subscale motor, Phase III, were developed. All efforts were integrated with systems studies and liquids technology through General Dynamics.

The three candidate hybrid concepts evaluated are illustrated in Figure 1. The classical hybrid has a solid fuel grain, with oxidizer injection at the head end. The afterburner hybrid is like the classical hybrid, but oxidizer is also injected in an afterburning combustion chamber. The gas generator hybrid is similar to a solid rocket; self-sustaining combustion results from having an oxidized fuel grain with no oxidizer injected down the fuel grain bore. It has the solid rocket regression rate correlation ($r = aP^n$) and burns fuel-rich with the balance of oxidizer added in an afterburning combustion chamber.
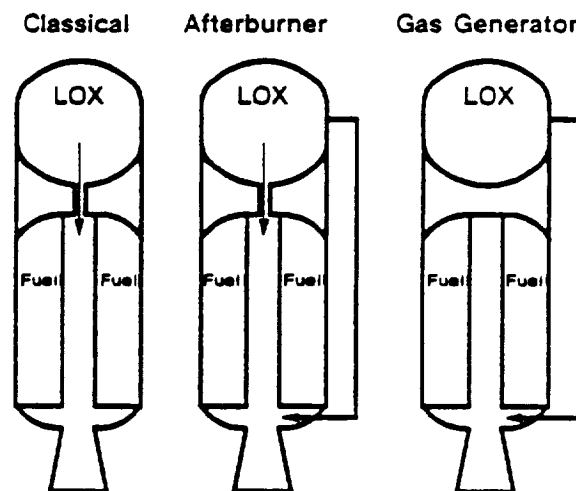
Note: Classical and afterburner hybrids use inert fuel. Gas generator hybrid uses live fuel.

CSA024094a

Figure 1. Candidate hybrid concepts.

1

Results of the trade studies and analyses are illustrated in Figures 2 and 3 for the full- and quarter-scale boosters, respectively. Both pump- and pressure-fed systems were evaluated for a total of six designs for each booster size. Performance evaluation was based on ideal velocity calculated for an assumed trajectory. Based on performance alone, a pump-fed afterburner configuration would have been selected for

Concept / Parameter	Classical	Afterburner	Gas Generator
● Pump Fed	Flexseal	Flexseal	Flexseal
● TVC	Hypergolic	Hypergolic	Hypergolic
● Ignition	4	4	1
● # Ports	608	693	741
● P$_{ave}$ (psi)	9,132	9,180	8,794
● ΔV (ft/sec)	HTPB/GAP/Zn	HTPB/GAP/Zn	HTPB/AN/Al
● Fuel	LOX	LOX	LOX
● Oxidizer			
● Pressure Fed	Flexseal	Flexseal	Flexseal
● TVC	Hypergolic	Hypergolic	Hypergolic
● Ignition	4	4	1
● # Ports	480	469	741
● Pave (psi)	8,703	8,718	8,581
● ΔV (ft/sec)	HTPB/GAP/Zn	HTPB/GAP/Zn	HTPB/AN/Al
● Fuel	LOX	LOX	LOX
● Oxidizer			

Figure 2. Summary of full-scale booster trade studies/analyses.

Concept / Parameter	Classical	Afterburner	Gas Generator
● Pump Fed	Flexseal	Flexseal	Flexseal
● TVC	Hypergolic	Hypergolic	Hypergolic
● Ignition	4	4	1
● # Ports	809	757	777
● P$_{ave}$ (psi)	9,136	9,120	8,887
● ΔV (ft/sec)	HTPB/GAP/Zn	HTPB/GAP/Zn	HTPB/AN/Al
● Fuel	LOX	LOX	LOX
● Oxidizer			
● Pressure Fed	Flexseal	Flexseal	Flexseal
● TVC	Hypergolic	Hypergolic	Hypergolic
● Ignition	1	1	1
● # Ports	480	469	741
● Pave (psi)	8,703	8,718	8,581
● ΔV (ft/sec)	HTPB/GAP/Zn	HTPB/GAP/Zn	HTPB/AN/Al
● Fuel	LOX	LOX	LOX
● Oxidizer			

CSA024095a

Figure 3. Summary of quarter-scale booster trade studies/analyses.

both full- and quarter-scale boosters. This information was conveyed to General Dynamics for integration into the overall concept evaluation. In considering other factors for safety, reliability, and cost, performance alone is outweighed. As indicated by the shaded regions in Figures 2 and 3, the simpler, less costly, classical configuration was selected for both the full- and quarter-scale boosters. This result evolved from the top-level trade study performed by General Dynamics. Completion of the trade studies and analyses provided the baseline for which shortcomings in state-of-the-art technology were identified, and technology acquisition planning was then developed to resolve these deficiencies. Areas needing improvement are summarized as follows:

- Nozzle materials
- Insulation materials
- Propellant (fuel and oxidizer)
- Ignition
- Combustion and flowfield modeling

A fully integrated two-year plan, Technology Acquisition, was prepared for Phase II. Technology Acquisition will consist of testing motors representative of the selected concept and large enough to minimize problems of scale. The Phase II program will culminate with the static test of a 160,000-lb thrust motor. The motor will provide for verification of technology developments in each of the areas of concern. The size and evolution of motors from conception through full-scale development are summarized in Figure 4.
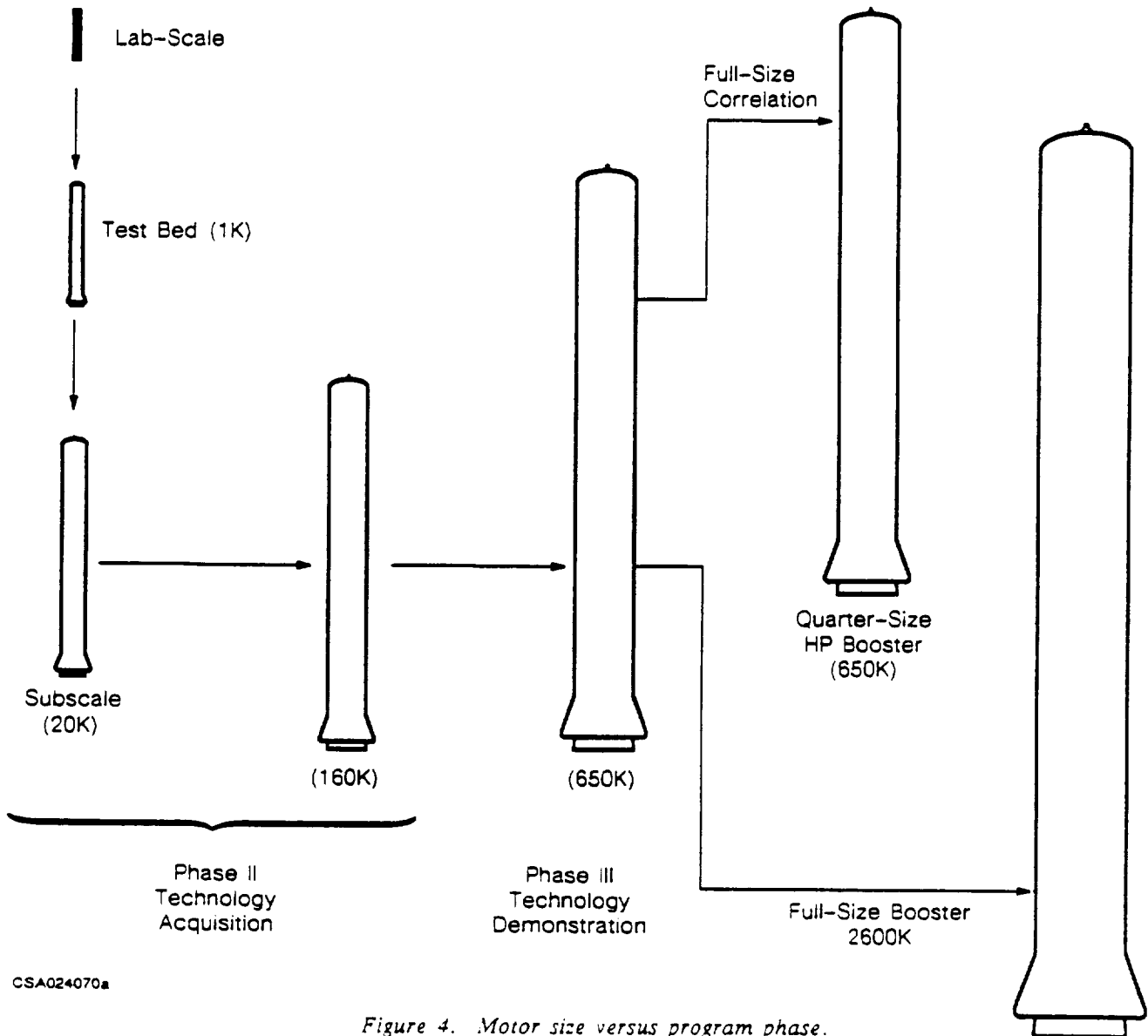
CSA024070a

Figure 4. Motor size versus program phase.

Our approach to Phase III, Technology Demonstration, is to integrate technologies developed in Phase II with engineering development including design and testing into one hybrid propulsion motor. This motor will demonstrate the hybrid propulsion technologies, model performance predictions, behavior, and other characteristics at thrust levels representative of large-scale booster application.

General Dynamics accumulated information from a variety of sources to develop the overall plan for Phase III. Thiokol developed SRM cost and schedule input for the overall plan. Estimated costs for development and fabrication of SRM components to support three 90-in. hybrid motor tests is $8.8 million.

3.0 TRADE STUDIES AND ANALYSES

Analyses and trade studies were conducted to refine preliminary hybrid propulsion concepts into their optimum configuration. Analyses and trade studies were conducted independently by trade study leaders. Key information evolving from initial trade study/analyses results, in many cases, provided input to other trade studies. Interaction between trade studies and update of information was maintained through completion of all trade studies/analyses. Thiokol was responsible for propellant, ignition, combustion stability, thrust vector control (TVC), and motor performance trade studies/analyses.

Propellant selection and motor performance were considered essential to establishing feasibility of hybrid propulsion and identification of the optimum hybrid propulsion concept. Therefore, these two trade studies/analyses were treated more rigorously than trade studies/analyses of lesser importance. All trade studies and analyses are documented in the sections that follow.

3.1 PROPELLANT SELECTION

Due to the unique nature of the hybrid rocket propulsion concept, a vast array of fuel and oxidizer combinations is conceivable for application, and an effort to narrow this field for large booster feasibility studies was necessary. The propellant selection trade study concentrated on two distinctly different booster designs: the classical/afterburner hybrid, with forward injection only or with supplemental aft oxidizer injection; and the gas generator approach in which conventional solid propellant is used to provide a fuel-rich exhaust which further undergoes combustion in an aft chamber via oxidizer injection.

Requirements/goals used to narrow the field of options for both classical/ afterburner and gas generator hybrid approaches are summarized as follows:

1. Performance—Theoretical density and vacuum I_{sp} was determined at 1000 psi and 10:1 supersonic expansion, with the performance to meet or exceed current shuttle.

2. Exhaust Environmental Hazards—Clean exhaust products were given a premium. Common toxic species such as HCl, HF, Cl_2, F_2, NOx, and so forth were minimized.

3. Hazards—Chemical (highly reactive oxidizers) and explosive (certain oxidizers and gas generator propellants) hazards were identified. Both potential production and pad or range safety concerns were considered.

4. Reliability—The potential for operation failure modes as well as ingredient stability, producibility, and reactivity in compromising reliability or reproducibility were considered.

5. Cost—Relative costs or anticipated costs of ingredients were considered in conjunction with grain and system production costs as directly related to the propellant system.

6. Ballistic Performance—Burning rate or regression rate characteristics, where known, were also figured in estimating relative merits of candidate propellant approaches.

7. Extinguishment—Fuel grains that extinguish upon oxidizer cutoff were determined.

The above considerations represent the major aspects used in determining which propellant or propulsion concepts to pursue further in conducting systems performance trades and designs. Each aspect has varying nuances and complex interactions but conducting the trade studies (Figures 5 and 6) proved to be adequate for narrowing the available options.

3.1.1 OBJECTIVE. In conducting the Propellant Trade Study, the primary objective was to conduct theoretical trade studies of various propellant combinations and determine the optimum approach for each of the hybrid propulsion concepts. The specific objective of this study was to conduct a series of trade studies utilizing both experimental and theoretical data to arrive at a recommended approach for further development of hybrid booster technology.

3.1.2 CONCLUSIONS. The classical hybrid concept of an inert fuel grain operated with supplemental head-end oxidizer injection meets the goals for large booster application. Historic ballistic shortcomings of this approach may be potentially overcome by the use of glycidyl azide polymer (GAP) or other additives providing equivalent response, and high performance (density I_{sp}) may be achieved by inclusion of dense metals (aluminum, zinc, tungsten). Performance of propellant selected for the classical and afterburner
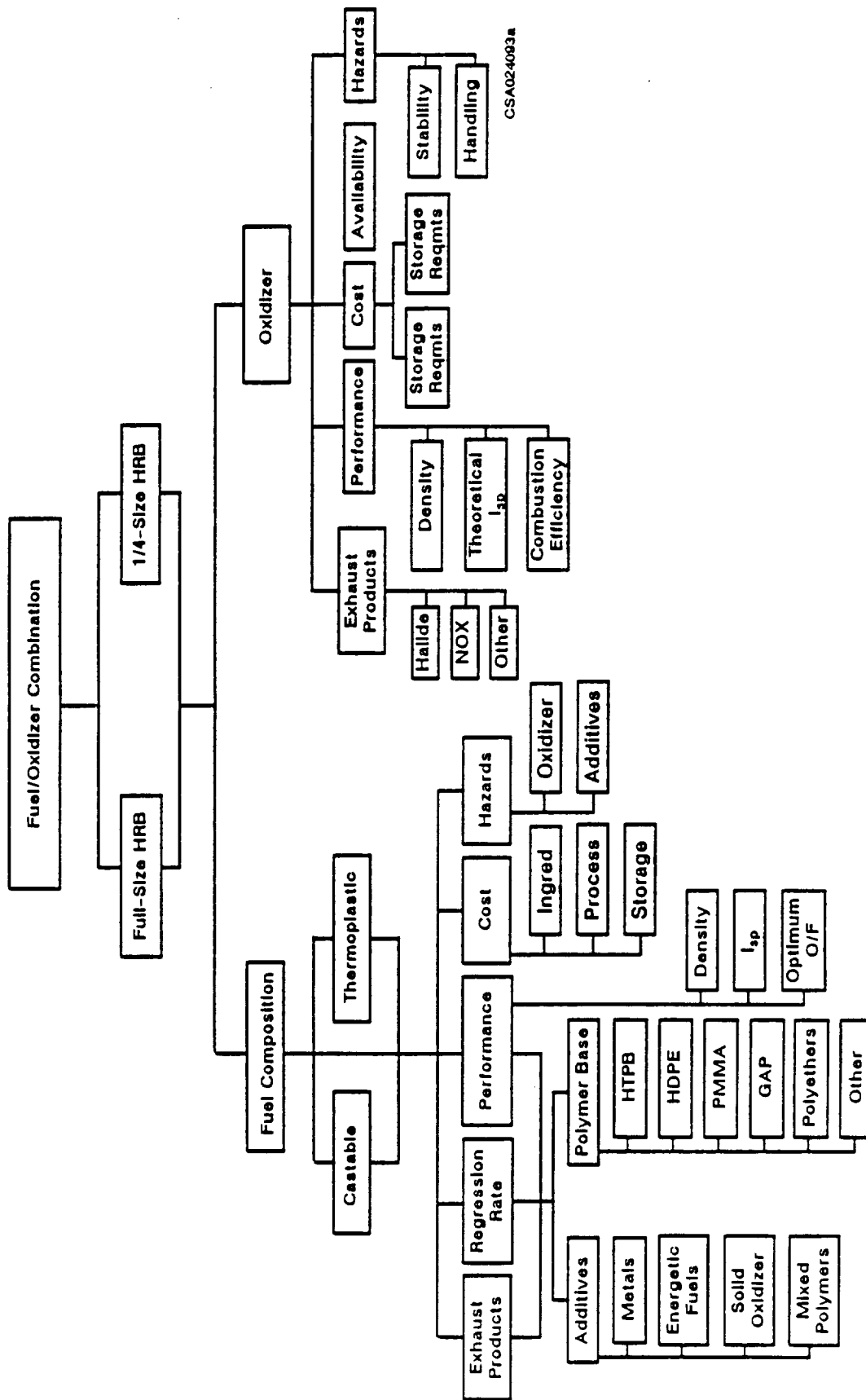
Figure 5. Propellant selection trade tree classical and afterburner concepts.

CSA024093a
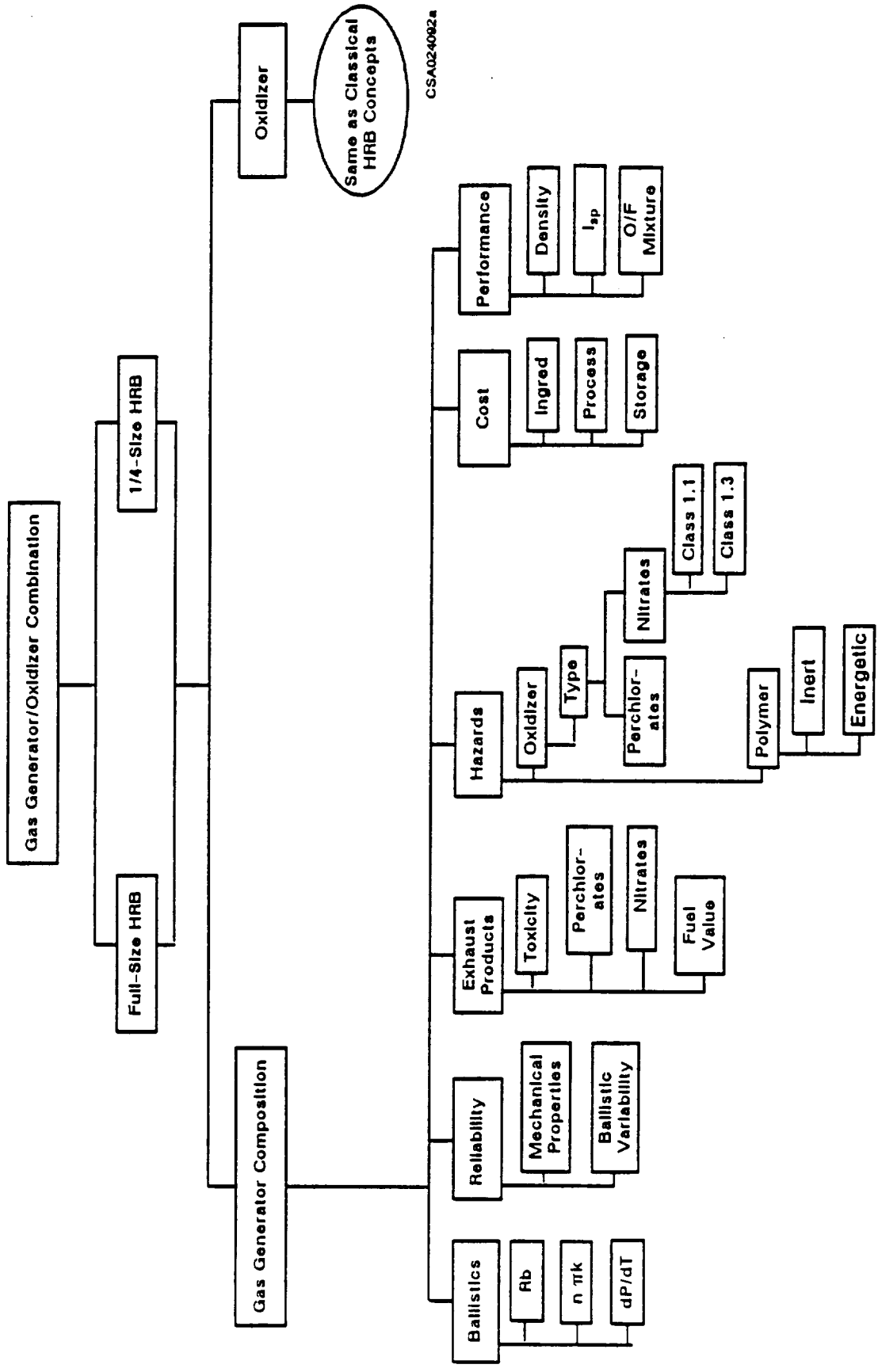
Figure 6. *Propellant selection trade tree for gas generator concept.*

hybrid concepts (HTPB/GAP/Zn/LOX) is far superior to propellant selected for the gas generator (HTPB/AN/Al/LOX).

3.1.3 DISCUSSION

Oxidizers

A number of both cryogenic and storable liquid oxidizers were examined with HTPB serving as the baseline fuel to compare the performance of these compounds. Candidate oxidizers are summarized in Table 1 and represent most classes of liquid oxidizing compounds, including nitrogenous, halides, and oxygen-based materials. The relative I_{sp} of these oxidizers with HTPB are shown in Figure 7 which plots I_{sp} as a function of mixture ratio. Not surprisingly, the fluorine-based oxidizers, F_2, FLOX ($F_2 + O_2$), F_2O, and F_2O_2, yield extremely high I_{sp} performance, particularly with the endothermic F_2O and F_2O_2

Table 1. Oxidizer trades with HTPB fuel.

Oxidizer	Class	BP (°C)	Density (g/cc)	ΔHf (kcal/mole)
O_2	Cryogenic	-183	1.149	-3.1
F_2	Cryogenic	-188	1.696	-3.0
O_3	Cryogenic	-112	1.614	+30.9
F_2O	Cryogenic	-145	1.650	+2.5
F_2O_2	Cryogenic	-57	1.450	+4.7
N_2O	Cryogenic	-88	1.226	+15.5
N_2O_4	Storable	+21	1.449	+2.3
IRFNA	Storable	80-120	1.583	-41.0
H_2O_2	Storable	+150	1.463	-44.8
ClO_2	Storable	+11	3.090	+24.7
ClF_3	Storable	+11	1.810	-44.4

90209-1.4
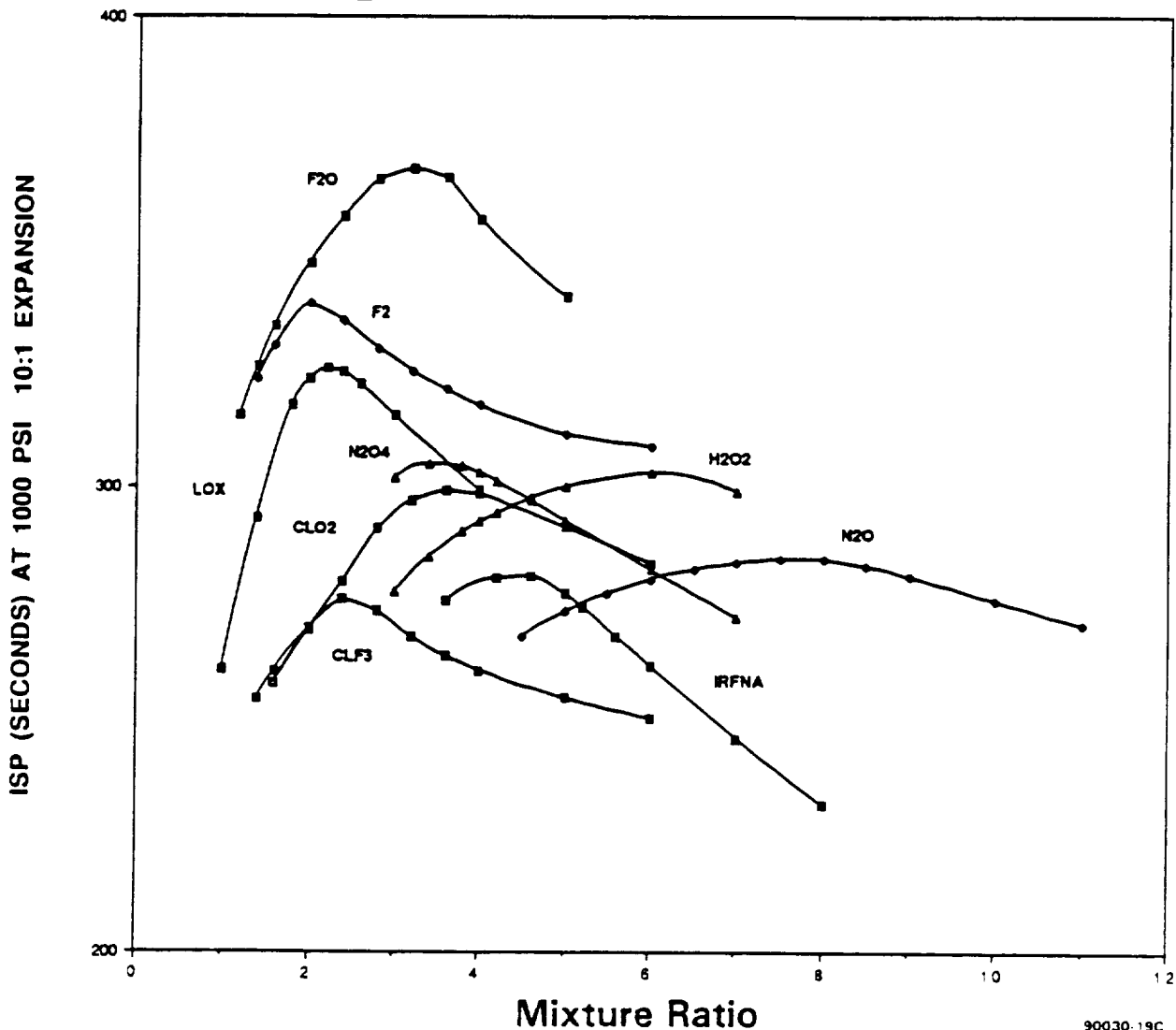
Figure 7. Vacuum I_{sp} (lbf·sec/lbm) comparing liquid oxidizers with HTPB fuel.

90030-19C

compounds. Unfortunately, these do not represent environmentally benign options since major exhaust products are HF and elemental fluorine (at high oxidizer-to-fuel (O/F) ratios), both of which are intensely toxic and corrosive. A potential means to alleviate these byproducts was examined via the inclusion of magnesium metal in the fuel formulation, whereby the stable salt MgF_2 would replace the free HF and F_2 species in the exhaust. Figures 8 and 9 illustrate the theoretical exhaust product distribution for a FLOX-type mixture based on this approach and suggests that free HF may be substantially reduced with magnesium. The uncertainty in completely eliminating these toxic products is great enough to still suggest that use of fluorine is not acceptable for the purposes of this application.

The same considerations hold true with the storable alternate halogen oxidizer candidates such as ClF_3, ClO_2, NF_3, and hydrated perchloric acid.

Of the remaining nitrogen- and/or oxygen-based oxidizers, oxygen is the most attractive. The nitrogen materials, N_2O_4, HNO_3 (IRFNA), and N_2O, tend to suffer from low performance and relatively high (>1000 ppm) NOx production in the exhaust, a source of potential serious atmospheric pollution.[1] Although densities are attractive, in the case of N_2O_4 and IRFNA, liquid-to-gas conversion in the motor system presents potential complications. A large amount of experience with these two oxidizers as hybrid components has been gained with the development of small motors,[2] although handling these materials on the scale required
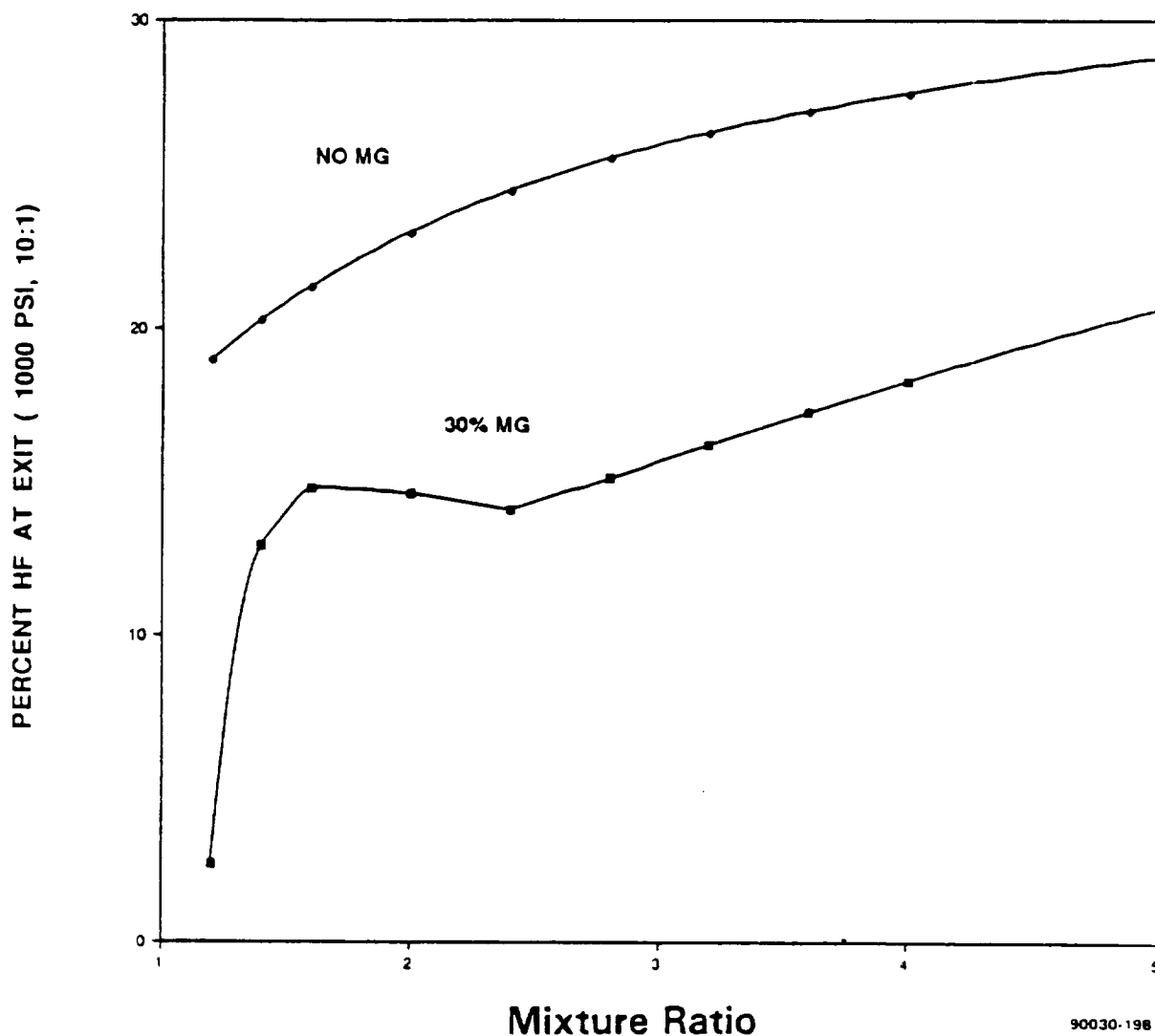
Figure 8. Production of HF in FLOX/HTPB hybrid and effect of including Mg in the fuel.

90030-198

3
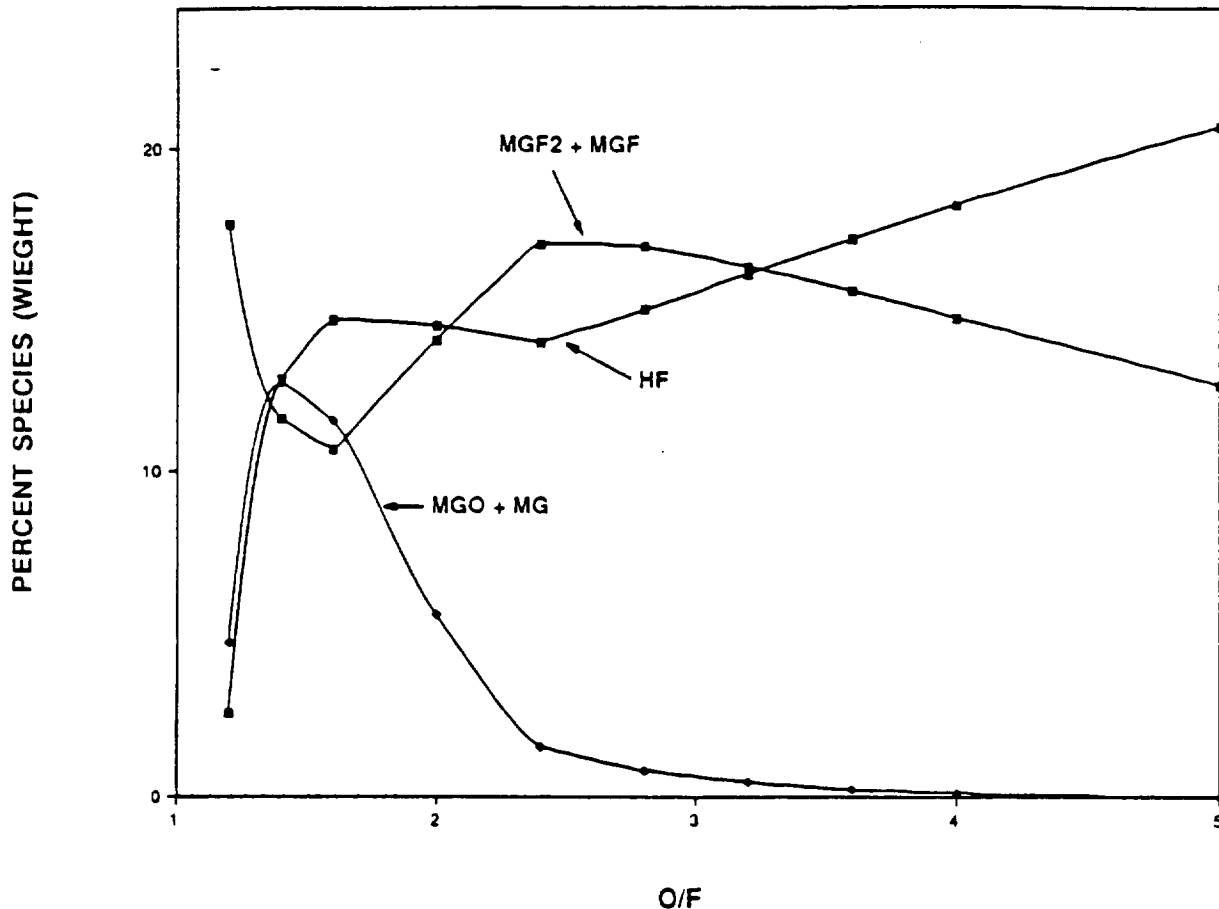
Figure 9. Relative concentrations of HF, MgO, and MgF times species in exhaust of FLOX/HTPB/Mg hybrid--lower temperatures at low mix ratios promote MgF_2 formation.

for large booster applications may pose some serious technical challenges both with regard to pad hazards and motor operation. The same handling reservations exist with concentrated (over 90 percent) hydrogen peroxide although gasification of liquid H_2O_2 to H_2O and O_2 can be accomplished catalytically, effectively circumventing injection/combustion problems.[2] The property of catalytic decomposition of H_2O_2 also contributes to undesirable stability problems with very concentrated material, which tends to make the handling and storage hazards an issue.

LOX, despite being cryogenic, clearly appears to be the best choice as an oxidizer candidate. LOX has been used for liquid rocket motors for years and thus enjoys an enormous experience base and is routinely handled in large quantities. With the exception of the fluorine oxidizers, LOX offers the highest performance of the oxidizers examined and is environmentally sound. One attractive energy growth option of the LOX-based oxidizer system identified in these trade studies is the inclusion of ozone. Figures 10 and 11 illustrate the

energy growth of both theoretical I_{sp} and density I_{sp}, with a potential energy possible of up to 50 percent ozone in the oxidizer. In general, cryogenic ozone is a marginally stable compound capable of mass detonation, but O_2/O_3 mixtures containing 25 percent or less ozone are suggested to be stable.[3] The production of ozone from oxygen on a large scale is a relatively mature technology and ozonized air (1 to 5 percent O_3) has been used for large-scale drinking water purification for a number of years.[4] Thus, ozonization of O_2 and subsequent liquefaction may potentially offer a viable means for increasing the available oxidizer enthalpy and density for rocket motor application. Another possible advantage of ozonization lies in the chemical reactivity of this species as an oxidizing agent. Ozone is intensely reactive toward hydrocarbons, being similar to fluorine, and thus may appreciably enhance regression rate characteristics of a given hybrid fuel formulation. It has been demonstrated that oxidative degradation at the fuel surface in polymer-based hybrid fuel combustion is a key element in fuel vaporization rates in addition to thermal degradation[5] and ozone can be expected to

9
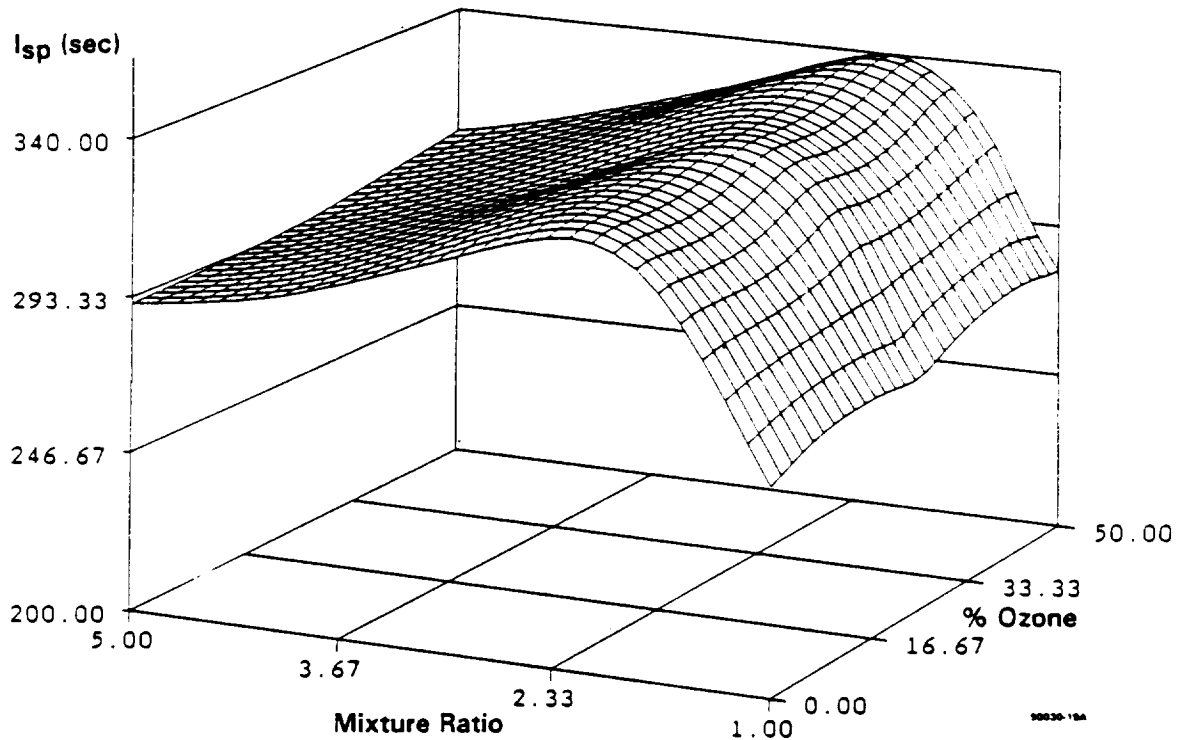
Figure 10. I_{sp} *versus mixture ratio and percent ozone--HTPB/ozone/LOX hybrid (1000 psi, 10:1 area ratio).*
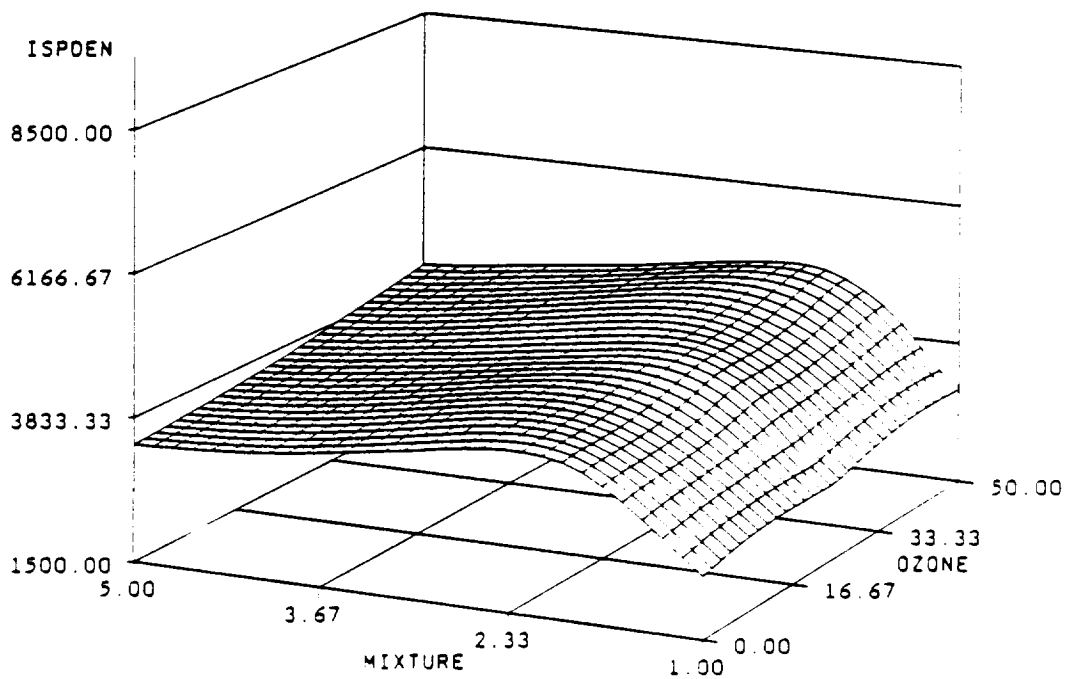
Figure 11. *Vacuum I_{sp} (lbf·sec/lbm) and density I_{sp} trends for HTPB fuel with LOX/ozone mixtures--increased energy and density of ozone make an attractive energy growth option.*

markedly enhance this process. Thus, experimental exploration of ozone/ oxygen mixtures as hybrid oxidizers should be considered seriously in further technology acquisition.

A summary of the various trade factors for each oxidizer candidate is given in Table 2, along with pertinent comments on the relative rankings. In general, due to exhaust product hazards and performance considerations, the oxygen-based candidates LOX, LOX/O_3, and H_2O_2 were selected for further trade studies with respect to fuel formulation and gas generator evaluation. The major emphasis for further studies is placed on LOX which is the least expensive, least hazardous, and most available high-performance oxidizer with any measure of experience.

Classical/Afterburner Fuel Formulations

Binders—As mentioned in the preceding section on oxidizer trades and selection, the baseline fuel formulation for classical concept studies is cured HTPB. From both a practical and performance point of view, HTPB is an excellent choice as a inert fuel matrix for the classical hybrid approach. Being a castable liquid, the material is easily formed into complex grain geometries, may be filled to relatively high solids loadings, and has a very large experience base with respect to handling, properties, etc., in the solid propellant industry. As the theoretical I_{sp} data of Figure 12 show, HTPB is one of the highest performance polymer fuels examined in these studies, exceeded only by polyethylene (presumably due to the more favorable hydrogen-to-carbon

balance in the latter). The trends in theoretical I_{sp} (Figure 12) also serve to underscore the fact that oxygenated polymer species (PolyTHF, PEG, Delrin) tend to degrade perform-ance and drive optimization levels to lower O/F ratios, contrary to what is observed with conventional solid propellant formulations. In addition to performance and handling considerations, relative ballistic performance as determined by regression rate characteristics also tend to favor HTPB over other polymer materials. Figure 13 plots experimentally determined regression rate as a function of motor pressure and oxidizer mass flux (gaseous O_2 (GOX)) for HTPB and polyethylene, respectively, while Table 3 compares the regression rates of several polymeric materials at similar oxidizer flux. The data clearly show HTPB to provide substantially higher regression rates than the other materials.

Costwise, HTPB also compares favorably with the various thermoplastics and other polymers considered. Liquid polybutadienes such as HTPB are available in several grades, with R-45M (commonly employed for solid propellant manufacture) being the most expensive (ca. $2.75 per pound). Use of R-45M for solid propellant formulating is principally driven by its high stress and strain capability relative to the less expensive grades. Due to the inert nature of the hybrid fuel grain, the less expensive materials are quite adequate. Bulk grade HTPB, as represented by R-45HT, costs roughly $1.25 per pound which makes it cost competitive with commodity polymers such as polystyrene, PEG, etc.

Table 2. *Oxidizer trade studies ranking and comparison.*

Oxidizer	Total Score	Performance (20)	Hazards (10)	Exhaust (20)	Cost (10)	Reliability (20)
LOX	70	15	5	20	10	20
FLOX	31	20	0	0	1	10
F_2	28	17	0	0	1	10
Ozone/LOX	54	17	2	20	5	10
N_2O	43	5	8	10	5	15
H_2O_2	47	10	2	20	5	10
N_2O_4	38	10	3	5	5	15
HNO_3 (IRFNA)	37	7	3	5	7	15
ClF_3	19	7	1	0	1	10
ClO_2	19	15	0	2	0	5

• Overall choice

  • LOX with LOX/ozone and H_2O_2 as alternates

11
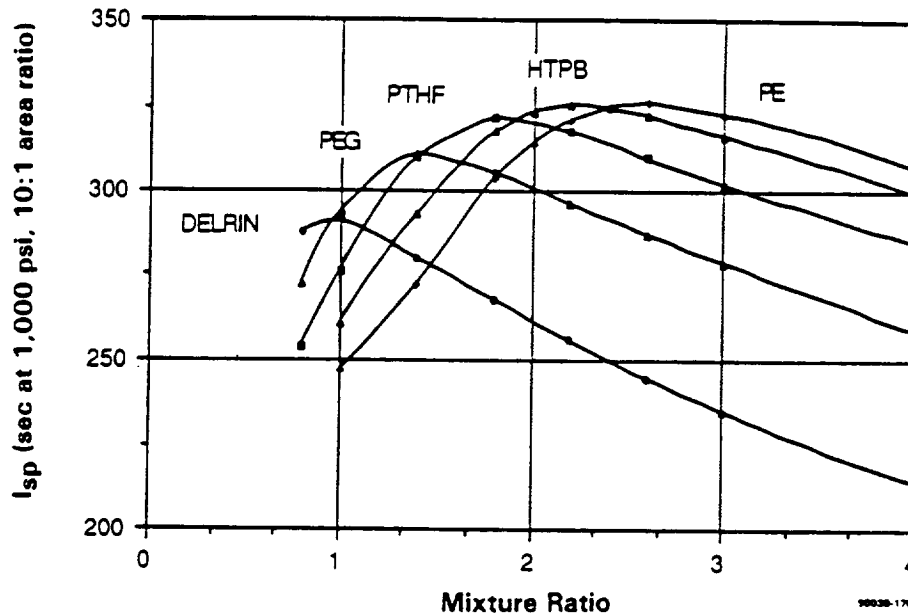
Figure 12. Comparison of vacuum I_{sp} (lbf·sec/lbm) at 1000 psi, 10:1 area ratio for several polymer fuels with LOX–oxygenated binders significantly lower performance potential of system.

Polyethylene, however, is substantially less expensive (ca. $.50 to $.60 cents per pound) than HTPB, but processing costs associated with thermoplastic injection or rotational molding on the scale required for large booster grain forming would add a substantial premium to the final fuel cost per pound. This, coupled with the limited solids-loading capability of high polymer thermoplastics such as polyethylene, leads us to favor bulk grade HTPB as the base fuel for hybrid grain formulating.

Table 3. Regression rate comparison of polymer fuels in a GOX hybrid motor.

Polymer Type	O_2 Mass Flux (lb/sec/in.²)	Motor Pressure (psi)	Regression Rate (ips)
HTPB	0.0441	88	0.0122
	0.0827	172	0.0169
HDPE (polyethylene)	0.0425	86	0.0042
	0.0785	179	0.0086
Delrin (polyformaldehyde)	0.0426	72	0.0040
	0.0818	132	0.0061

90209-1.3

Additives—The aforementioned regression rate characteristics of the fuel formulation with the selected oxidizer has long been one of the greatest challenges to hybrid motor application technology. Typically, low grain regression rate during operation tends to necessitate complex, high surface area grain designs which result in poor volumetric loadings and large case requirements. This is further aggravated by overall low system propellant densities, particularly with LOX/ polymer fuel combinations which are similar to LOX/RP-1 or kerosene–type liquid systems. Thus, low density and low mass flow combine to seriously impair the realistic adaptation of a hybrid motor to large boosters.

A large body of literature exists pertaining to improving both the ballistic (regression rate) characteristics and density performance of solid fuel hybrid motors. Principally, such approaches have concentrated on either using very reactive oxidizers (e.g., OF_2), endothermic fuel additives, metalization, or combinations of all.[1,6,7] Since fluorinated oxidizers were eliminated early from consideration due to hazards and environmental toxicity, concentration was placed on evaluating various fuel additive and mixture concepts in conducting further trade studies.

Two additive candidates showing promise with energetic oxidizers such as OF_2 are the lithium compounds LiH and $LiAlH_4$ (LAH). The light atomic weight and high hydrogen content, combined with low-temperature decomposition (assist in surface gassification), have made these attractive additives in solid propellant formulations. Based on a LOX hybrid system, only the LAH exhibits any potential for energy growth over HTPB alone (Figure 14). These additives

12
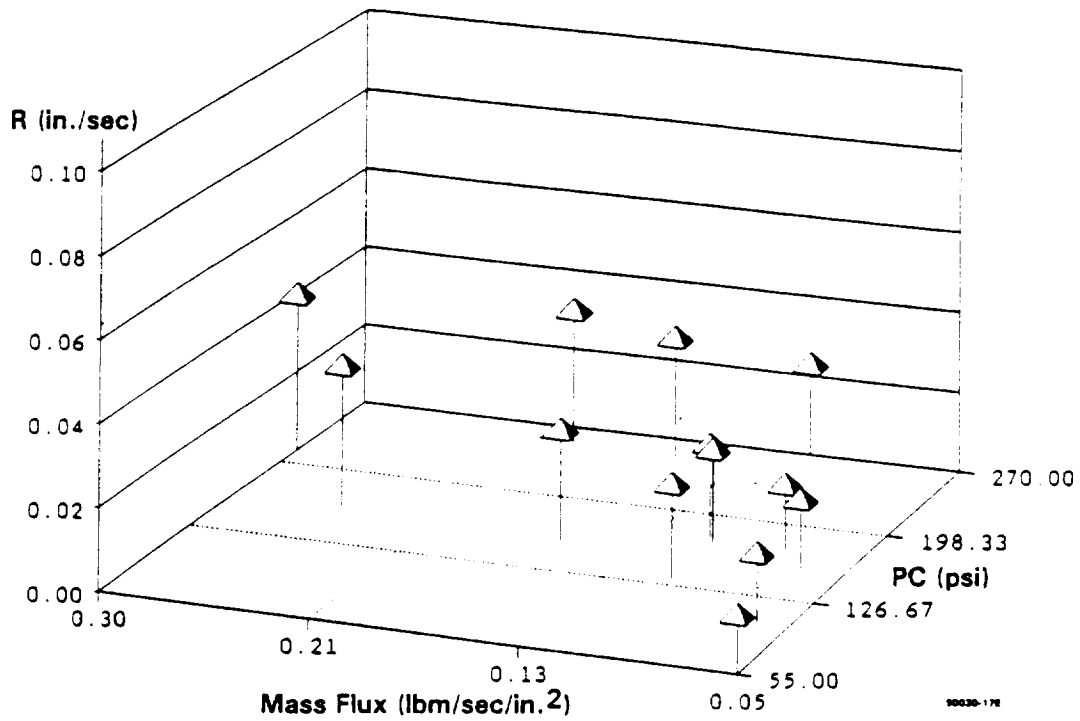
a. *HTPB fuel with oxygen.*
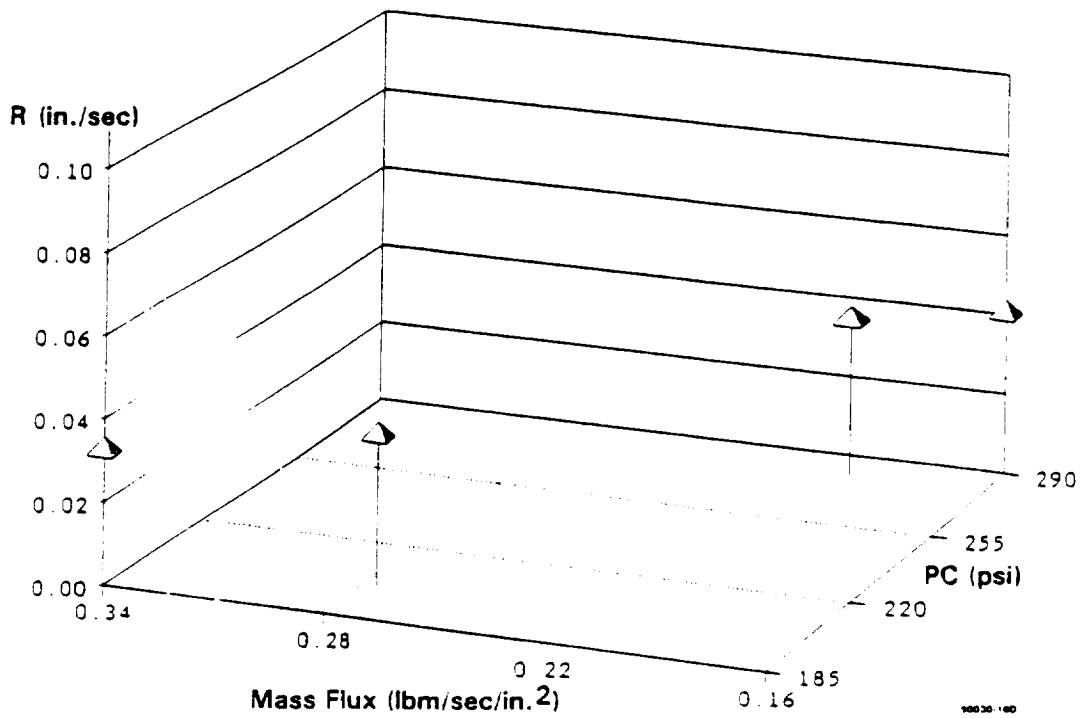
b. *HTPB/AN (20%) fuel with oxygen.*

Figure 13. Regression rate versus mass/flux and motor pressure.
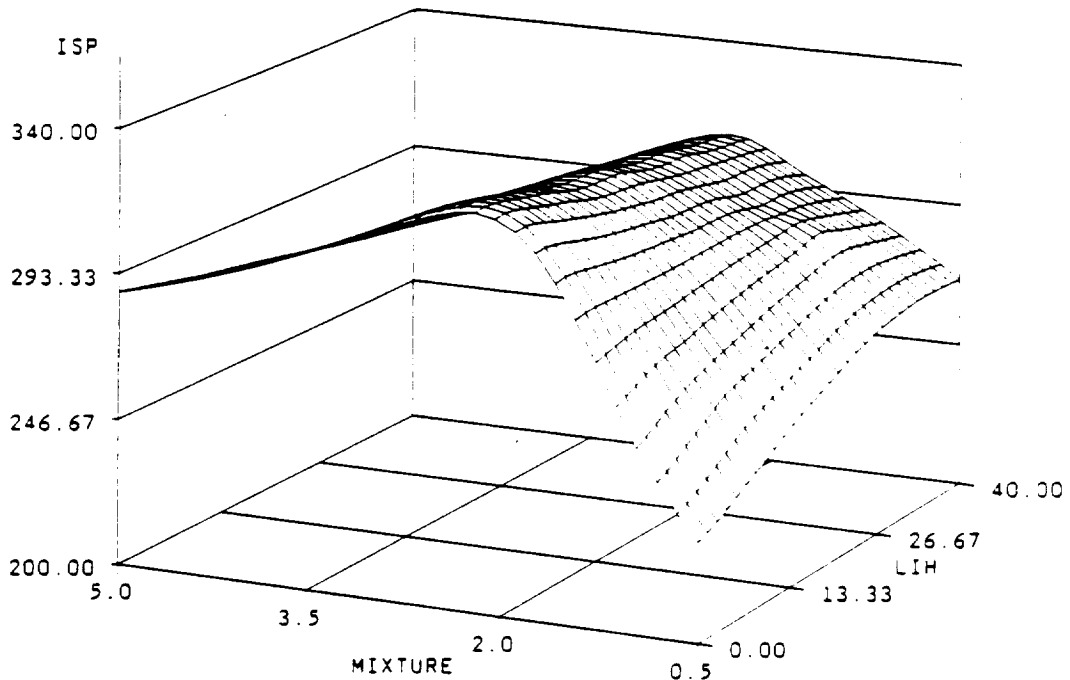
a. *HTPB/Li hydride (LiH)/LOX hybrid.*
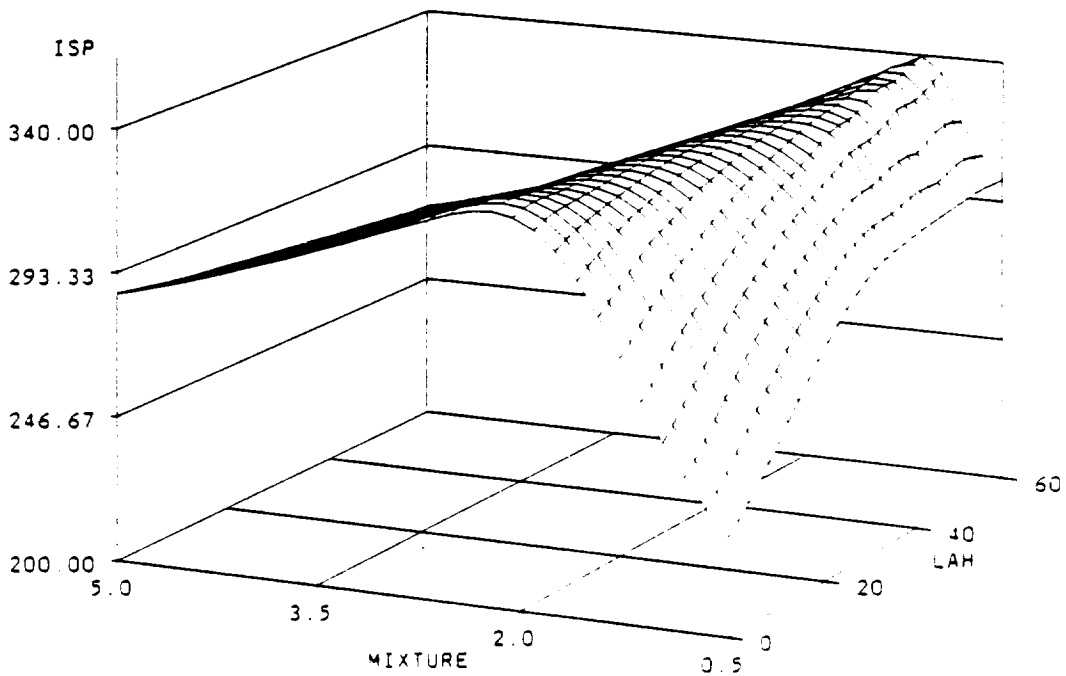
b. *HTPB/LiAlH₄ (LAH)/LOX hybrid.*

Figure 14.   Vacuum I_{sp} (lbf·sec/lbm) at 1000 psi, 10:1 area ratio for LOX HTPB.

also suffer from very low densities (due to the steric demands of the hydride anion) and, consequently, density I_{sp} is substantially degraded relative to HTPB (Figure 15). The surprisingly poor performance of these compounds, combined with their high chemical reactivity (particularly towards moisture), resulted in considering the addition of light hydrides to not be a viable option.
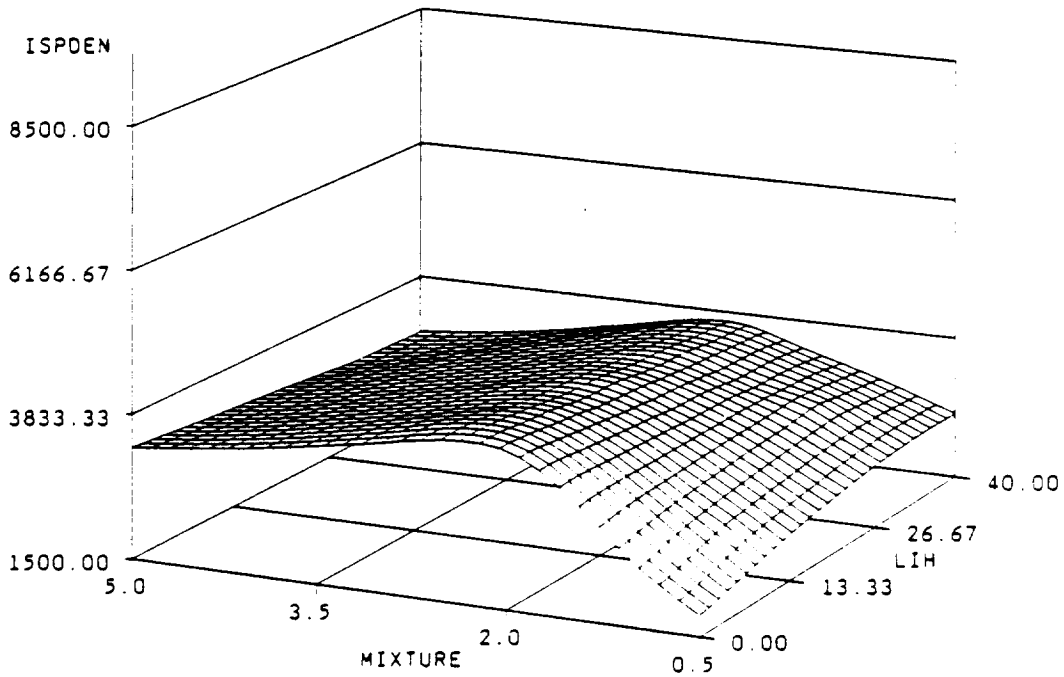
a. HTPB/Li hydride (LiH)/LCX hybrid.
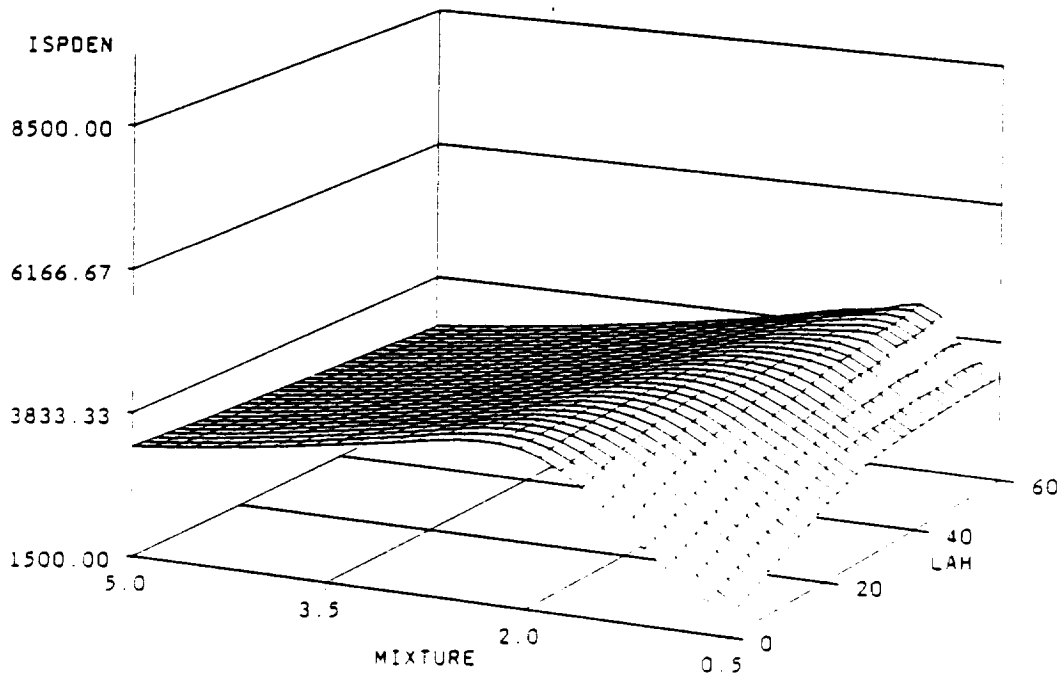
b. HTPB/LiAlH₄ (LAH)/LOX hybrid.

Figure 15. Density I_{sp} comparison of LiH and LAH additives in HTPB/LOX hybrid--low densities of metal hydrides result in density I_{sp} value less than HTPB alone.

Metalization, on the other hand, appears to offer substantial energy growth, particularly with respect to density I_{sp} for hybrid fuel grains. As mentioned previously, numerous metals have been employed in hybrid fuel studies, typically those traditionally included in solid propellant or pyrotechnic compositions such as aluminum, lithium, and magnesium due to high heats of oxidation and ease of combustion. Figure 16 illustrates the effect of aluminization of HTPB with regard to theoretical I_{sp} and density I_{sp} for LOX, H_2O_2, and LOX (75%)/ozone (25%) oxidizer systems. For comparison, the theoretical I_{sp} and density I_{sp} for a conventional high-performance aluminized solid propellant are plotted as a function of aluminum and total solids in Figure 17 under similar conditions. For clarity, expanded scale versions of these two figures are given in Figure 18 revealing the relatively sharp local maximum occurring in the 88 to 89 percent solids regime, which is where most high-performance composite propellants are formulated. Comparison of these energy surfaces for the various hybrid combinations and solid propellants suggests that propellant density I_{sp} values approaching or exceeding those of state-of-the-art solid propellants may readily be achieved, particularly with the denser H_2O_2 oxidizer or the more energetic LOX/ozone combination. In addition, a shift in the maximum I_{sp} O/F combination to lower mixture ratios enhances the total motor density advantage with metalization since less of the lower density oxidizer is required for maximum I_{sp} performance, resulting in a rapid increase in density I_{sp} at higher metal loadings.

From a combustion/ballistic standpoint, metalization of the fuel formulation has been found to enhance regression rate characteristics. Figure 19 illustrates the effect of aluminum content on the regression rate (with GOX) of two polymer fuels, HTPB and polyTHF. Curiously, the metalization effect was much more pronounced with the lower initial regressing fuel, polyTHF, resulting in equivalent regression rates being observed at high (>40 percent) metal loadings. The mechanism of regression rate enhancement through metalization has been investigated at length and is generally accepted to involve increased radiative heat feedback to the fuel surface.[6] This becomes less effective with increased metal content as increased fuel flux (blowing), resulting from improved heat feedback, tends to insulate the fuel surface until a leveling effect is produced, thus, the apparent limit on regression rate enhancement (Figure 19).

Taking the idea of increasing density I_{sp} via fuel metalization a step further, it was decided to examine the theoretical aspects of two rather unconventional metallic propellant additives, zinc and tungsten. These both represent combustible metals but carry density

(and molecular weight) to an extreme. For example, Zn with a density of 7.14 g/cc and tungsten with a density of 19.3 g/cc are several factors more dense than aluminum (2.7 g/cc), but due to high atomic weight and low heat of combustion (relative to aluminum) they are typically disastrous for I_{sp} when included in solid propellant formulations. Surprisingly, under the conditions of the hybrid configuration, both metals give reasonable theoretical impulse, as shown in Figure 20 (HTPB/Zn) and Figure 21 (HTPB/W) with LOX, H_2O_2, and LOX (75%)/ozone (25%). Combining the theoretical performance with the extreme densities involved results in density I_{sp} values substantially greater than previously supposed. Figure 22 illustrates this by comparing the density I_{sp} of HTPB/Al, HTPB/Zn, and HTPB/W with LOX as a function of metal and mixture.

A note of caution should be included at this point with respect to the zinc I_{sp} data. An unfortunate deficiency in the thermochemistry computer code used for calculating the theoretical I_{sp} exists in which, at temperatures above about 2300°K, the combustion product ZnO is returned to Zn(O) in the gas phase. Although this should not impact the exhaust mean molecular weight, an erroneous temperature (and characteristic velocity (C^*)) may be resulting. Whether this will favorably or unfavorably impact the I_{sp} and whether the error is significant is unknown at this time. However, a full set of products for tungsten does exist within the code, giving confidence in these data. The fact that the theoretical I_{sp} values for zinc and tungsten are consistently similar tends to suggest that the impulse values being used for zinc are conservative due to the large difference in oxide molecular weights. Further support for this assumption arises from an experimental comparison of hybrid motor combustion ballistic data conducted by us in which aluminum-, zinc-, and tungsten-containing fuels were evaluated with GOX.

As mentioned previously, one of the major shortfalls of the classical hybrid motor as an approach to large booster design is the low regression rate behavior of the fuel grain. This aspect has been the subject of numerous investigative programs examples of which are summarized in References 6 and 7. Among the approaches that have been explored, one of the more common is to formulate the fuel grain with a solid oxidizer (e.g., AP, AN) to provide surface combustion enhancement to the overall regression mechanism. In general, this has had limited success and only at solid oxidizer loadings capable of providing self-sustaining combustion (30 percent AP, 50 percent AN) are substantial increases in regression obtained.[6,7] This approach tends to drive the overall configuration of the hybrid motor to an auxiliary oxidizer augmented SRM as occurs with the gas generator hybrid concepts.
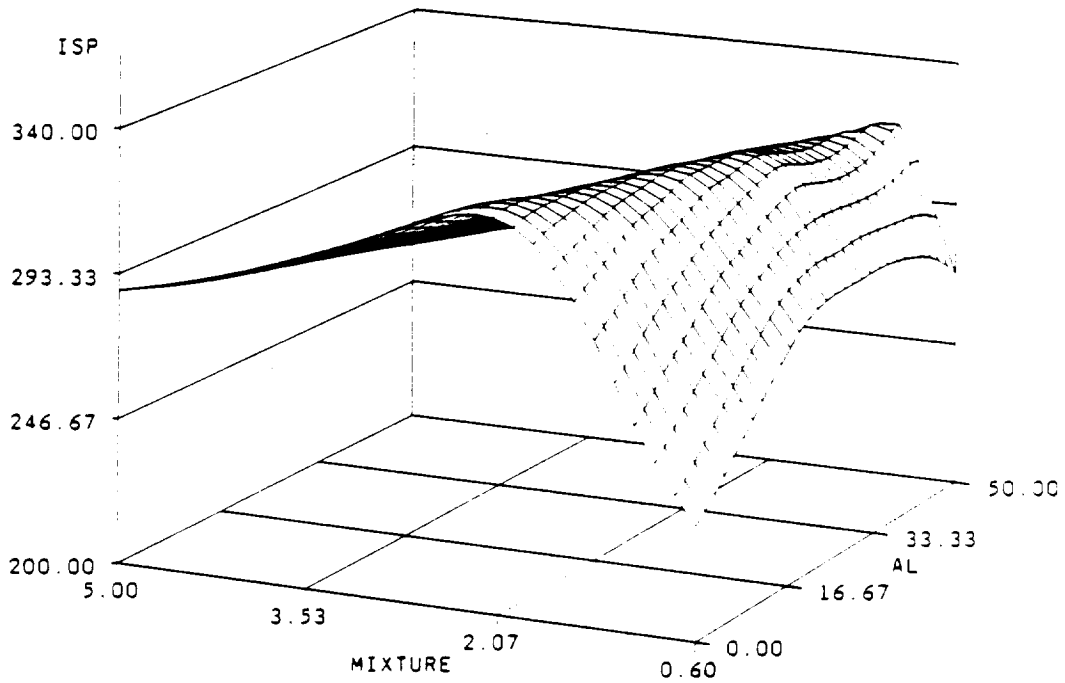
a. HTPB/Al/LOX
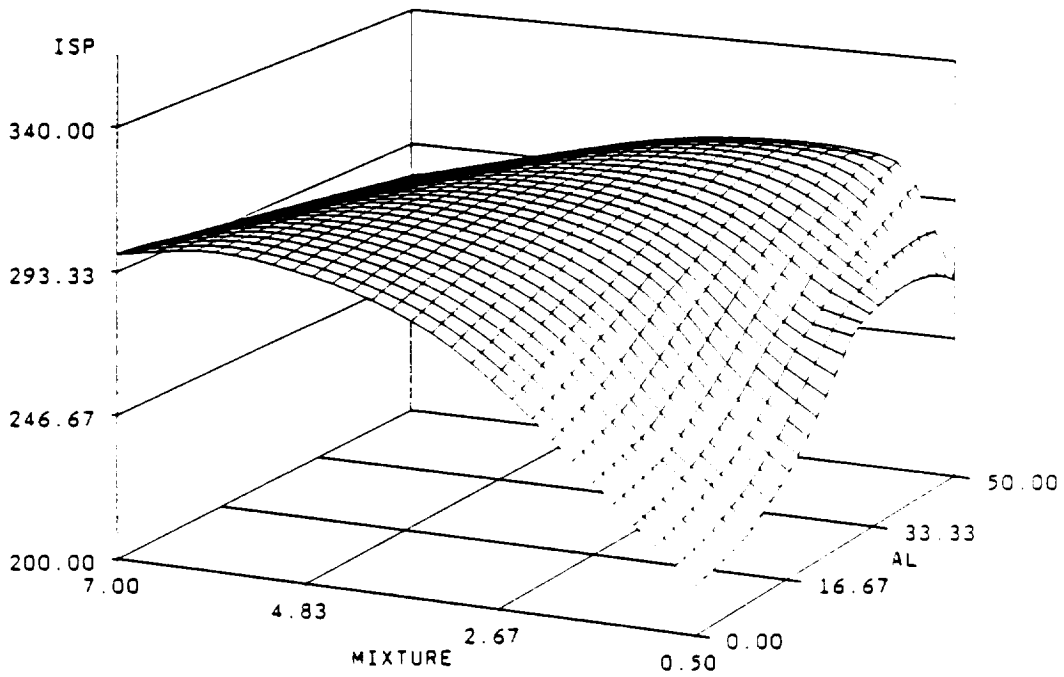
b. HTPB/Al/H₂O₂ hybrid.

Figure 16. Effect of aluminization of HTPB fuel on vacuum I_{sp} (lbf·sec/lbm) and density I_{sp} at 1000 psia, 10:1 area ratio--aluminization greatly increases density without significantly degrading I_{sp}--low levels of Al improve I_{sp} with H_2O_2.
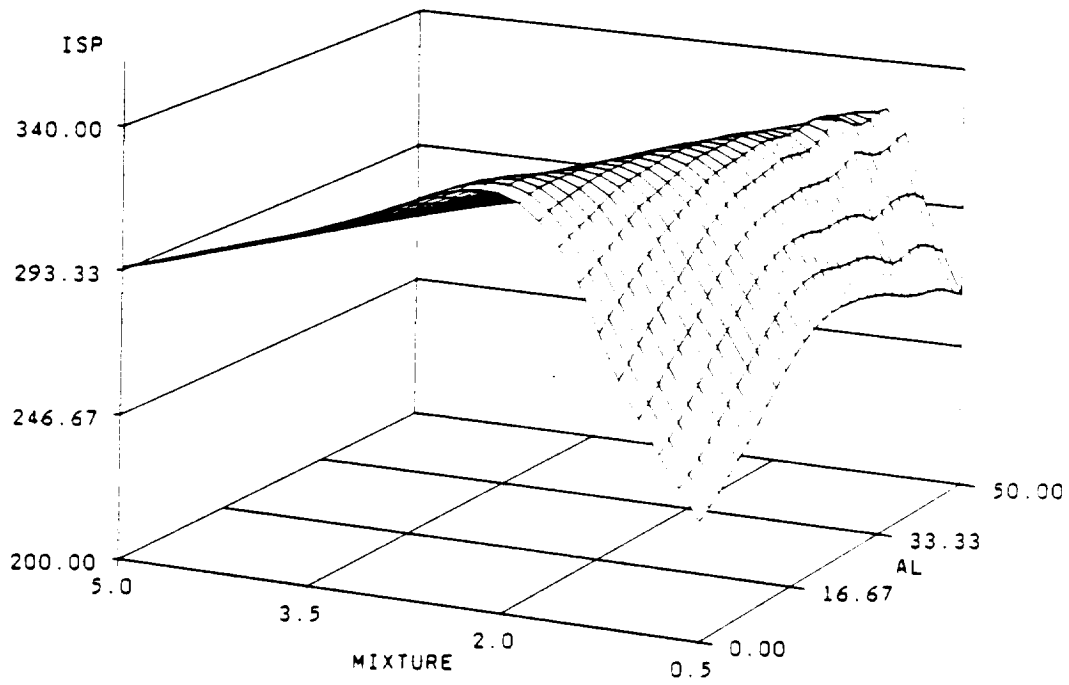
c. HTPB/Al/LOX-ozone hybrid.
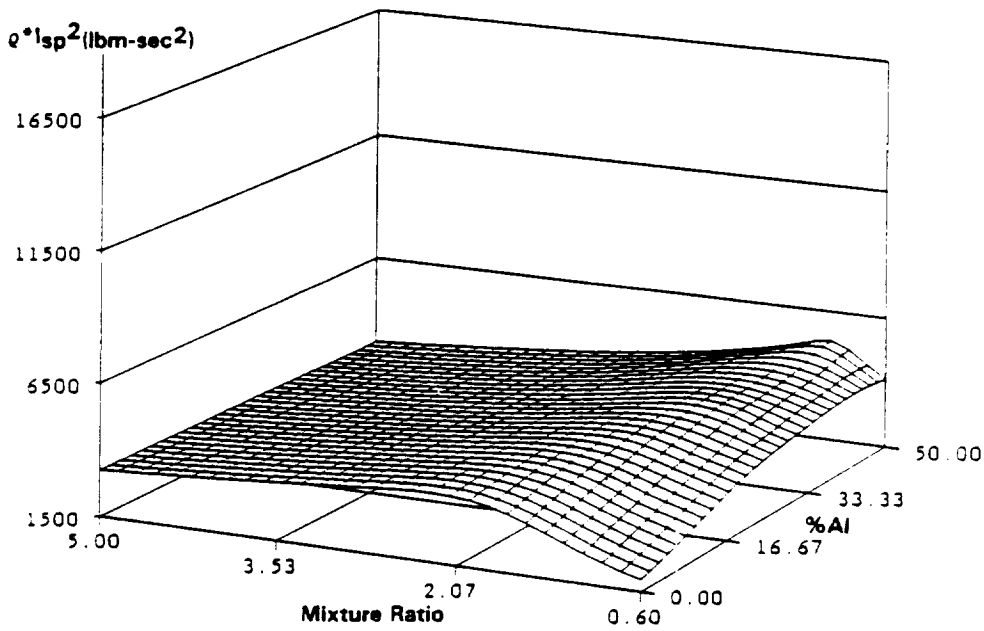
d. HTPB/Al/LOX.

Figure 16. Effect of aluminization of HTPB fuel on vacuum I_{sp} (lbf·sec/lbm) and density I_{sp} at 1000 psia, 10:1 area ratio—aluminization greatly increases density without significantly degrading I_{sp}—low levels of Al improve I_{sp} with H_2O_2 (cont).
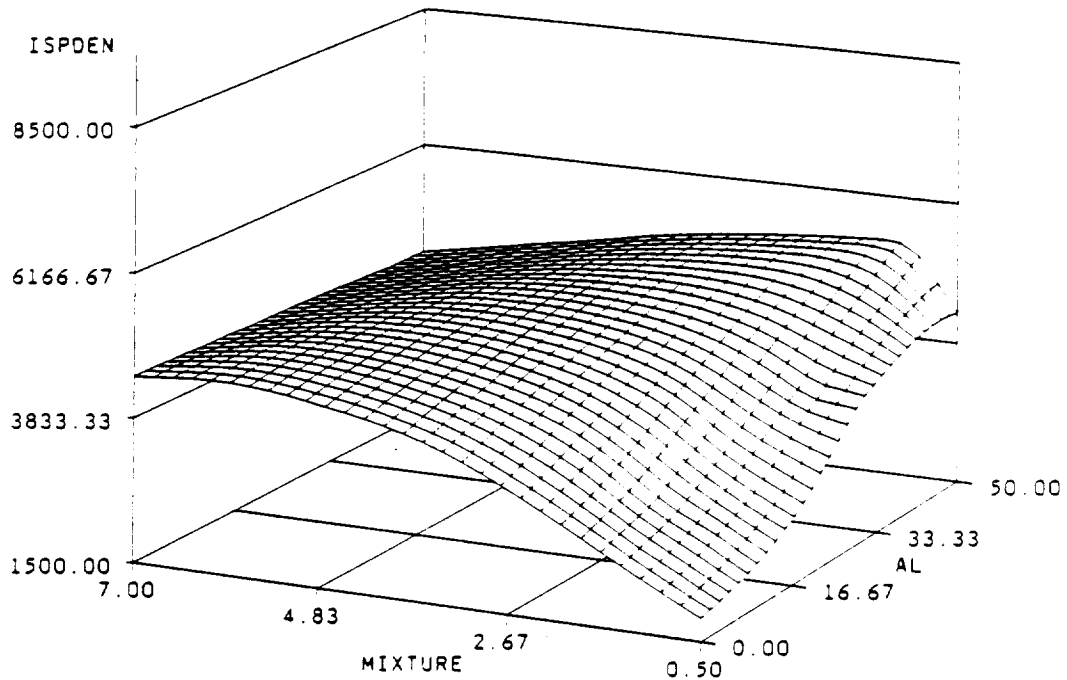
e. HTPB/Al/H₂O₂ hybrid.
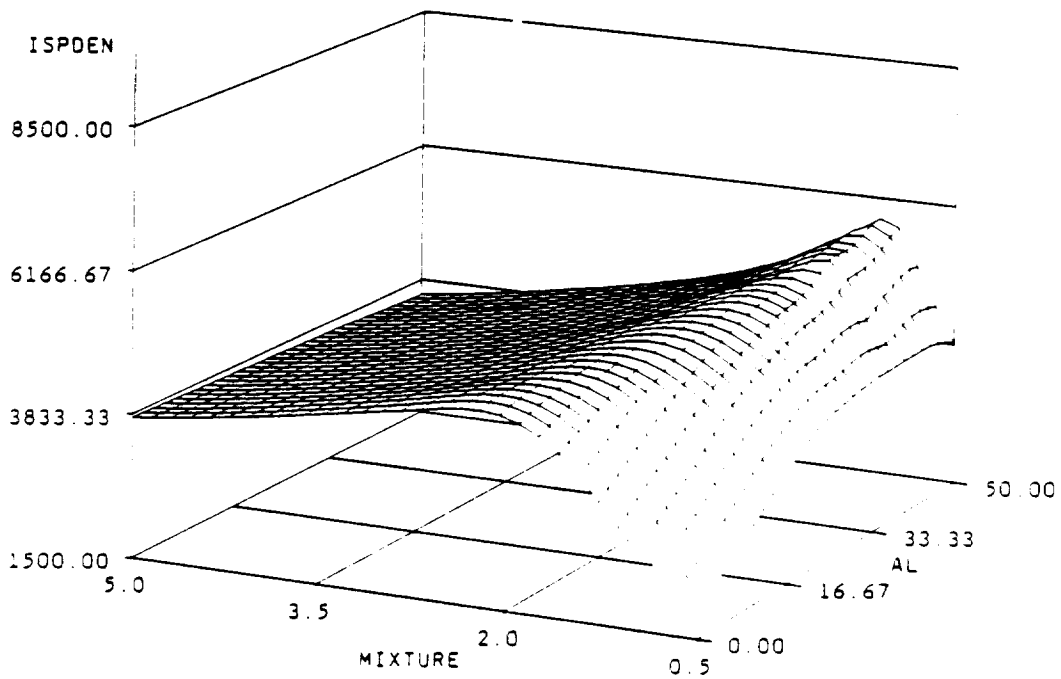
f. HTPB/Al/LOX-oxone (75/25) hybrid.

Figure 16. Effect of aluminization of HTPB fuel on vacuum I_{sp} (lbf·sec/lbm) and density I_{sp} at 1000 psia, 10:1 area ratio--aluminization greatly increases density without significantly degrading I_{sp}--low levels of Al improve I_{sp} with H_2O_2 (cont).

19
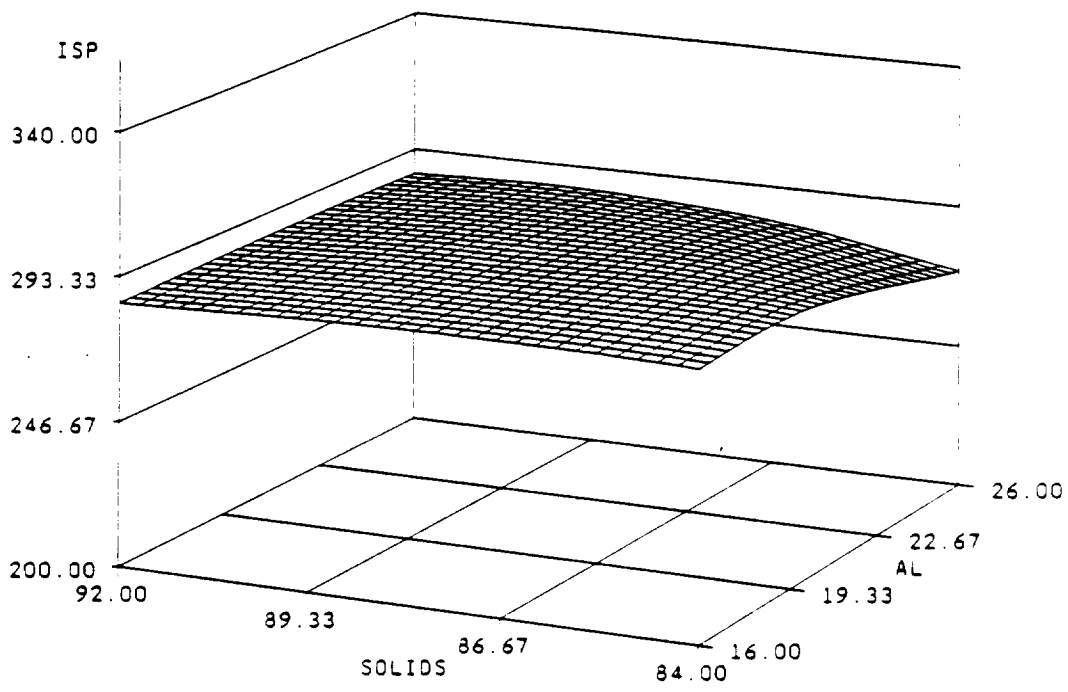
a. HTPB/Al/AP propellant.
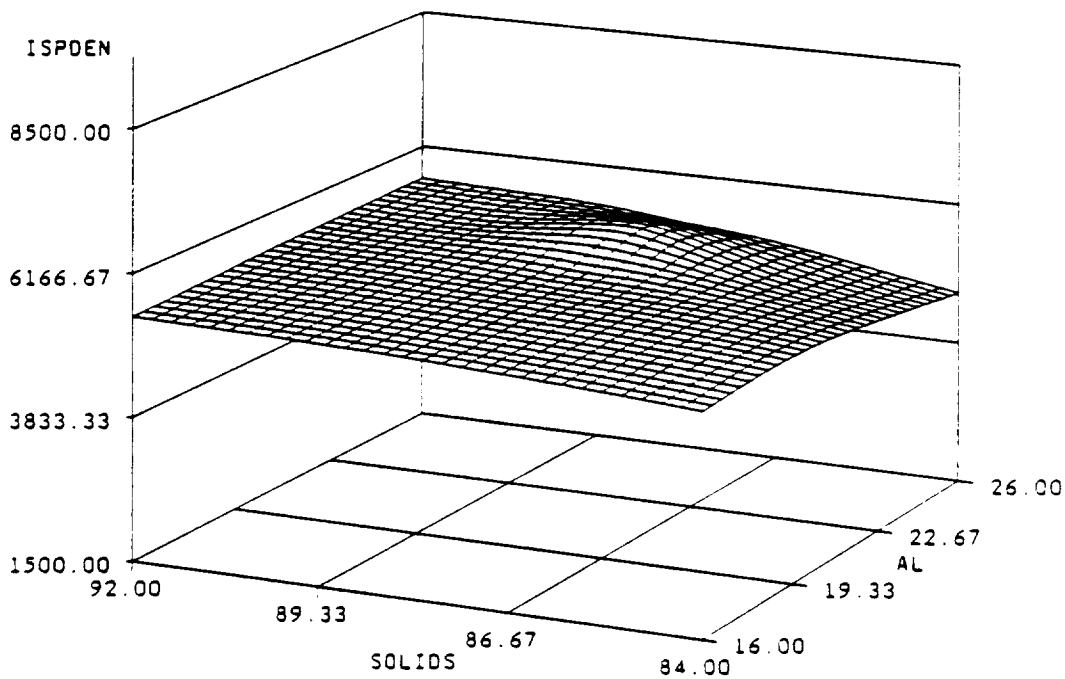
b. HTPB/Al/AP/propellant.

Figure 17. Vacuum I_{sp} (lbf·sec/lbm) and density I_{sp} trends of conventional high-performance composite solid propellants as a function of Al content and percent solids.
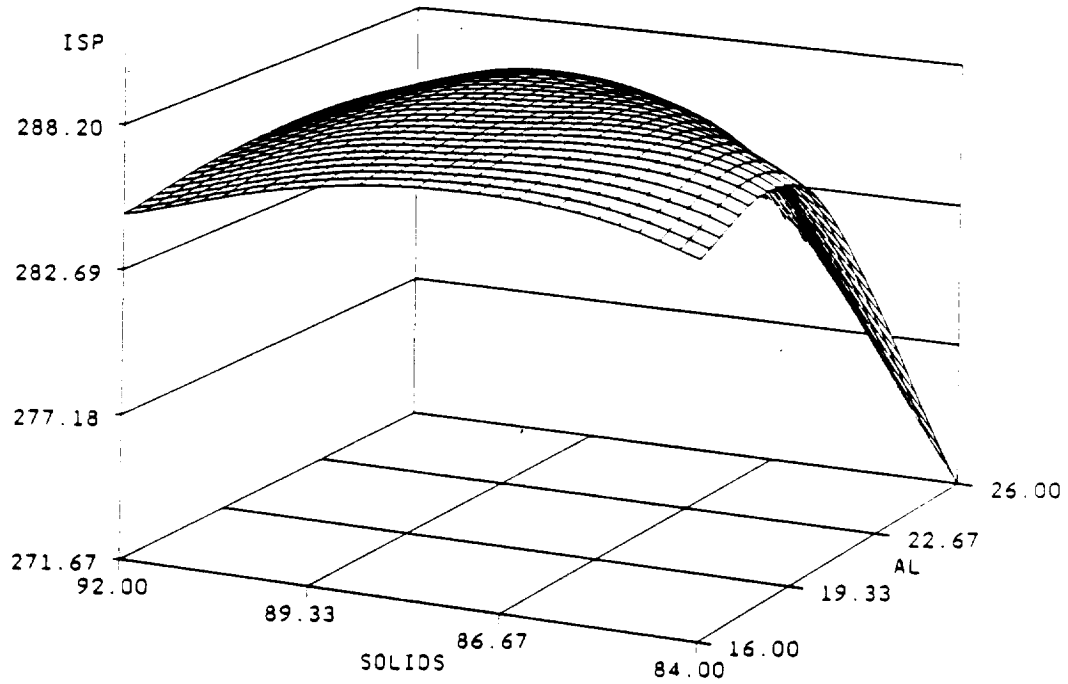
a. *HTPB/Al/AP propellant.*
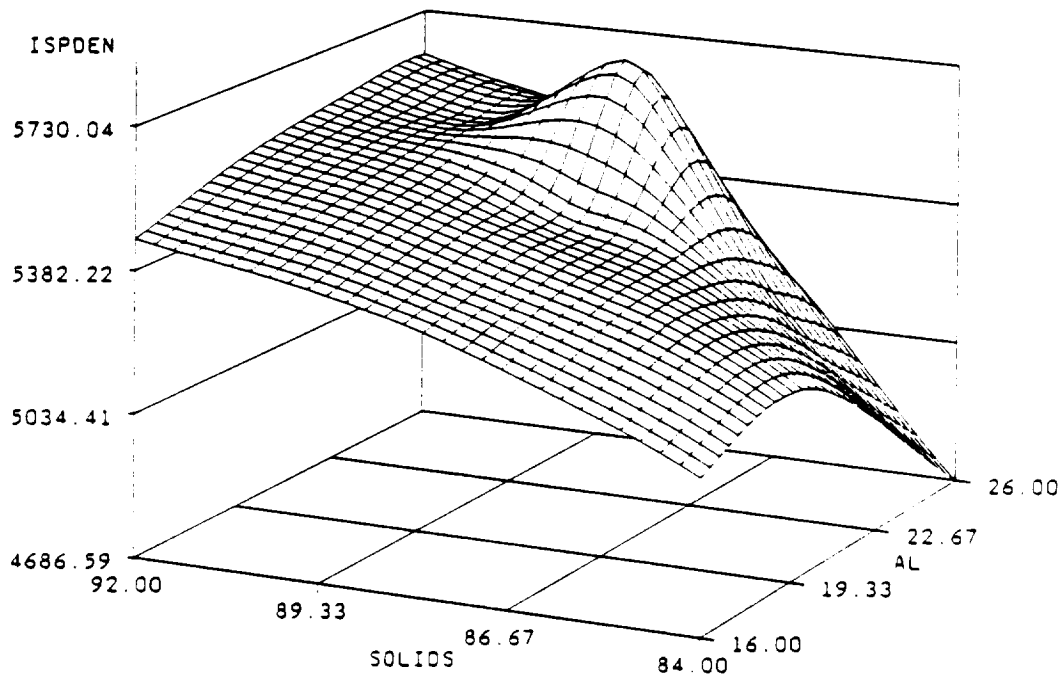
b. *HTPB/Al/AP propellant.*

Figure 18. Expanded scale showing strong local maxima of energy surfaces--conventional solid propellants are formulated in these regions to maximize performance.
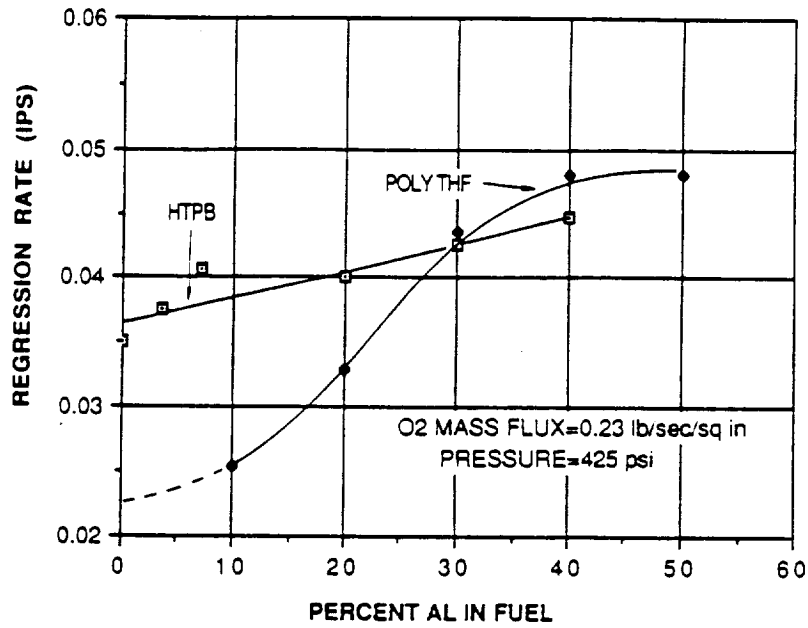
Figure 19. Effect of aluminum content on regression rates of HTPB and polyTHF with GOX.
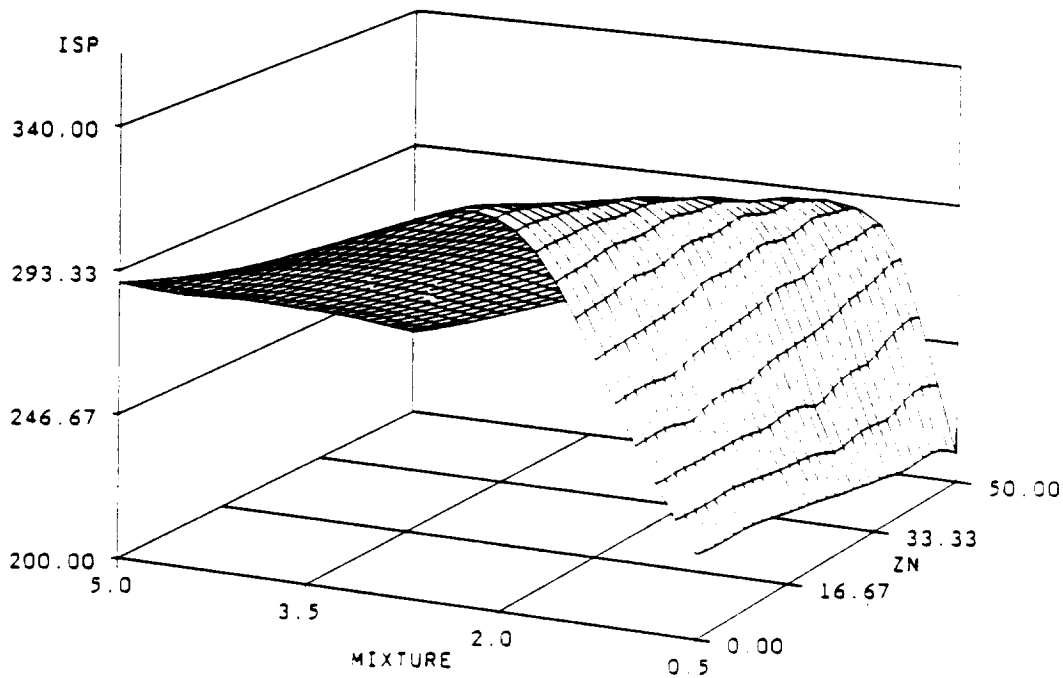
a. HTPB/Zn/LOX hybrid.

Figure 20. Vacuum I_{sp} (lbf·sec/lbm) at 1000 psi, 10:1 area ratio of HTPB/Zn fuels.
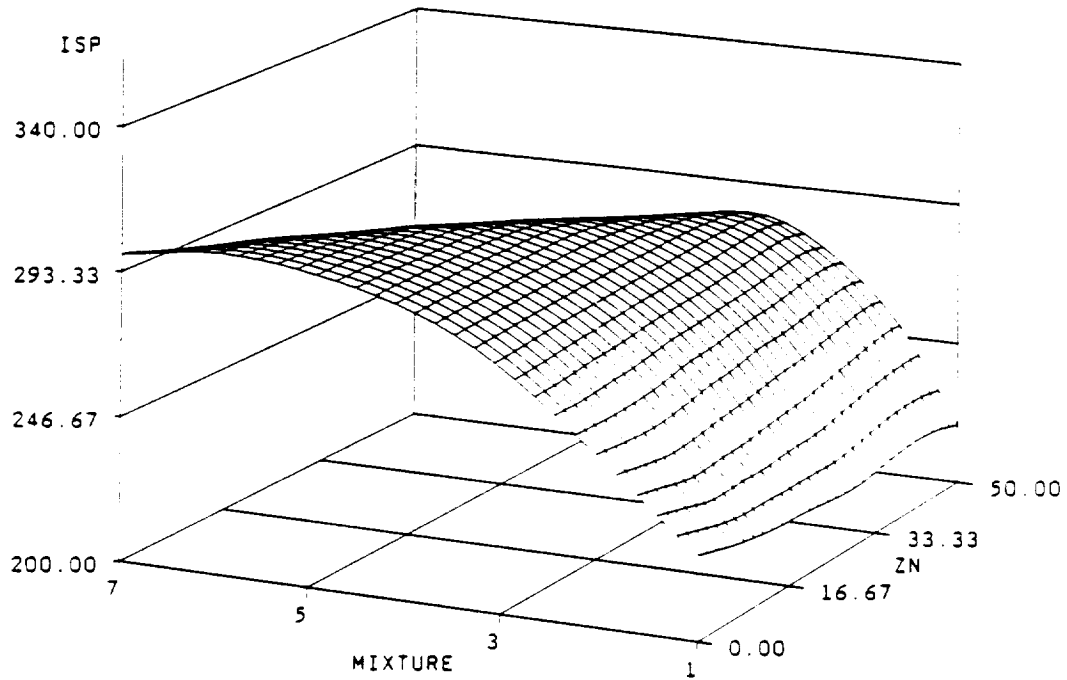
b. HTPB/Zn/H₂O₂ hybrid.
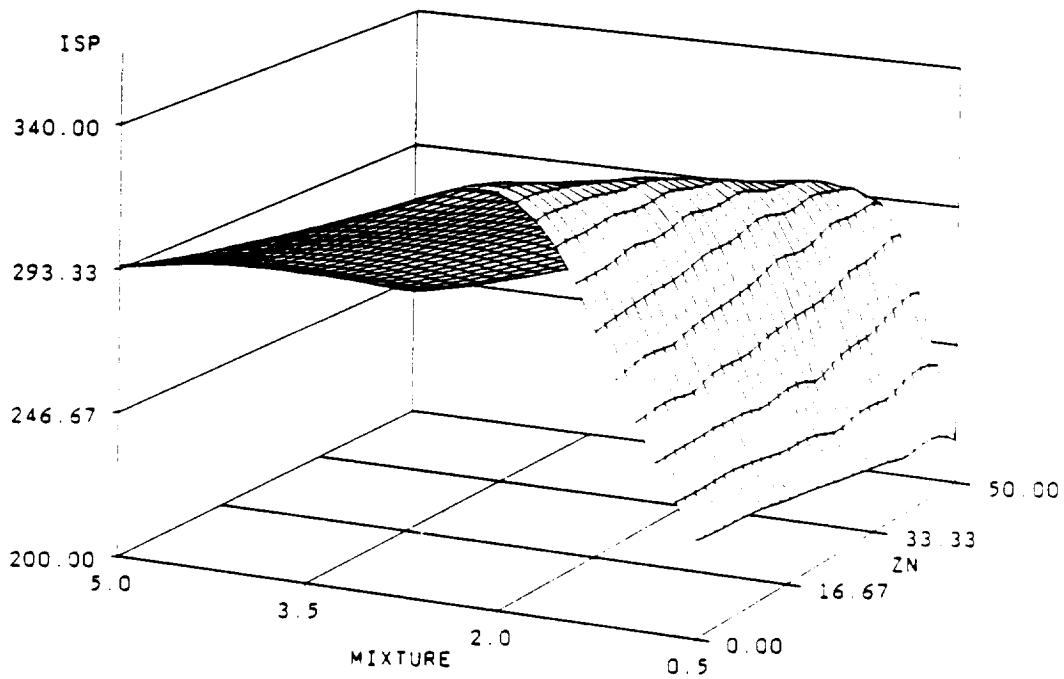
c. HTPB/Zn/LOX-ozone hybrid.

Figure 20. Vacuum I_{sp} (lbf·sec/lbm) at 1000 psi, 10:1 are ratio of HTPB/Zn fuels (cont).
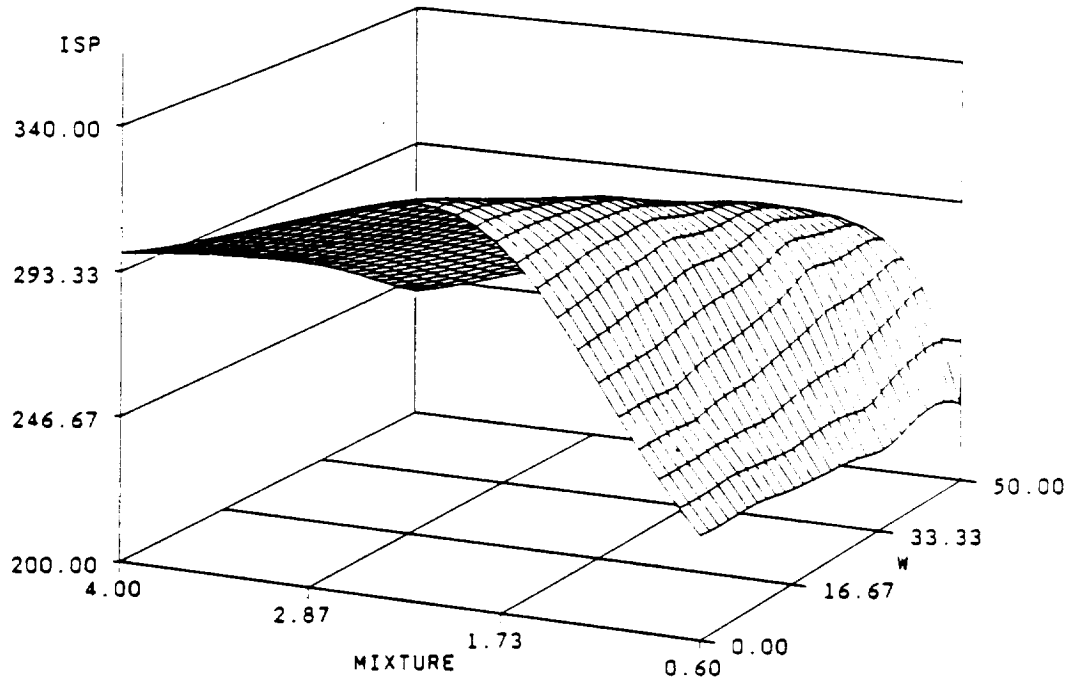
Figure 21. Effects of tungsten on HTPB/LOX hybrid vacuum I_{sp} (lbf·sec/lbm) at 1000 psi, 10:1 area ratio.
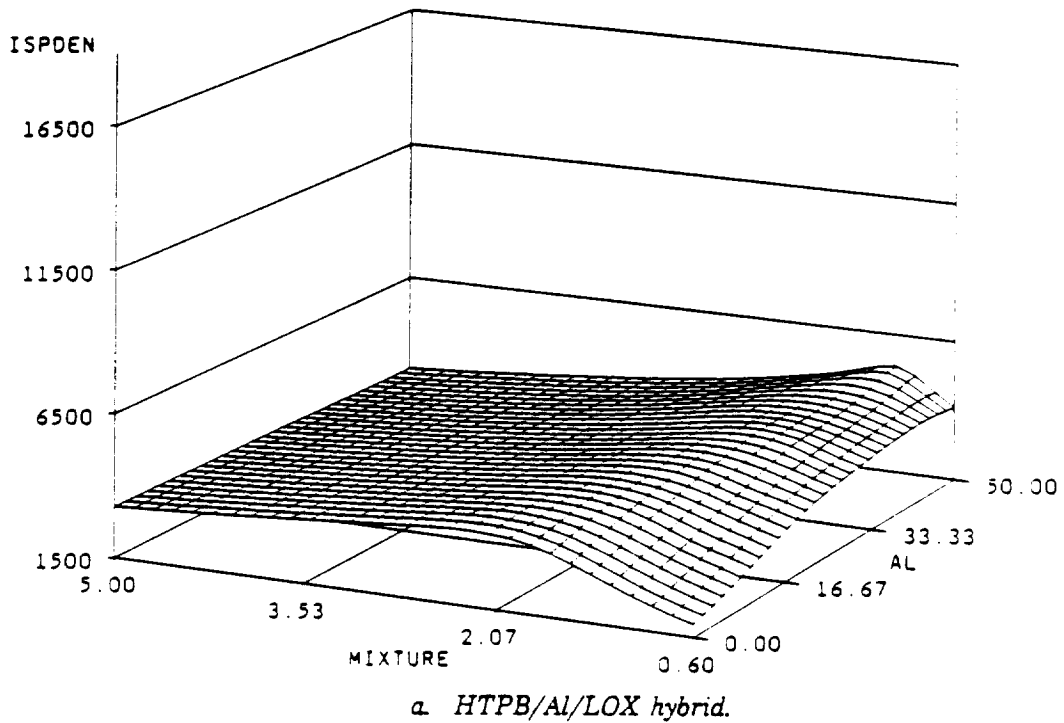
a. *HTPB/Al/LOX hybrid.*

Figure 22. Comparison of density I_{sp} at 1000 psi, 10:1 area ratio versus metal content--high densities of Zn and W contribute to large values of density I_{sp} far surpassing typical solid propellants.
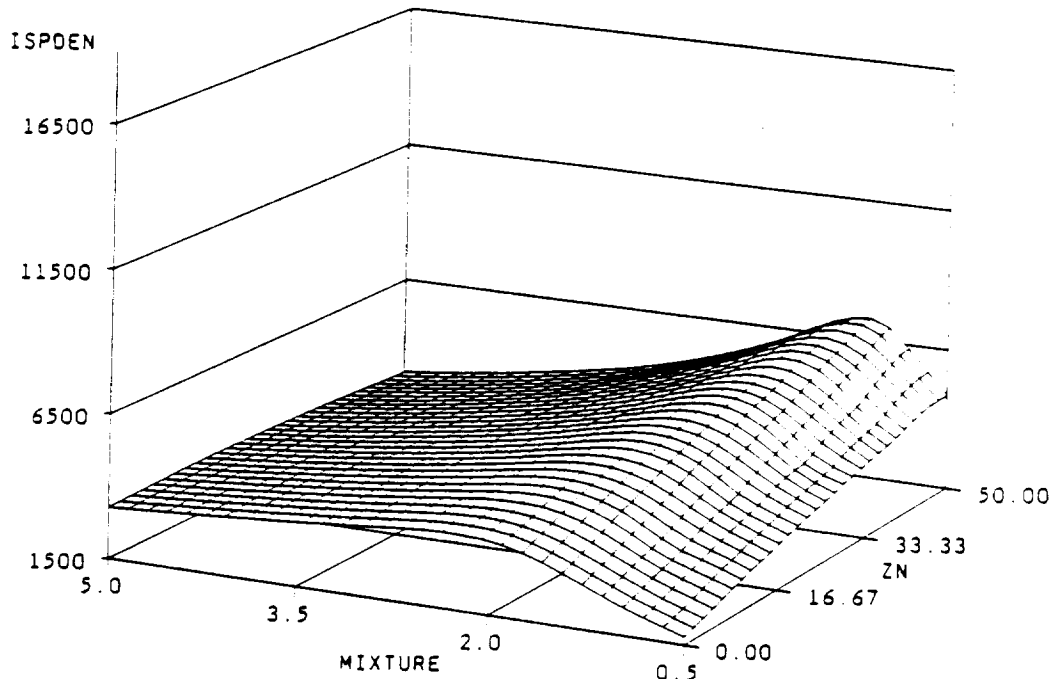
b. *HTPB/Zn/LOX*
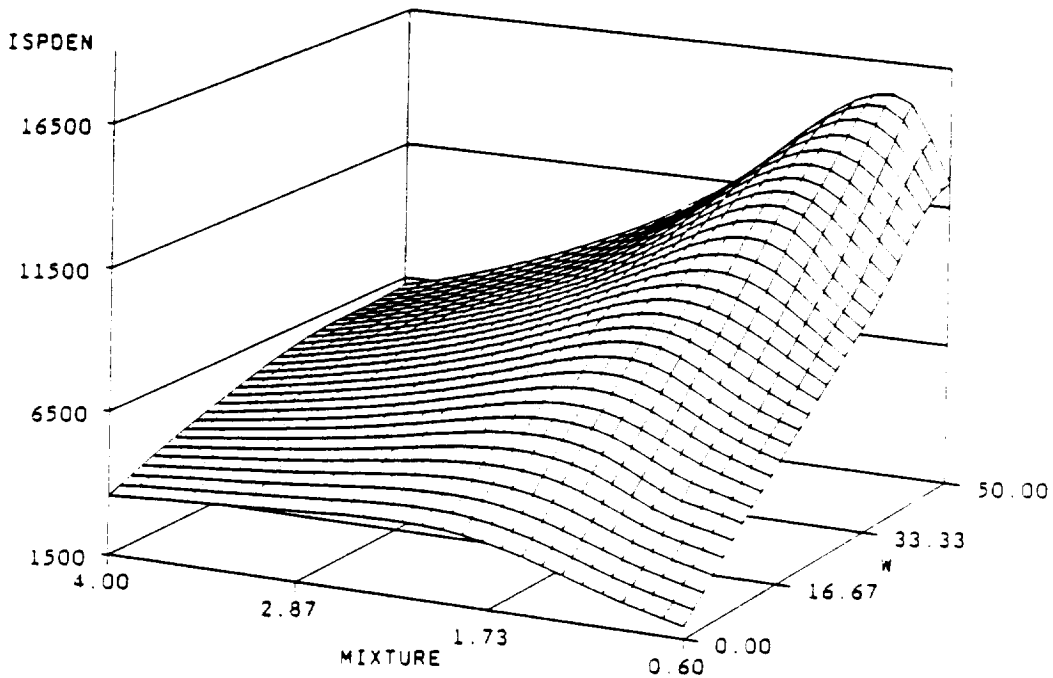
c. *HTPB/W/LOX hybrid.*

Figure 22. Comparison of density I_{sp} at 1000 psi 10:1, area ratio versus metal content--high densities of Zn and W contribute to large values of density I_{sp} far surpassing typical solid propellants (cont).

This, then, begins to defeat a number of the advantages accrued in the classical system, most notably the safety aspects associated with processing, handling, and storing an inert fuel grain as opposed to a live propellant. Alternatively, endothermic additives decomposing thermally in the fuel grain, such as light metal hydrides (LiH, LAH) or polynitrogen compounds (tetrazoles, diazo compounds, etc.), have also been explored as a means for increasing regression rates. As part of a discretionary funded parallel effort to this program, we have experimentally revisited a number of these approaches, in addition to metalization, for increasing regression rates of polymer-based (particularly HTPB) fuel formulations with GOX injection. A summary of additives and fuels examined to date are given in Table 4.

Table 4. Experimental fuel ingredients for GOX hybrid evaluation.

Polymers	Metals	Additives
HTPB Al	AN	
Polyethylene	Zn	Aminotetrazole (AT)
PolyTHF	Mg	Carbon black
Polyformaldehyde (Delrin)	W	
Butylmethacrylate	Reticulated Al	
Nitrocellulose	Structures	
GAP	–	

90209-1.1

Generally, it was found that metalization in combination with additives resulted in regression rate increases on the order of 20 to 50 percent over the baseline formulations, consistent with the literature. In addition, most combination fuels resulted in significant pressure dependence being observed, with pressure exponents typically on the order of 0.3 to 0.4, similar to that obtained with solid propellants. Although a combination of pressure and flux dependency is useful for simplifying grain configurations, only one additive was found to influence regression rates enough to actually begin to make a large hybrid design appear realistic.

The energetic binder GAP was found to produce very large increases in regression rates when blended with HTPB or other inert binders such as polyTHF. This material is unique in being self-deflagrating in the neat form but is rendered extinguishable at concentrations up to 70 percent by weight in HTPB. As shown in Figure 23, the effect on regression rate in the hybrid motor is dramatic. Blends of HTPB and GAP (typically 30 percent GAP) were found to respond quite well to metalization, with aluminum, zinc, or tungsten giving

regression rates at least twice those obtained with HTPB alone at relatively low oxidizer flux and motor pressures (Figure 24). Interestingly, motor pressure and regression rate were quite similar for aluminum and zinc, suggesting similar C^* are being obtained.

From a performance standpoint, addition of GAP to HTPB results in slight I_{sp} degradation, a shift to lower optimum O/F and an increase in density I_{sp} relative to HTPB alone (Figure 25). Metalization with aluminum, zinc, or tungsten (Figure 26) gives similar results to those observed with metalization of HTPB and at levels of up to 20 percent metal (GAP (70%)/HTPB (30%)), which are probably more realistic than the very high (40 to 50 percent) levels shown in earlier figures.

Despite the extremely attractive ballistic and performance aspects resulting from the use of GAP in a hybrid fuel formulation, there are aspects of this material that need to be addressed in seriously considering its use for hybrid fuel formulation. First is the fact that GAP is classified as a Class B explosive due to its ability to deflagrate under pressure. It does, however, self-extinguish at ambient pressures and it is not an oxidizing agent. Thus, it is rapidly desensitized upon dilution with inert materials as is reflected in the true start/stop behavior of compositions containing up to 70 percent by weight GAP. Another obstacle associated with GAP is that it is expensive. GAP is a developmental material available in up to 1000-lb quantities, and is currently priced at roughly $100 per pound. Future cost projections of $8 to $10 per pound have been mentioned, but for now price remains an issue. Consequently, a GAP substitute for hybrid application is highly desirable. Several promising options with the same regression rate mechanism are being explored under continued discretionary funded research activities by Thiokol Corporation.

Relative costs also constitute selection issues with respect to metal for the candidate hybrid fuel formulation. Strictly from a performance (density I_{sp}) point of view, use of tungsten in combination with GAP and HTPB is the obvious choice. Tungsten is, however, a relatively expensive metal and its large-scale availability is uncertain.

Moreover, the environmental impact of the exhaust products from tungsten combustion may pose a potential threat. Zinc and aluminum, on the other hand, are quite common in the environment, and both metals are available in abundance with zinc being considerably less expensive than aluminum ($.65 to $.85 per pound versus $1.65 to $2.70 per pound). Neither oxide is excessively toxic, both being used in common products as pigments, ointments, etc. although fine dusts may represent inhalation hazards.[8] The combination of very low cost, high density, and acceptable performance

26
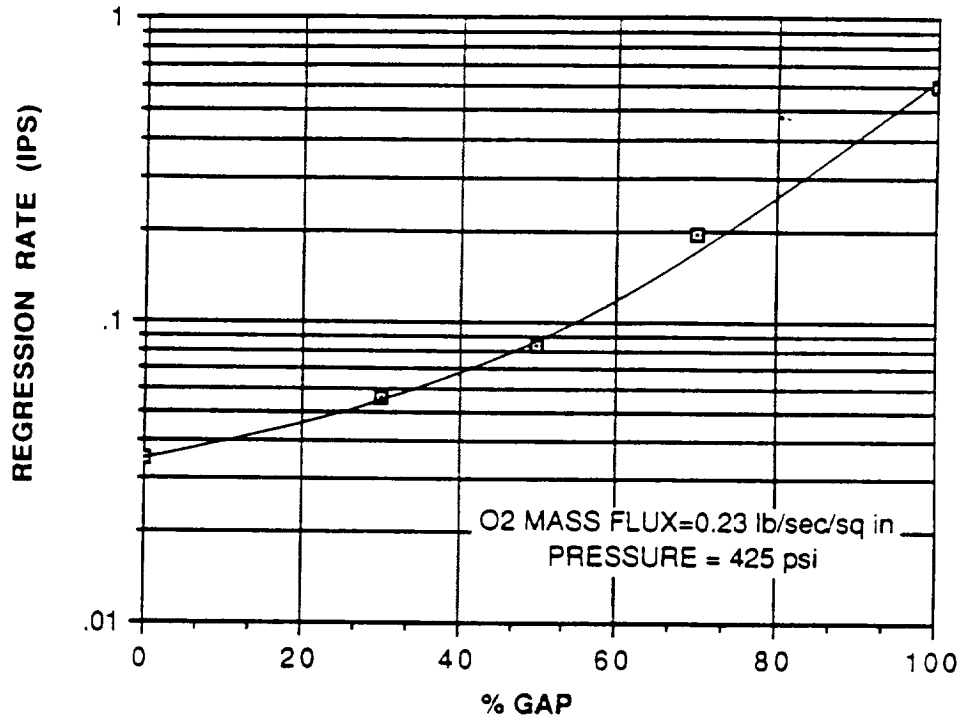
Figure 23. Effect of GAP on regression rate of HTPB/GOX hybrid--concentrations of 70 percent or less GAP exhibit start/stop behavior; 100 percent GAP is self-deflagrating.
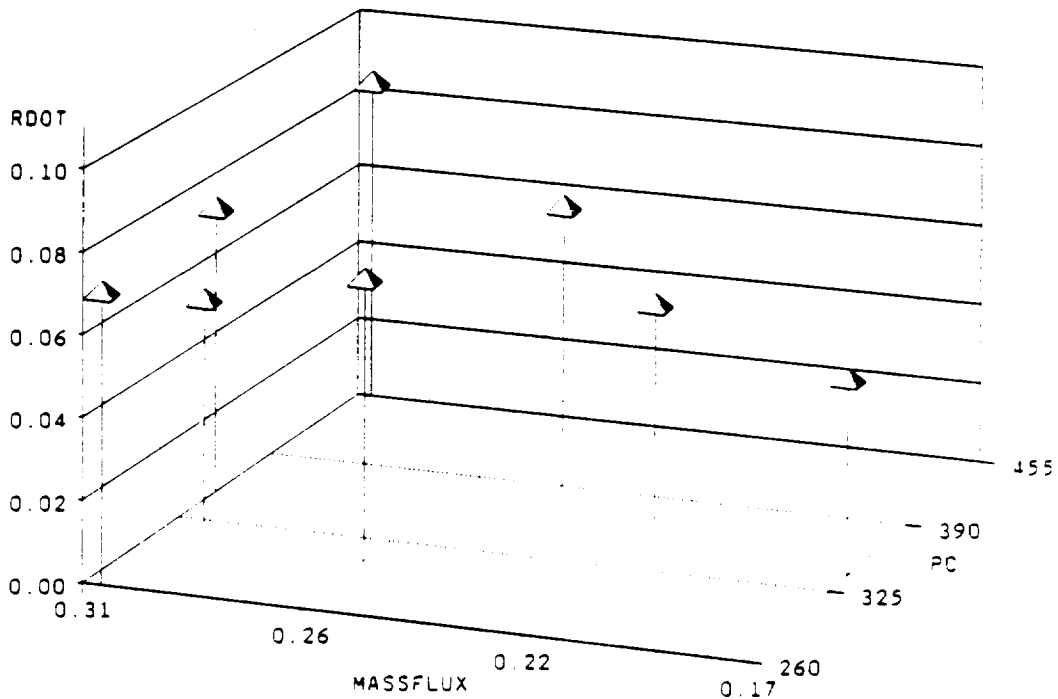
a. HTPB (54%)/GAP (26%)/Al (20%) fuel with oxygen.

Figure 24. Regression rate characteristics of metalized HTPB/GAP fuels--all exhibit high regression rates relative to HTPB alone with Al and Zn giving similar values.
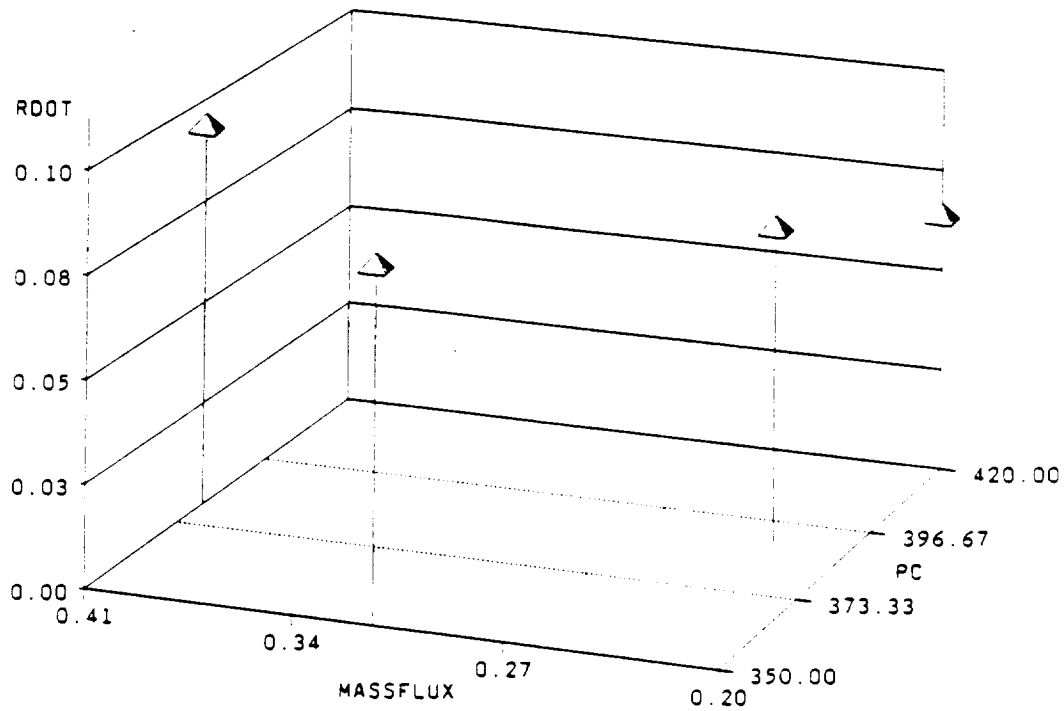
b. *HTPB (63%)/GAP (27%)/Zn (10%) fuel with oxygen.*
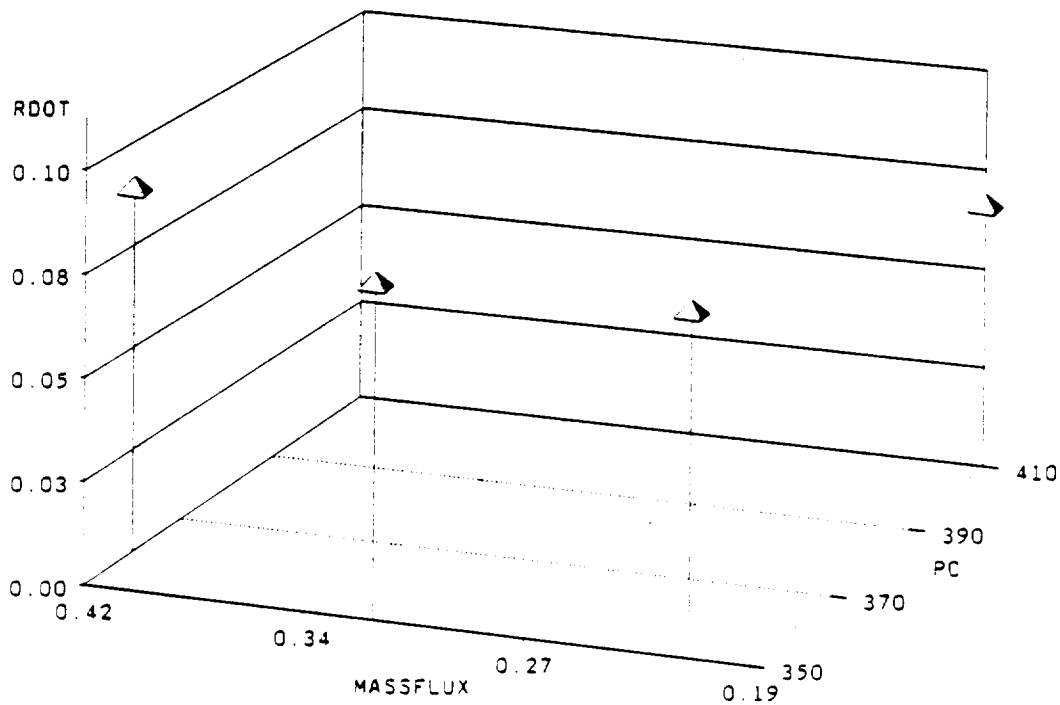
c. *HTPB (63%)/GAP (27%)/tungsten (10%) fuel with oxygen.*

Figure 24. Regression rate characteristics of metalized HTPB/GAP fuels--all exhibit high regression rates relative to HTPB alone with Al and Zn giving similar values (cont).

28
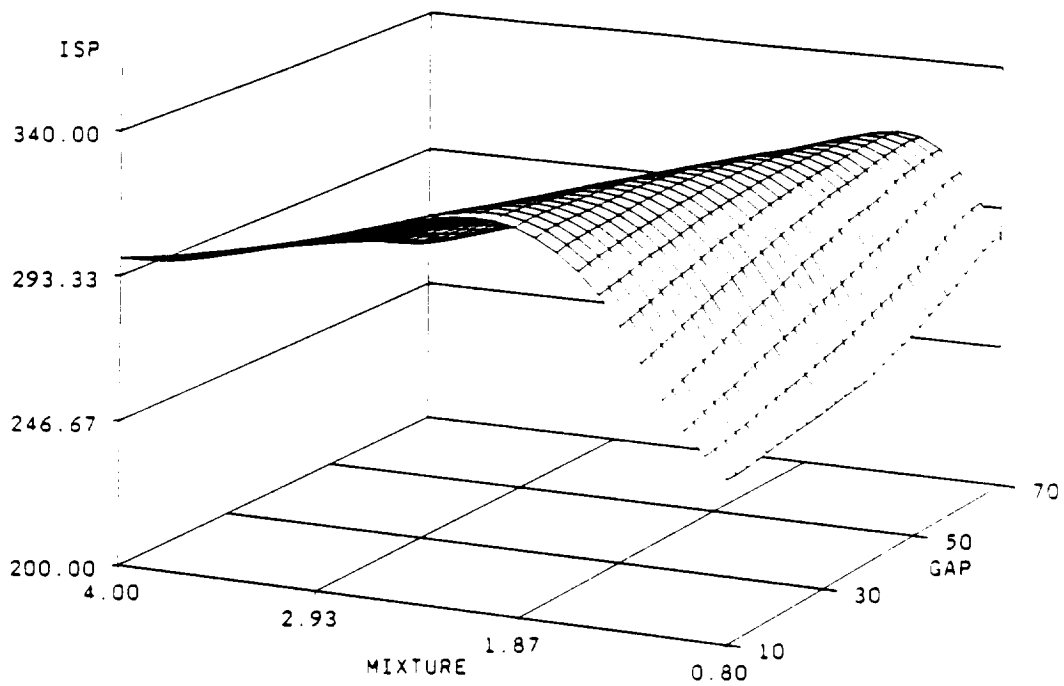
a. HTPB/GAP/LOX hybrid.
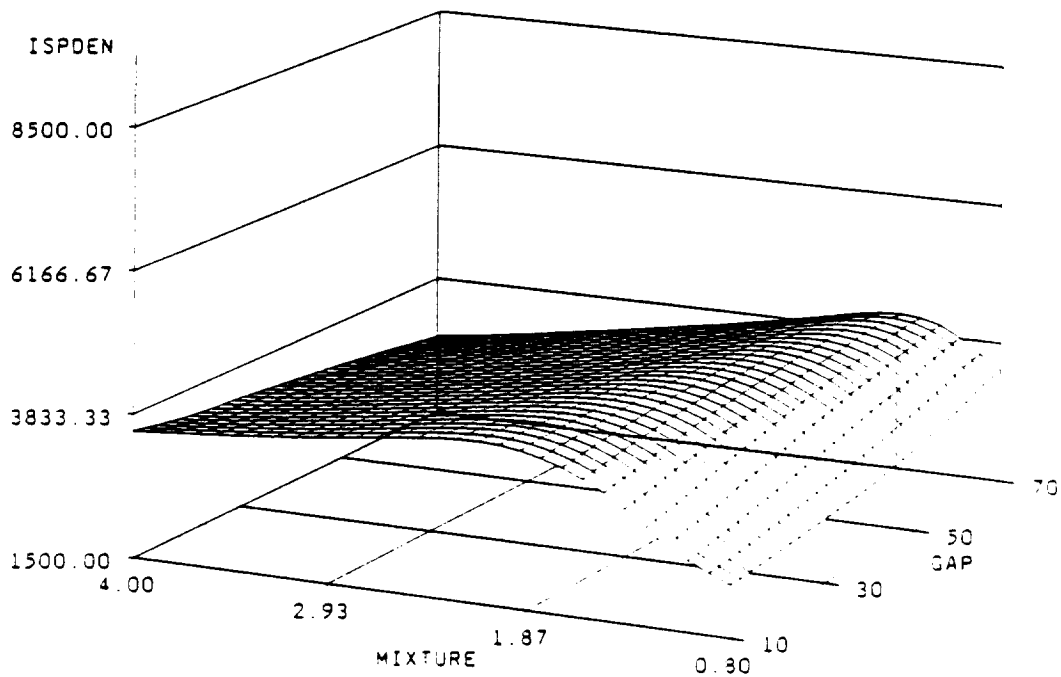
b. HTPB/GAP/LOX hybrid.

Figure 25. Effect of addition of GAP to HTPB on Vacuum I_{sp} (lbf·sec/lbm) and density I_{sp} at 1000 psi, 10:1 area ratio.
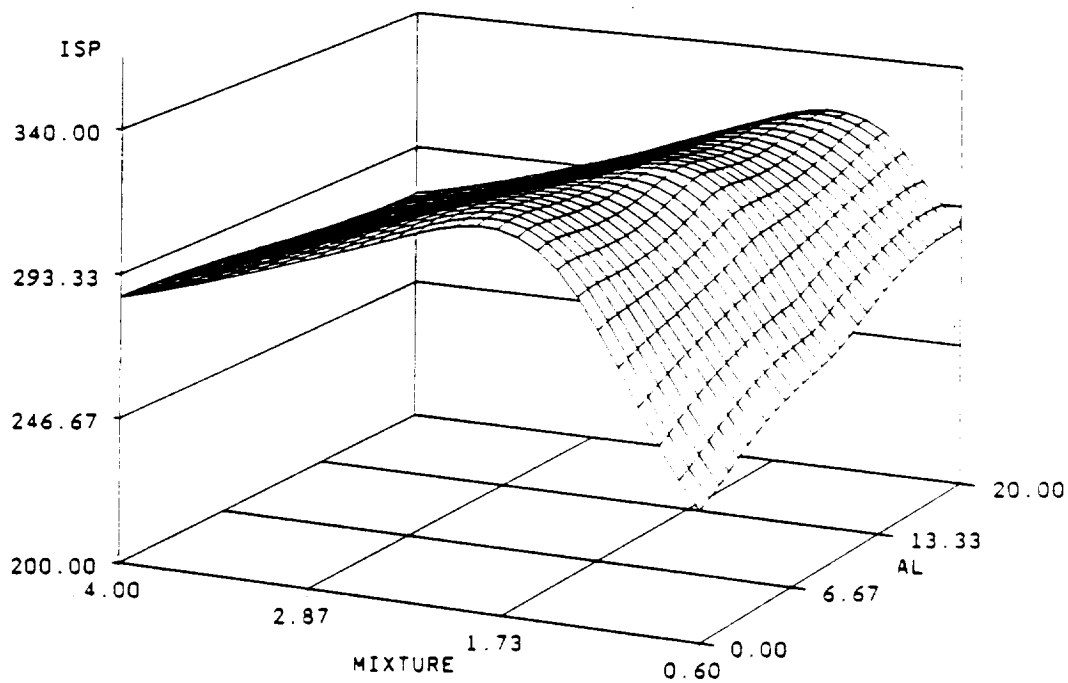
a. HTPB (70%)-GAP (30%)/Al/LOX hybrid.
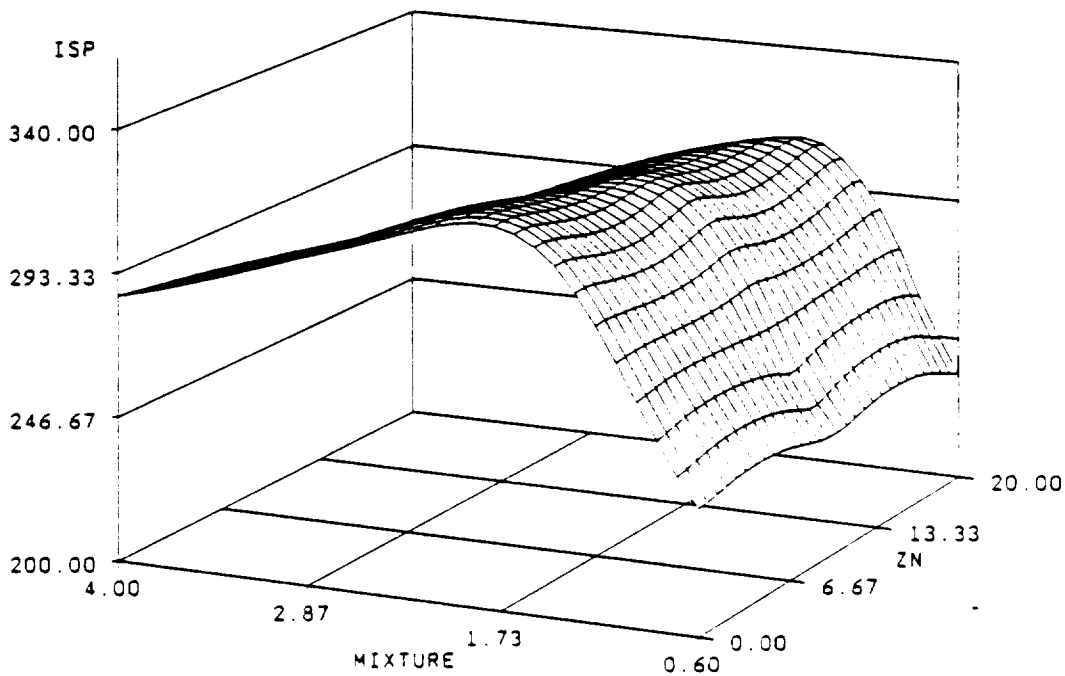
b. HTPB (70%)-GAP (30%)/Zn/LOX hybrid.

Figure 26. *Effect of metalization of GAP/HTPB fuel on vacuum* I_{sp} *(lbf·sec/lbm)* *and density* I_{sp} *at 1000 psi, 10:1 area ratio.*
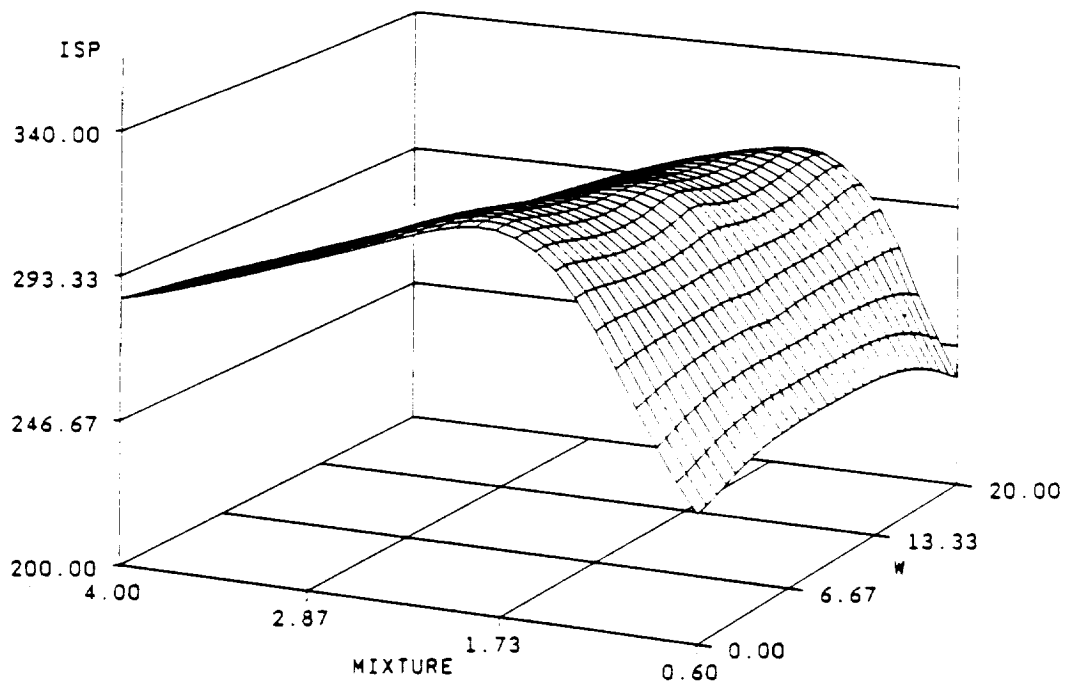
c. *HTPB (70%)-GAP (30%)/W/LOX hybrid.*
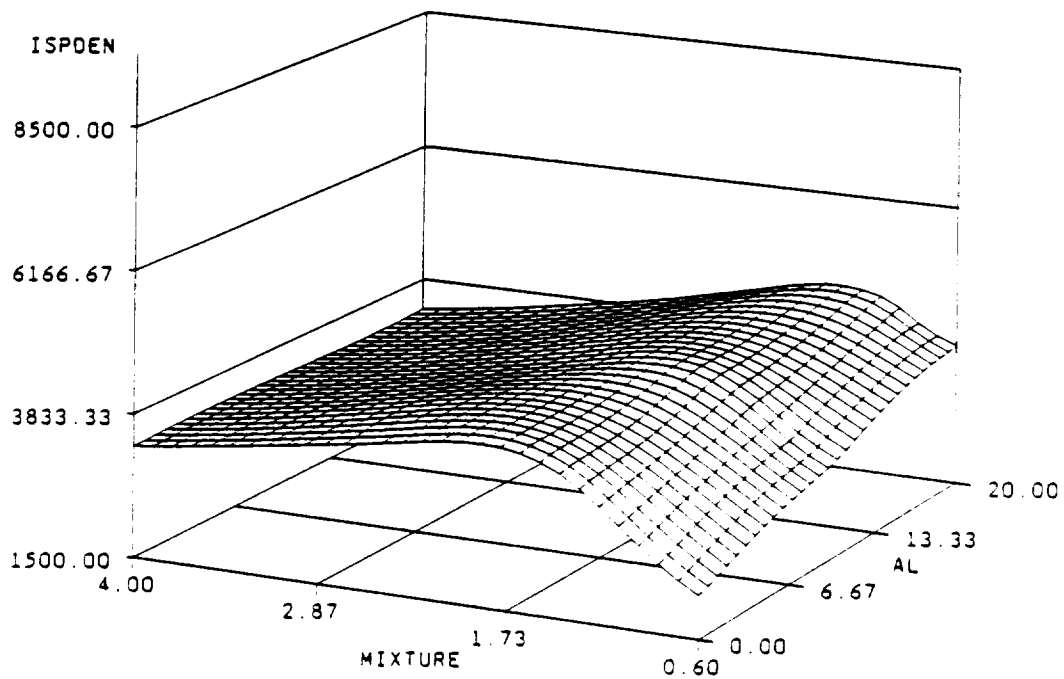
d. *HTPB (70%)-GAP (30%)/Al/LOX hybrid.*

Figure 26. Effect of metalization of GAP/HTPB fuel on vacuum I_{sp} (lbf·sec/lbm) and density I_{sp} at 1000 psi, 10:1 area ratio (cont).
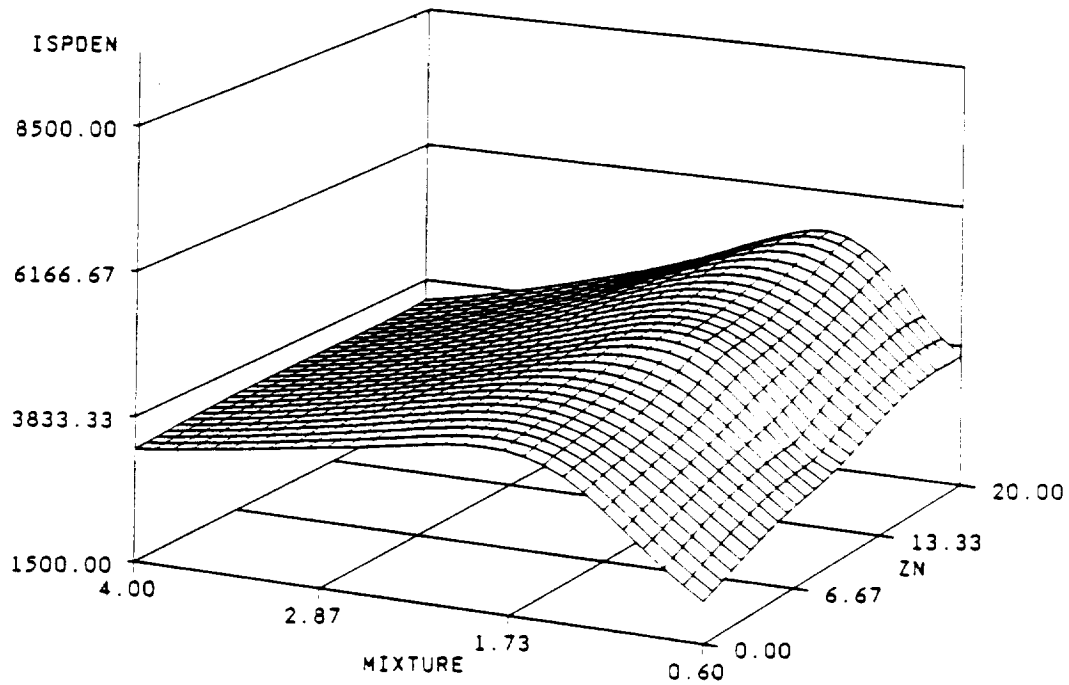
e. HTPB (70%)-GAP (30%)/Zn/LOX hybrid.
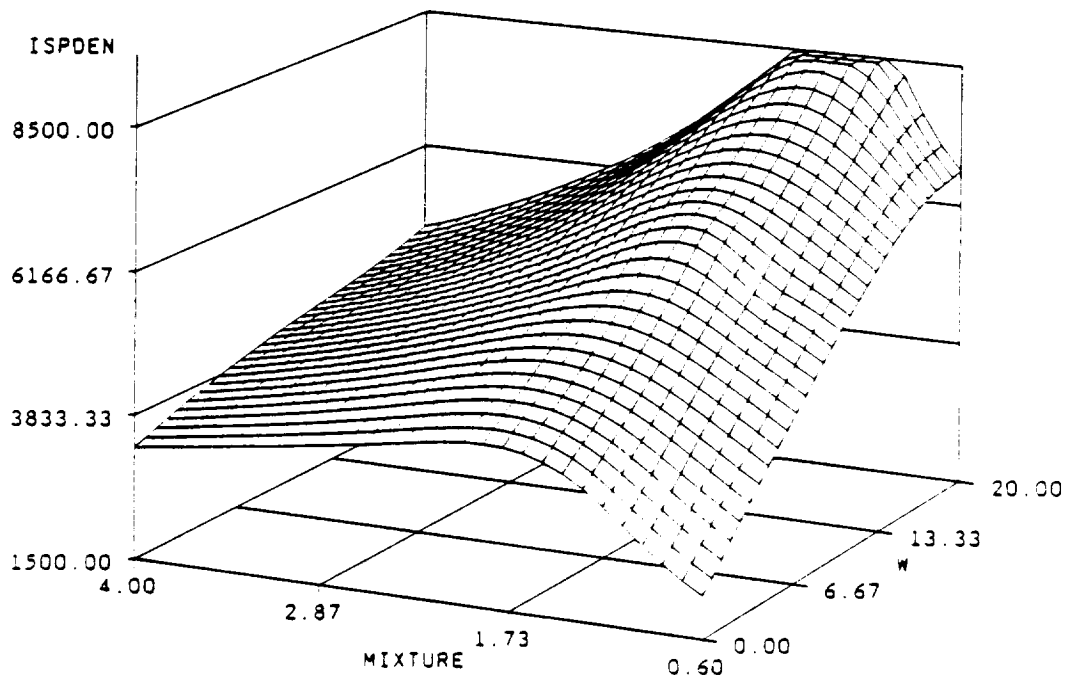
f. HTPB (70%)-GAP (30%)/W/LOX hybrid.

Figure 26. Effect of metalization of GAP/HTPB fuel on vacuum I_{sp} (lbf·sec/lbm) and density I_{sp} at 1000 psi, 10:1 area ratio (cont).
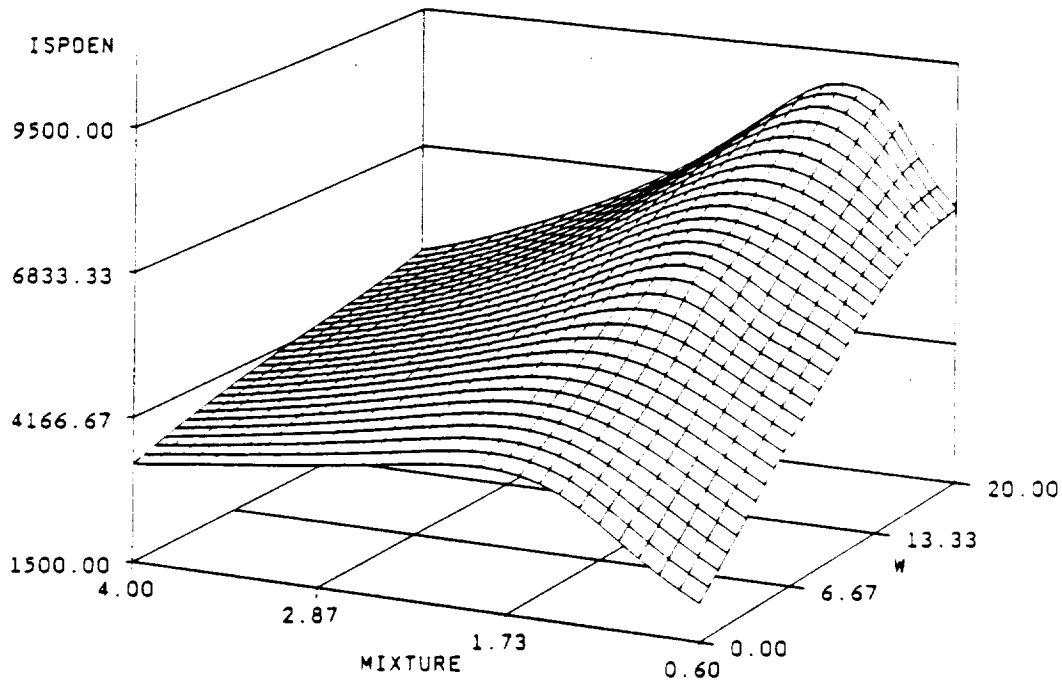
g. *HTPB (70%)-GAP (30%)/W/LOX hybrid.*

Figure 26. *Effect of metalization of GAP/HTPB fuel on vacuum I_{sp} (lbf·sec/lbm) and density I_{sp} at 1000 psi, 10:1 area ratio (cont).*

leads us to favor zinc metal as a candidate component in hybrid fuel formulations for classical system trade studies. A summary of the various candidates considered for fuel formulation trade studies is given in Table 5.

Table 5. *Fuel component trades.*

Material	Total Score	Performance (20)	Hazards (10)	Exhaust (20)	Cost (10)	Reliability (20)
HTPB	75	18	10	20	9	18
Polyethylene	66	19	10	20	7	10
Polyethers/esters	55	10	10	20	5	10
GAP	47	15	5	15	2	10

Material	Total Score	Performance (20)	Hazards (10)	Exhaust (20)	Cost (10)	Reliability (20)
AN	34	10	3	10	3	8
Metal Hydrides	36	15	5	10	1	5
AT	53	15	8	15	5	10
Al	60	15	8	15	7	15
Zn	66	18	8	15	10	15
W	56	20	8	10	3	15
Mg	54	12	7	15	5	15

• Overall best choices

  • HTPB/GAP/Zn—High density performance and high regression rates

  • HTPB/Zn—High density performance, low cost, and moderate regression rates

33

Gas Generator Formulations

As an alternate approach to the classical hybrid, the concept of a self-sustaining, fuel-rich propellant augmented by supplemental oxidizer injection was given consideration. Presumed advantages to this approach are primarily of a ballistic nature. Complications arising from classical hybrid combustion boundary layer combustion, low regression rate, aerodynamics of the combustion chamber, and changing combustion chamber volume would be circumvented by providing an aft-fixed volume combustion chamber into which supplemental oxidizer and fuel-rich generator exhaust are introduced for final combustion.

In performing the formulation trade studies for this approach, we limited consideration of solid oxidizer to nitrate salts, principally due to the previously discussed ground rule of no halides (i.e., perchlorates), due to environmental exhaust toxicity. Nitrates known to be high explosives, such as RDX, HMX, nitroglycerin, etc., were also not considered due to excessive hazards and critical diameter-driven detonation susceptibility known to occur with the use of such compounds. Consequently, AN becomes the primary candidate for gas generator compositions.

This material has been with the rocket propulsion industry since its infancy and has received renewed attention in the solid propellant arena as a potential clean solid oxidizer replacement for AP. As mentioned earlier, use of AN as a supplemental oxidizer in hybrid fuel grains has been explored both by Thiokol and others.

The theoretical performance potential of this approach is much more limited than that available from the classical approach. The I_{sp} versus mixture curves of several AN formulations are compared to HTPB with LOX augmentation in Figure 27. In this case,
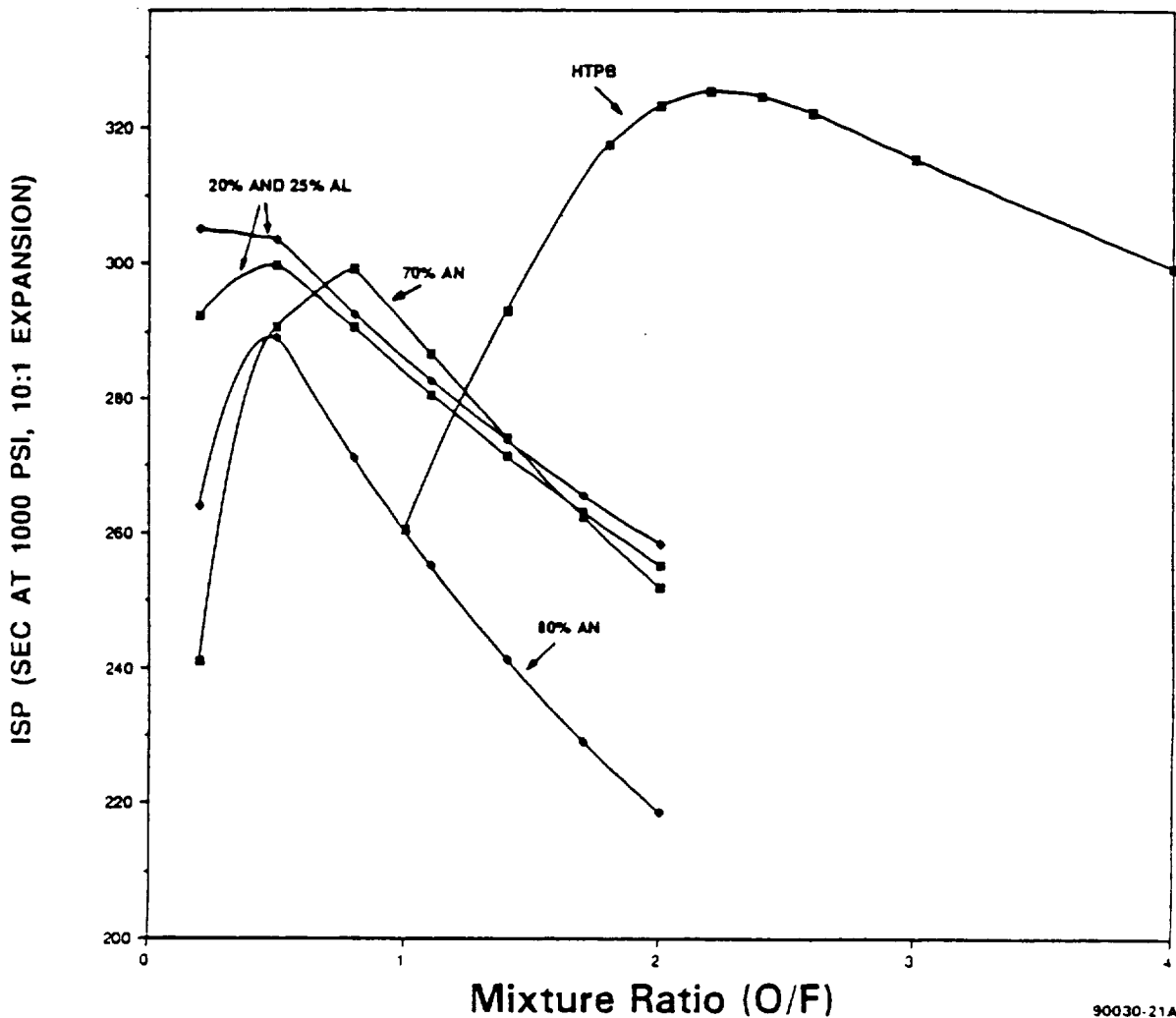
Figure 27. Comparison of vacuum I_{sp} (lbf·sec/lbm) of AN-based gas generator formulations with HTPB hybrid--generally, lower I_{sp} and O/F optimization is observed with gas generators.

34

metalization (with aluminum) improves I_{sp} performance as well as density but optimum mixture ratios are very low, typically less than 0.5. Additional energy growth options for the nitrate-based propellant, substituting the more energetic materials, hydrazine mononitrate (HN) or hydroxylamine nitrate (HAN) for AN, are shown in Figure 28 and suggest that some performance growth potential exists but involves the use of exotic and potentially explosive ingredients.

Unlike AP-based solid propellants, AN- (or HN, HAN) oxidized solid propellants tend to exhibit very low burning rates and extremely poor combustion efficiency in the presence of aluminum. This may be partially relieved by the use of magnesium metal as the fuel, but both density and I_{sp} are adversely affected (Figure 29). Based on the data presented in Table 6 for the ballistic behavior of several AN-based propellant

formulations, it is apparent that little is to be gained in ballistic performance by employing a clean gas generator propellant as the basis of a hybrid motor, over some of the previously discussed classical options.

The data of Table 6 do suggest that burning rates may be enhanced by binder changes, with rates up to 0.2 ips being attainable with GAP. Unfortunately, this results in a substantial energy loss in the hybrid system performance (Figure 30). In spite of improved ballistic response with the more energetic materials, gross amounts of slag are produced with the aluminized formulations, implying combustion efficiency must be improved. Consequently, it is likely that any application of aluminized AN gas generator propellants to the hybrid concept will need to incorporate supplemental oxidizer injection into the solid propellant bore.
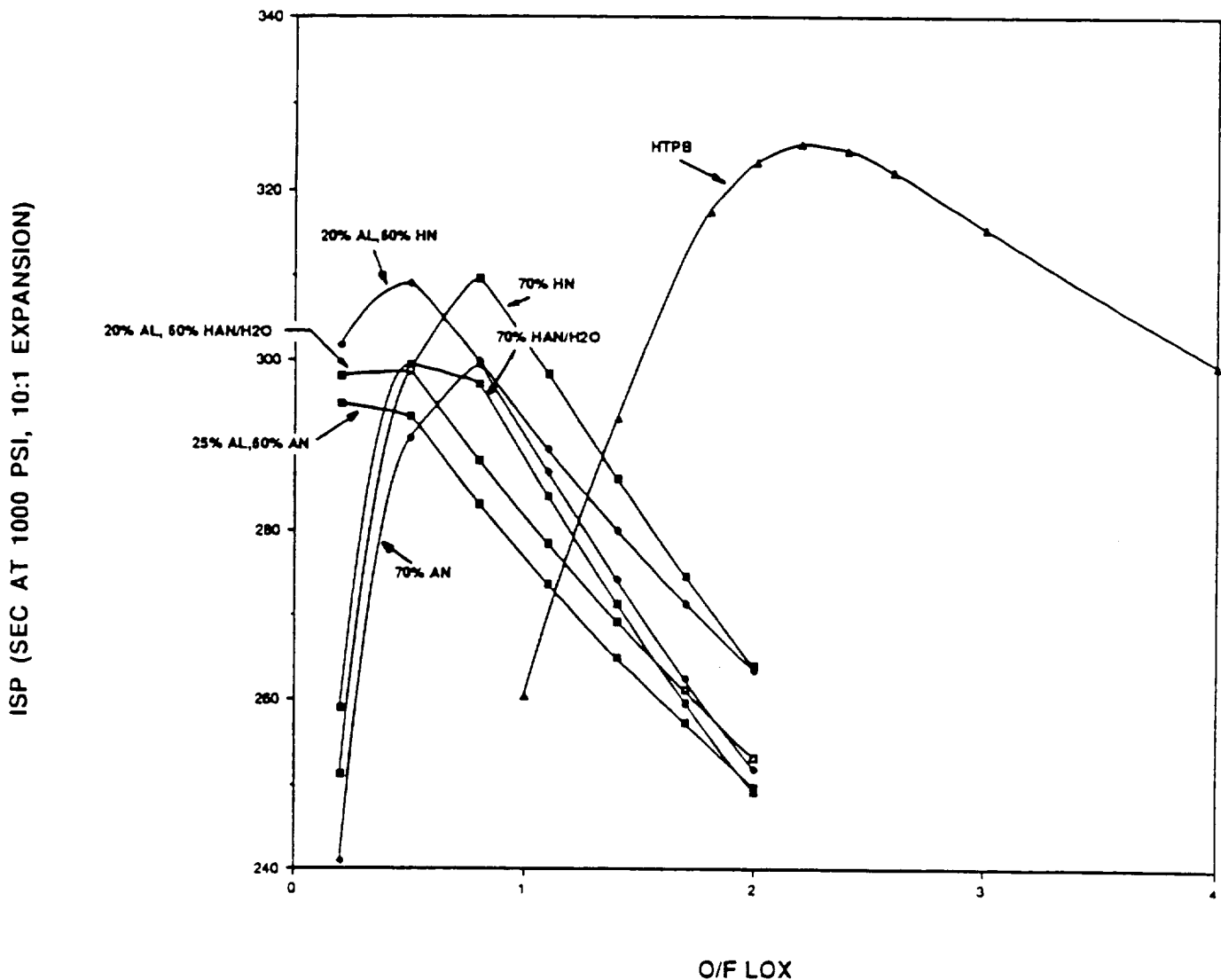
Figure 28. Theoretical performance comparison of energetic nitrate-based gas generator propellants with AN gas generants and HTPB classical hybrid.

35
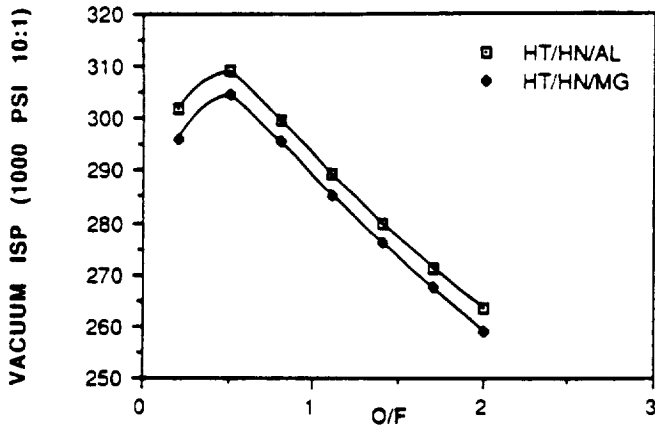
Figure 29. Comparison of HN-based gas generator hybrid compositions with I_{sp} (lbf · sec/lbm)--substitution of Mg for Al results in a 5-sec I_{sp}/loss.

Table 6. Ballistic properties of AN propellants.

Composition	R_b at 1000 psi (ips)	Pressure Exponent
HTPB/64%/AN/21% Al	No ignition	—
HTPB/60% AN/25% Mg	0.08 to 0.12	0.23 to 0.07
HTPB/62.2% AN/11.4% Mg 11.4% Al	0.10	0.20
PPG/55% AN/30% Mg	0.14	0.36
PPG/60% AN/25% Al	No ignition	—
GAP/52.5 AN/31.5 Mg	0.26	0.36
GAP/57% AN/27% Mg	0.17	0.96
GAP/55% AN/14.5% Mg 14.5% Al	0.21	0.44

90209-1.2
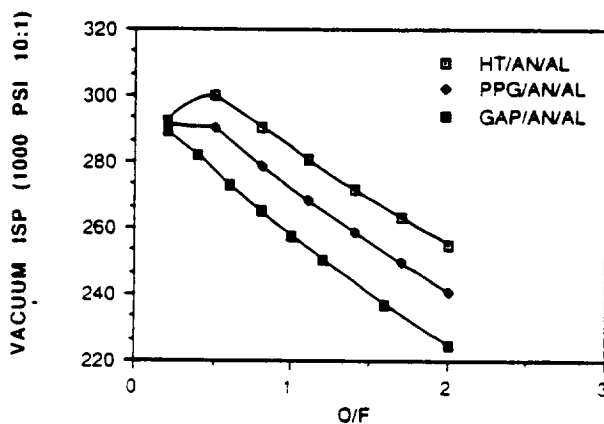
Figure 30. Vacuum I_{sp} (lbf · sec/lbm) comparison of propellants (80 percent solids) showing loss of I_{sp} relative to HTPB--the opposite trend occurs in the absence of supplemental oxygen.

Probably the greatest objection to the gas generator solid propellant hybrid approach relative to the classical configuration lies in the fact that the tremendous cost and reliability advantages of the inert fuel grain in the classical system are lost with the gas generator approach. Although raw material cost differences are minor, the expenses associated with producing and handling a live propellant, particularly on the scale of a large booster, are astronomical compared to processing completely inert components. This is further aggravated when it is considered that, in the case of the live propellant, reliability issues associated with grain flaws, bondline integrity, environmental storage, etc., become very important, whereas, with the inert fuel classical hybrids (outside of gross flaws, grain cracks, deformities, etc.) have very little influence on motor operation and reliability.[2] Thus, sacrificing substantial life cycle cost advantages, performance, and safety of the inert fuel classical hybrid for questionable ballistic gains with the solid propellant gas generator approach is not recommended.

The regression rate advancement of inert fuel grain/oxygen classical hybrids demonstrated by the use of GAP as a fuel additive has effectively advanced the ballistic potential of the classical hybrid to that available in clean gas generator propellants. Consequently, the full potential of the performance, safety, and cost advantages of the classical hybrid system may actually be realized, and thus represents our recommended approach for further development. Trade studies between these two concepts reflecting relative rankings are summarized in Table 7.

3.2 IGNITION

Hypergolic ignition systems have typically been utilized for hybrid motors. Ignition of a hybrid motor is different from a solid or liquid motor in that ignition timing and the ignition transient are a function of fuel volatility and initial oxidizer flow rate, respectively. Providing enough initial heat to the fuel grain in the presence of an oxidizer promotes ignition in a hybrid. This has the potential for greatly simplifying hardware requirements for motor ignition.

3.2.1 OBJECTIVE. The overall objective is to identify the most cost-effective, reliable ignition system for hybrid applications.

3.2.2 CONCLUSIONS. A hypergolic ignition system is the best off-the-shelf ignition system for hybrid applications. However, this system contains toxic and hazardous materials. Other simpler, more cost-effective techniques for heating the hybrid grain and providing motor ignition need further development and evaluation through testing.

3.2.3 DISCUSSION. Ignition concepts considered (Figure 31) fall into four basic categories: chemical,

36

Table 7. Ballistic performance comparison.

	Classical (HTPB/GAP/Zn/LOX)		Gas Generator (HTPB/AN/Al/LOX)	
Performance (20)	15	Moderate I_{sp} High density Improved ballistics	10	Low I_{sp} Moderate density baseline ballistics
Cost (10)	7	GAP is expensive	2	Inexpensive raw materials. Live processing
Hazards (10)	7	GAP is Class B explosive	2	Live propellant
Exhaust (20)	18	Inert fuel advantages	10	Potential for NOx very high
Reliability (20)	18	Inert fuel advantages	10	Live grain disadvantages. Sensitive to grain flaws. Design limits stricter
Total	62		34	

90030-21C
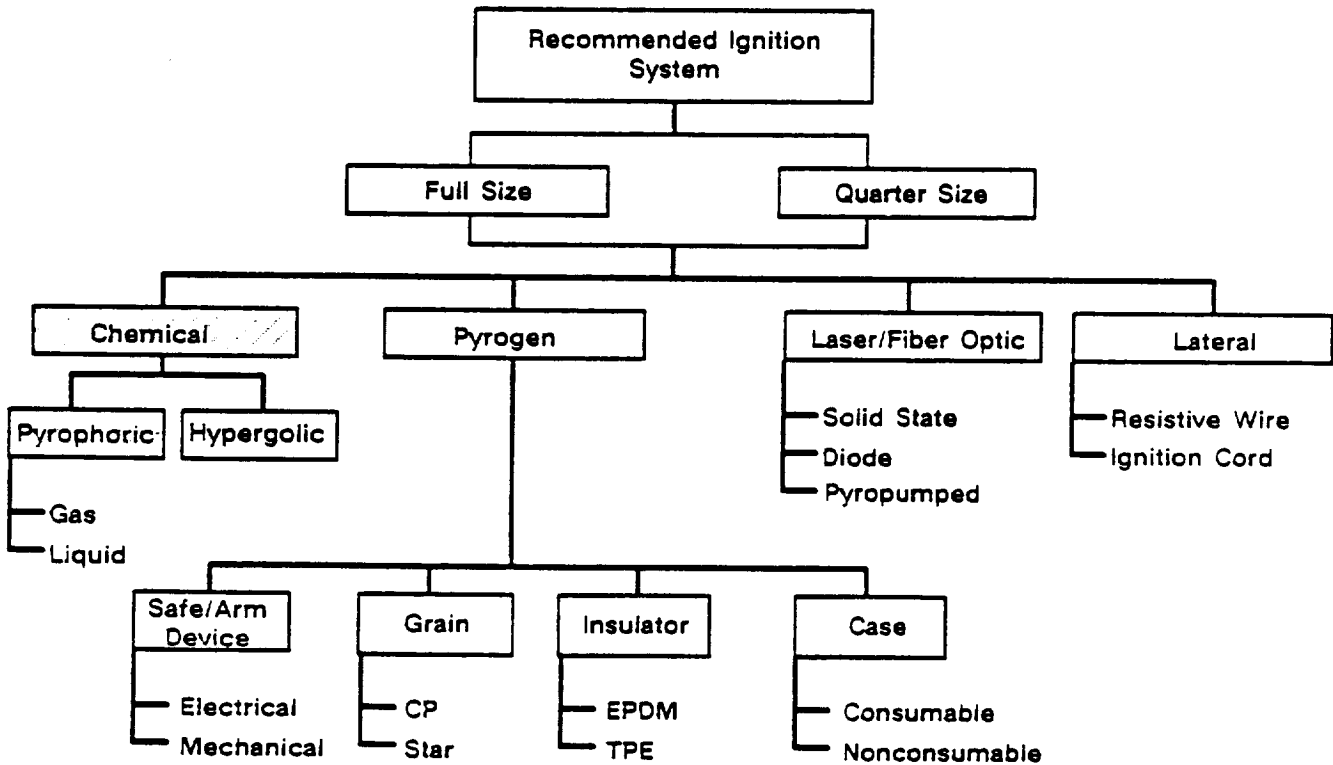
Figure 31. Igniter trade tree.

37

pyrogen, laser/fiber optic, and lateral. Each of these candidate approaches has advantages and disadvantages relative to the evaluation criteria. Chemical- and pyrogen-type igniters are well proven approaches using mature technology. Grain heating approaches offer significant cost and safety benefits but the technology required is undeveloped. Reliability of these advanced approaches is uncertain. Evaluation of these concepts is summarized in Tables 8 and 9.

3.3 COMBUSTION STABILITY

Pressure oscillations are inherent to typical hybrid systems. Nonacoustic pressure oscillations are associated with injection of high mass fluxes of liquid oxidizer and fuels that are combustible with a melt layer or formation of metal oxide. Because the oscillations are nonacoustic, i.e., totally random, the potential for catastrophic failure resulting from hybrid stability is virtually nonexistent.

Table 8. HPT system analysis and trade studies —ignition system concept ranking explanation.

| Criteria | Concept | | | |
	Chemical	Pyrogen	Laser/Fiber Optic	Lateral
Flight Safety	Complex; carried for some portion of flight	Complex; carried for some portion of flight	Simple; consumable	Simple; unknown effects
Reliability	Demonstration-level maturity	Proven SRB system	Research-level maturity	Immature
Nonrecurring Life Cycle Costs	No S/A[1]; partial development program costs	S/A required; demonstration program costs	S/A required; partial development program costs	S/A required; full development program costs
Recurring Life Cycle Costs	No S/A, squibs, or igniter initiator; less complex	Complex	Few components; simple	Few components; simple
Performance, Mass, and Energy Transfer	Mature science; requires hybrid development	Reproducible and predictable mass flow; proven SRB	Mature research; requires hybrid development	Immature; requires hybrid development
Launch Site Considerations	Inert when separate	Proven; complex	Inert; insensitive to electric fields	Electric field sensitivity; unproven

[1]Safe/arm or safe/arm/fire device

Table 9. Ignition concepts ranking.

| Criteria | (Rating Factor) | Concept | | | | | | | |
| | | Chemical | | Pyrogen | | Laser/Fiber Optic | | Lateral | |
		Score[1]	Weighted Score	Score[1]	Weighted Score	Score[1]	Weighted Score	Score[1]	Weighted Score
Flight Safety and Reliability									
Flight Safety	(0.20)	85	17	85	17	90	18	60	12
Reliability	(0.20)	80	16	85	17	75	15	50	10
Life Cycle Costs									
Nonrecurring	(0.15)	90	13.5	80	12	70	10.5	90	13.5
Recurring	(0.150)	75	11.25	60	9	80	12	90	13.5
Performance		100	20	100	20	100	20	100	20
Operational Considerations									
Launch Site	(0.10)	90	9	85	8.5	95	9.5	95	9.5
Total		86.75		83.5		85		78.5	
Rank		1		3		2		4	

[1]Scored from 0 to 100, where 100 is the best

The fundamental causes of hybrid instability are summarized as follows:

- Coupling of liquid droplet vaporization and heat transfer to grain surface results in nonacoustic instability, eliminated by a high degree of droplet atomization
- Shedding and combustion of molten metal droplets or liquid phase fuel
- Pressure coupling of combustion process in pressure/flux coupled regimes

Each of these causes can be addressed through appropriate design practices.

3.3.1 OBJECTIVE. The objectives of the combustion stability analysis were to evaluate the potential for pressure oscillations in all three proposed hybrid configurations and to identify design approaches to minimize the potential for combustion instabilities.

3.3.2 CONCLUSIONS. The classical and afterburner hybrid concepts offer the least potential for pressure oscillations because of the nonexistent or relative small dependence of burn rate on pressure. Pressure oscillations in the classical and afterburner design can be minimized by incorporating the following design features:

- Vaporized oxidizer
- Metalized fuel
- Low pressure/large throat
- Fuels that vaporize directly to gas phase
- Pressure–insensitive fuels

3.3.3 DISCUSSION. To date, there is no industry standard combustion stability model for predicting hybrid stability which is analogous to existing liquid or solid propellant rocket models. Consequently, complete combustion stability predictions are currently not possible for hybrid rocket motor designs. However, there are a number of wave–damping mechanisms that are valid for both solid and hybrid rocket motors, including nozzle damping and particle damping.

Nozzle damping is a fairly complex phenomenon that is related to the gas dynamics of the flowfield in the vicinity of the nozzle throat. As the combustion gases approach the nozzle throat, strong gradients in the density of the gas make the nozzle throat reflective to oscillations generated in the combustion cavity. Nozzle damping is also a function of nozzle throat size. If the throat is large, there is more nozzle damping than in a small throat. These principles will hold for hybrid motor designs, and various hybrid configurations can be successfully analyzed for nozzle damping. The design objective is to maximize the amount of nozzle damping to minimize pressure oscillations.

Another important solid rocket damping mechanism that is applicable to hybrid rockets is particle damping. Particle damping can be a very significant energy sink in SRMs and hybrid motors. This type of damping is most significant in SRMs at higher frequencies with propellants that produce smoke. Any metalized propellant will produce significant amounts of smoke as they burn. The smoke consists of small particles of oxidized metal which absorb large amounts of energy as they are vibrated by the pressure waves in the combustion chamber. The more particles or smoke, the more damping. This implies that hybrid formulations using significant amounts of metal (aluminum, magnesium, etc.) will provide extra margins for stable combustion.

Historically, hybrids have demonstrated strong coupling between chamber and oxidizer droplets, resulting in large amplitude pressure oscillations, particularly with high mass fluxes of liquid oxidizer. Instabilities of this type have been solved by a high degree of droplet atomization or by bringing the oxidizer into the chamber in vapor phase. An example of the effect of atomization or vaporization of the oxidizer is illustrated in Figure 32. Liquid oxidizer was temporarily replaced with gasified oxidizer. A marked reduction in pressure oscillations was observed. Smaller amplitude oscillations have been observed with fuels that form a melt layer on the grain surface. Periodic shedding of this layer with rapid combustion results in periodic increases of heat release into the combustion chamber, producing rough burning of the fuel activity.

Pressure coupling is a common source of acoustic energy in an SRM, and arises as a result of the pressure–dependent burning rate of solid propellant. The burning rate of most hybrid fuels is dependent on mass flux, not pressure. In these cases, pressure coupling will not be a factor in hybrid motor instability. Some of the hybrid formulations are slightly pressure-sensitive. Some form of pressure coupling could contribute to pressure oscillations in these cases, though there is existing no methodology to predict the magnitude or importance of the effect with these formulations.

3.4 THRUST VECTOR CONTROL

TVC for hybrid booster applications was determined by evaluating and ranking state–of–the–art TVC systems using reliability, cost, and performance criteria. Both fixed and movable nozzles were evaluated as shown in Figure 33. Within each class of TVC system, only those systems offering the greatest potential for payoff were evaluated. Developmental, or high risk systems were not evaluated; their reliability was assumed to be inferior. Primary TVC concepts are illustrated in Figures 34 and 35.

Temporary Gas Flow

P_C AV = 402 psig

Injector ΔP

Time (sec)

CSA024097a
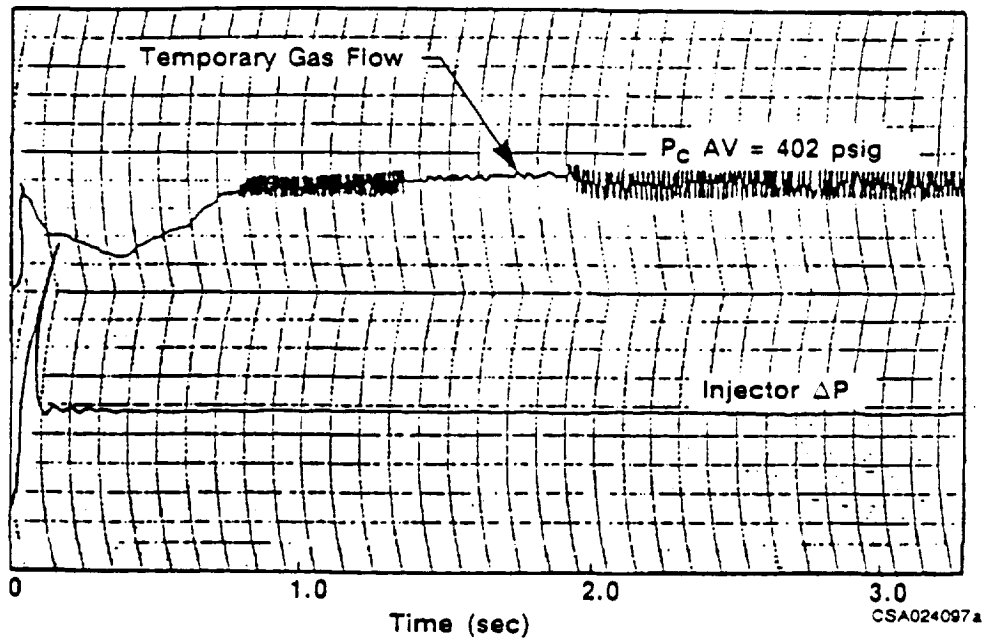
*FLOX/lithium/hydrocarbon binder fuel—"Investigation of Fundamental
Phenomena in Hybrid Propulsion," final report, Bureau of Naval
Weapons Contract NOW64-0659C

Figure 32. *Example of liquid phase oxidizer instability.*

TVC Systems

TVC Systems

TVC Systems

— Secondary Injection (1)
— Jet Vanes (1)
— Jet Tabs (1)
— Jet Probe
— Movable Plug

— Hot Ball and Socket
— Gimbal (1)
— Flexible Exit
— Thiovec (2)
— Techroll (1,3)
— Trapped Ball (1,3)
— Flexseal (1)

1 Primary Concepts
2 Trademark of Thiokol Corp.
3 Trademark of United Technology Corp.
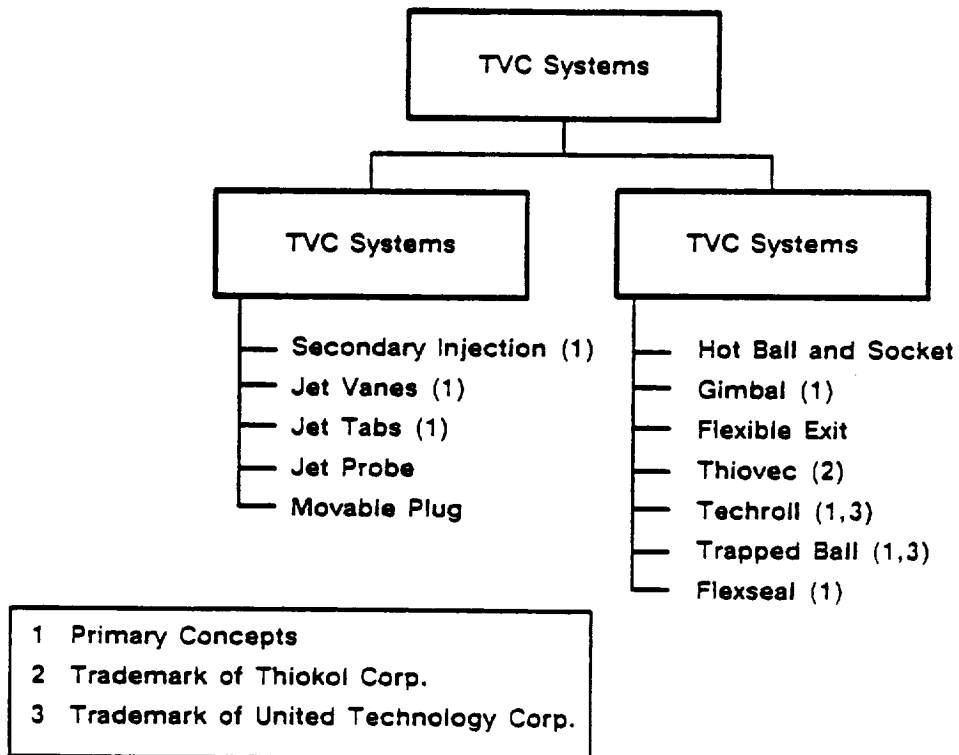
Figure 33. *Thrust vector control trade tree.*

Exit Cone

Fluid Tank ——► ⬤ Injection Valve

Secondary Injection

Exit Cone
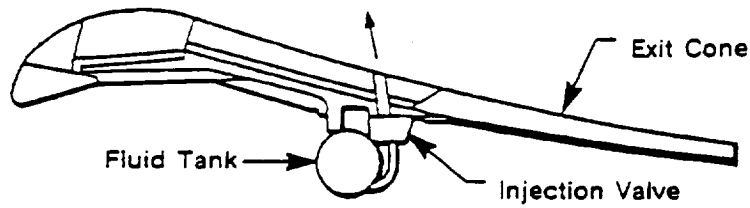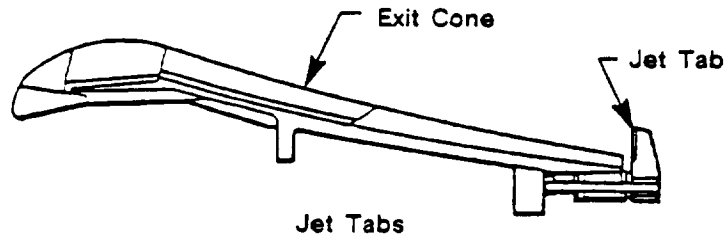
Jet Tab

Jet Tabs

CSA024096a

Figure 34. Primary TVC concepts—fixed nozzle.

Fixed Structure
Supersonic Splitline
Movable Nozzle

Forward
End Ring
Elastomer

Gimbal

Pivot-Point
Aft End Ring
Movable Nozzle
Fixed Structure
Ablative Protection
Reinforcement

Flexseal

Pivot-Point

Fabric Reinforced
Neoprene
Bladder

Movable Nozzle

Silicone Rubber Boot
Silicone Fluid
Fixed Structure

Techroll

Movable Nozzle

Teflon®
Fabric Seat

Antiroll
Pin

Storage Preload Ring
Fixed Structure
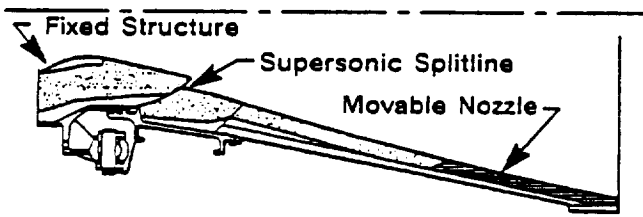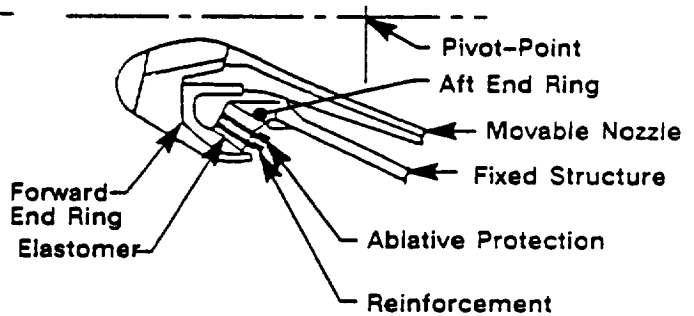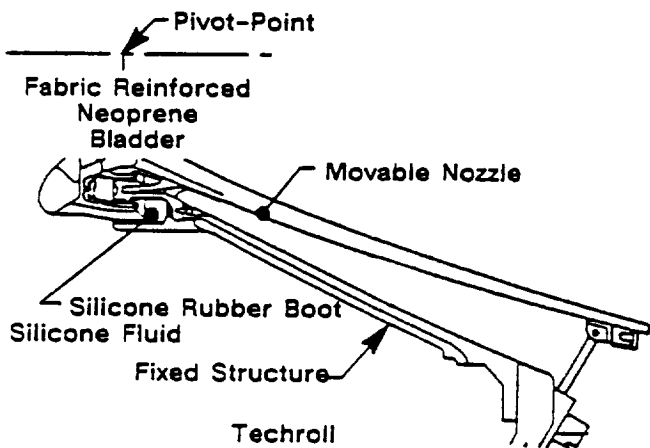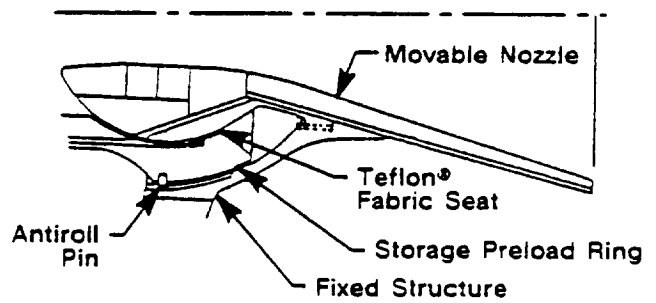
Trapped Ball

CSA024089a

Figure 35. Primary TVC concepts—movable nozzle.

41

Several key assumptions were required to narrow the field of candidate TVC systems. First, the trade study was limited to SRM technology. Movable combustion chambers with liquid cooled nozzles or throats, typical of liquid rocket engines, were considered more costly and raised many questions of reliability. Second, existing data from existing nozzle systems were considered applicable. Third, reliability would be assessed based on demonstrated flightworthiness, and fourth, TVC system selection was not considered an enabling hybrid technology and the trade study was performed independently of booster concept selection.

3.4.1 OBJECTIVES. The overall objective was to determine the optimum TVC concept for hybrid applications.

3.4.2 CONCLUSIONS. Flexseal® and trapped-ball TVC concepts are viable for hybrid applications. They offer the greatest reliability, cost advantage, and performance for solid and hybrid rocket motors. The Flexseal was selected in the final evaluation because of a small advantage in demonstrated reliability for large booster applications.

3.4.3 DISCUSSION. In identifying the optimum TVC candidate for hybrid rocket motors, the advantages and disadvantages of eight major types of TVC we.e considered. These types are:

TVC

Secondary injection

Jet tabs

Jet vanes

Trapped ball, insulated

Flex bearing, insulated

Gimballed nozzle (supersonic splitline)

Techroll

For performance considerations, these TVC systems were compared for their effects upon weight, thrust losses, TVC capability, and packaging constraints.

The vector angle capability for each of these systems is illustrated in Figure 36. All systems except for secondary injection have demonstrated vector angle capability in excess of seven degrees, which is more than adequate for large booster applications. Shuttle booster nozzle has 6.0 degrees of omniaxial capability. Limited capability of secondary injection makes it an unattractive candidate.

As illustrated in Figure 37, axial thrust losses resulting from TVC can be significant. Jet tabs and jet vanes disrupt the flow in the nozzle exit cone or at the exit plane, and therefore cause the largest thrust loss. The gimballed nozzle, with a supersonic splitline, also

disrupts flow in the nozzle and causes significant thrust losses at high TVC angles. Movable nozzles, such as Flexseal, trapped ball, and techroll, minimize thrust loss. Flow is directed without being disrupted to achieve the necessary TVC. A movable nozzle concept is preferred.

The advantages and disadvantages of the candidate TVC systems are summarized in Table 10. Primary applications and relative costs are also identified.

Numerical ranking of concepts is illustrated in Table 11. Using the weighting factors established for the program, the Flexseal is the optimum TVC concept for hybrid applications.

3.5 MOTOR PERFORMANCE

General Dynamics evaluated input from individual trade studies to identify the optimum booster concept. They made the overall determination based on flight safety, reliability, cost, and performance. Thiokol provided performance trade study input. The performance trade studies revealed the best performing designs, provided insight on hybrid operation, and uncovered technology areas needing advancement. Booster-level performance trade studies were conducted on grain design, fuel formulation, hybrid size, quarter-sized diameter, full-sized length, tank material, oxidizer feed system, and hybrid type.

3.5.1 OBJECTIVE. The overall objective of the performance trade studies was to optimize each booster concept and to provide a quantitative performance comparison between potential concepts.

3.5.2 CONCLUSIONS. Each potential hybrid concept was studied analytically. The key conclusion from the performance trade studies is that the pump-fed, afterburner hybrid propulsion concept offers the greatest performance for both quarter- and full-scale booster applications.

Other salient results from the performance trade studies are summarized as follows:

1. The pump-fed system offered the greatest performance increase. For the full-sized booster, the pump-fed system allowed an additional 18,700 lb of payload over the baseline pressure-fed design.

2. Lightweight graphite epoxy oxidizer tanks provided the second best performance gain. Lightweight tanks increased payload by 12,350 lb over the baseline aluminum tank design.

3. Although afterburner designs perform better, if the fuel regression rate is sufficiently tailorable, classical concepts can be designed with equal performance to afterburning concepts.

4. HTPB/Zn/GAP was identified as the best performing fuel. The high regression rate and high density of this
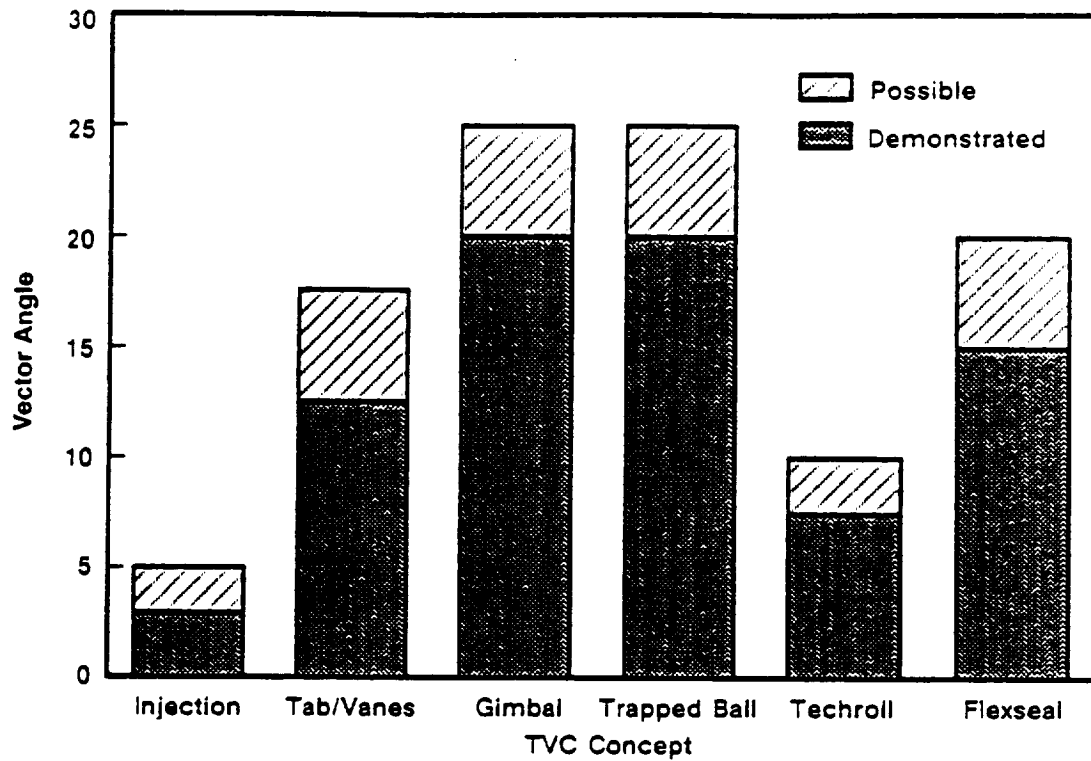
Figure 36. Vector angle capability.
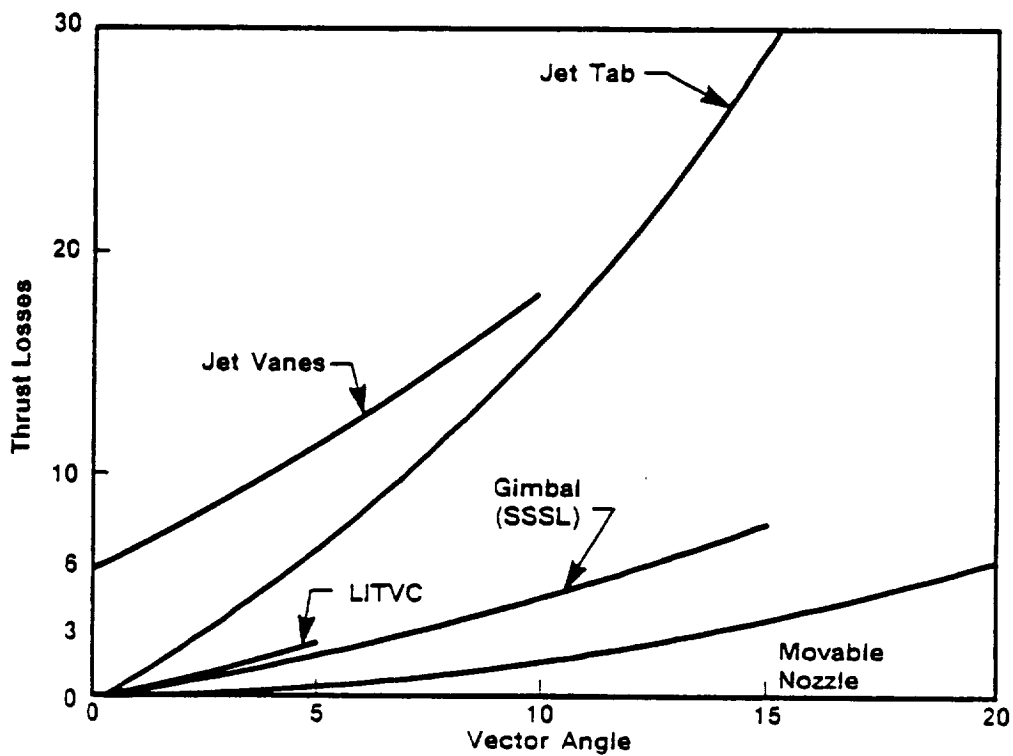
Figure 37. Percent axial thrust loss.

CSA024098a

Table 10. Advantages/disadvantages primary TVC systems.

System	Advantage	Disadvantage	Applications	Relative Cost
• Jet Tab/Jet Vane	• Actuation torques are low • Small installation envelope around nozzle • Power requirements are low, and thus actuator weights are low • Fast response capability	• Restricted to motors with low temperature propellant or short burn time • Caused significant local erosion in the nozzle • Large thrust loss (equal to generated side force) • Increase envelope requirements	• Sergeant, Talos, Pershing	6
• Secondary Injection • Liquid Injection	• State-of-the art • Liquid injection thrust adds to motor thrust • Little prelaunch checkout required • Fast response capability	• Limited thrust deflection • System weight is high • Careful attention must be given to selection of liquid and bladder material for long-term storage • A long hold period after the system is energized requires replenishment of the liquid and pressurization devices • Lack of flexibility for accommodation of changes in control requirements • Must be designed for worst-on-worst requirements	• Polaris A3, Minuteman III, demo motors	10
• Gaseous Injection	• Little prelaunch check-out required • Fast response capability • Lighter in weight than liquid injection systems	• Should be limited to applications with required thrust deflection angles less than 7 deg • Cannot be used where precise velocity control is required • Hot-gas valve is subjected to severe thermal environment • Warm-gas valve requires large and heavy gas generators • Additional propellant necessary to recover thrust losses • No production experience	• Demonstration	8

90209 2B

44

Table 10. Advantages/disadvantages primary TVC systems (cont).

- Ginbal

System	Advantage	Disadvantage	Applications	Relative Cost
• External	• Flexible duty cycle • Negligible thrust loss • Low torque • Low-to-medium blowout load • Low entry erosion	• High erosion and heat flux in splitline • Inflexible pivot-point locations	• Minuteman I, • Minuteman II, • Minuteman III. • Quickturn	5
• Submerged	• Minimum splitline erosion and heat flux • Minimum seal problem • Continuity of entry, throat, and exit cone • Flexible duty cycle • Negligible thrust loss • Large deflection capability • Long burn time durability • Low torque	• High blowout load • Large volume required within chamber • Medium entry erosion • Inflexible pivot-point location • Potentially large vectoring envelopes	• Demonstration motors	5
• Supersonic Splitline	• Attractive for submerged nozzle • Low entry erosion • Lightweight potential • Fast response capability • Low blowout load • Small deflection envelope	• Sealing and erosion problems at splitline • High actuation torque • Limited to small vector angles	• Demonstration motors	5
• Trapped Ball	• Potentially lightweight • Small envelope requirement • Large deflection capability • Flexible pivot-point location • Deflection of the seal region is minimized and seal gap is maintained by uniformly distributed load	• High friction torque • Potential sealing problem • Antirotation device required	• Tomahawk, Demonstration motors, Agile	3

90209 2C

Table 10. Advantages/disadvantages primary TVC systems (cont).

System	Advantage	Disadvantage	Applications	Relative Cost
• Flex Seal	• State-of-the-art • Flexible duty cycle • No splitlines • Large deflection capability • Flexible pivot-point location • Negligible thrust loss • Minimum seal problem • Can be used for deeply submerged nozzle • Fast response capability • Lightweight	• Joint requires thermal protection • Joint requires protection of elastomer during storage • Only small tension loads can be applied to joint • Joint pivot-point is floating, dependent on motor pressure and vector angle • Nozzle aligned only at one design pressure and misaligned at all other pressures • High torque at low temperature	• C3,C4,D5, SICBM, PK, SRM, Pershing II	4
• Techroll	• Low torque • Large deflection capability • Negligible thrust loss • Submerged nozzle • State-of-the-art	• Joint requires thermal protection • Potential fluid leakage • Fabrication difficulties (Kevlar®/Elastomer separation) • Nozzle alignment	• IUS	5

90209 2D

46

Table 11. Ranking of TVC concepts.

Concept / Criteria	Secondary Injection		Jet Tabs/Vanes		Trapped Ball		Gimbal		Techroll		Flexseal	
	Score	Weight	Score	Weight	Score	Weight	Score	Weight	Score	Weight	Score	Weight
Flight Safety (0.20)	90.0	18.0	90.0	18.0	90.0	18.0	95.0	19.0	90.0	18.0	100.0	20.0
Reliability (0.20)	90.0	18.0	90.0	18.0	90.0	18.0	95.0	19.0	90.0	18.0	100.0	20.0
Cost (0.30)	10.0	3.0	40.0	12.0	70.0	21.0	50.0	15.0	50.0	15.0	60.0	18.0
Thrust Loss Due to Vectoring (0.10)	95.0	9.5	85.0	8.5	98.0	9.8	98.8	9.8	98.0	9.8	98.0	9.8
Weight/ Packagibility (0.10)	100.0	10.0	100.0	10.0	85.0	8.5	70.0	7.5	75.0	7.5	85.0	8.5
Preflight Verification (0.10)	0.0	0.0	100.0	10.0	100.0	10.0	100.0	10.0	100.0	10.0	100.0	10.0
Total		58.5		76.5		85.3		79.8		78.3		86.3

Selected TVC Concept: Flex Seal

90209 2A

47

fuel allows the motor to meet the high thrust of the ASRM trace with compact grain designs. The low stochiometric O/F of HTPB/Zn/GAP minimizes the oxidizer required, reduces the size of the oxidizer tank, and enables the booster to approach the SRM envelope.

5. A driving assumption in this study was that the oxidizer tank was the same diameter as the fuel case and mounted in line. The oxidizer tank accounts for over one-half of the booster inert weight (for the baseline aluminum tank, pressure-fed designs), and it represents over one-half of the booster length (for all the designs). Since these boosters are intended to be used with a core vehicle which already has a large LOX external tank, the configuration in which the booster LOX is stored in a stretched core vehicle external tank should be investigated.

6. No significant performance differences were uncovered as a function of size or diameter. The primary effect of diameter size was that larger diameters required grains with a greater number of ports in order to match web-to-regression rate and achieve good volumetric loading.

Several areas requiring technology advancement were uncovered during the course of the study. These were:

1. Prediction and promotion of combustion efficiency in motors with large fuel grain ports, and low length-to-hydraulic-diameter (L/Dh) ratios.

2. Prediction of nozzle and insulation erosion.

3. The ability to tailor fuel regression rate characteristics.

4. Prediction of fuel regression rates in full-scale boosters from laboratory-scale tests.

These technology areas will be addressed in the optional Phase II of the HPT program.

3.5.3 DISCUSSION. For the performance trade studies, payload capability was considered to be the ultimate performance criteria and design optimization was formulated to maximize ideal velocity. Ideal velocity was defined as the vehicle ideal velocity at booster burnout. The Shuttle C configuration was simulated using the POST code to determine the validity of this approach. Figure 38 shows that the calculated payloads correlate well with ideal velocity.

The hybrid boosters had to satisfy several requirements. These were:

1. Match the ASRM NT-019 thrust trace (Figure 39).

2. Incorporate TVC.

3. Have no asbestos.

4. Have no environmentally degrading exhaust products.

5. Extinguish combustion with oxidizer shutoff.
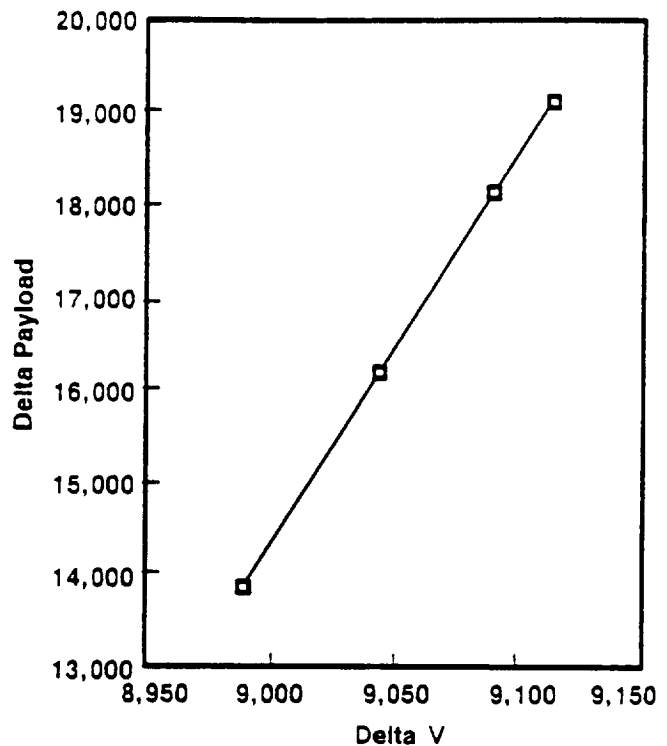
Figure 38. Correlation of payload with vehicle ideal velocity.

CSA024090a
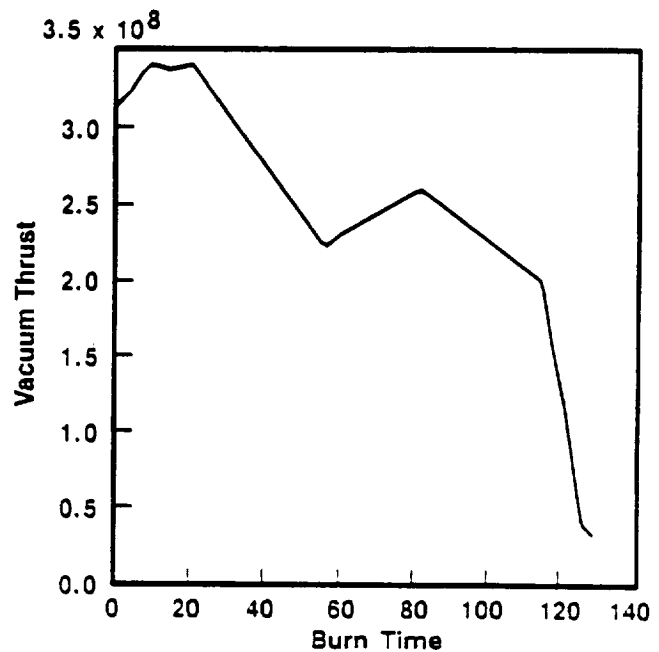
Figure 39. Thrust requirement.

48

One full-sized booster or four quarter-sized boosters burning together had to match the thrust trace. The nature of the thrust curve did impact the study. The ASRM trace is regressive, with very high thrust, and has a central bucket. These characteristics provided significant design challenges.

The requirements for TVC and nonasbestos materials did not affect the study, as neither requirement is viewed as a hybrid issue. The requirement for clean exhaust affected the fuel and oxidizer selection. Thiokol's laboratory conducted the initial fuel and oxidizer trade studies.[9] From the laboratory trade studies, the most promising fuel candidates were selected for propulsion-level studies.

The requirement to extinguish combustion with oxidizer cutoff is achievable with all hybrid types. In the statement of work, extinguishment was defined as having an initial thrust/weight of less than 70 percent. The inert fuels are not combustible without oxidizer. The gas generator fuel includes AN oxidizer. Depending upon design details, it may extinguish completely following oxidizer cutoff and the resultant rapid depressurization, or it may continue to be combustible at a low thrust level.

Several constraints and assumptions were imposed on the designs.

1. Case outside diameter $\leq$ 150 in.

2. Nozzle exit outside diameter $\leq$ case outside diameter.

3. Initial nozzle exit pressure $\geq$ 9 psia.

4. Grain initial port (L/Dh) $\leq$ 30.

5. Liquid tank was the same diameter as the fuel case and mounted in-line.

6. For classical hybrids, the fuel case tangent-to-tangent length was equal to the fuel grain length.

7. For hybrids with afterburners, the fuel case tangent-to-tangent length was 50 in. longer than the fuel grain.

The full-sized motors were held to the ASRM diameter of 150 inches. The quarter-sized motors did not have a diameter constraint. The nozzle exit outside diameter proved to be an active constraint. Many designs would have performed better if this constraint were lifted. The nozzle exit pressure constraint was included to avoid flow separation. This constraint was not active since the nozzle exit outside diameter constraint was always reached first.

The grain port L/Dh constraint was imposed to promote even grain regression. This constraint was consistent with published data.[10] The hybrid ballistics model employs zero-dimensional equilibrium ballistics, and assumes even regression. The L/Dh constraint was generally active for low-density fuels, but was not active for high-density fuels. Oxidizer flux was not constrained in this study, although high flux levels may cause a variety of problems. L/Dh and flux limits need to be established for Thiokol's proposed system. These limits would be established through experiment and analysis during the optional Phase II of the HPT program.

Case length was estimated since the volume which several key components need has yet to be defined. The front dome volume was reserved for oxidizer injection. The aft dome was reserved for a mixing chamber. For the afterburning hybrids, 50 in. was added to the case length, in order to have room for the aft LOX injection.

The trade study matrix included several design configurations consisted of combinations of the discrete variables listed below.

Hybrid Configuration Discrete Variables

Hybrid Type	Fuel Formulations
Classical	TPB
Afterburner	HTPB/Zn
Gas generator	HTPB/Zn/GAP
Hybrid Size	**Tank Material**
Full-size	2219 Al
Quarter-size	Graphite epoxy
Oxidizer Deliver	**Grain Design**
Pump fed	CP (single port)
Pressure fed	Multiport wagon wheel (2-8 ports)

The large number of discrete variables precluded examining every possible combination. The fuel formulation and tank material trade studies were conducted on the full-sized, classical, pressure-fed configuration only. The assumption was that the trends noted for this configuration would hold for the other configurations. During the trade studies, the grain design was matched to the achievable regression rate and the motor diameter. In general, the higher the regression rate and the smaller the diameter, the fewer number of ports were necessary.

The computer code used was Thiokol's hybrid preliminary design code. It is based on Thiokol's Automated Design Program (ADP). The hybrid design code consists of a hybrid ballistics module, several component design modules, liquid oxidizer system weight correlations, and an optimization module (OPTDES.BYU). The component design modules for nozzle, case, insulation, and intertank structure are ADP subroutines for SRMs. These routines should

apply equally well to hybrids. The liquid oxidizer system weight correlations were supplied by General Dynamics and updated as their studies progressed. Initial and final weight correlations are summarized as follows:

Initial Correlations

Pressure Feed

2219 $W_t = (10.55 + 0.113\ P_t)\ 0.001\ W_o/V_1$

Graphite $W_t = (4.65 + 0.039\ P_t)\ 0.001\ W_o/V_1$
Epoxy

$$P_{syswt} = 0.001193\ P_{max}\ V_t$$

Pump Feed

$$W_t = (47.2 - 0.115\ D_t)\ W_o/V_1$$

$$\text{Pump wt} = 70.9\ (h\ R_{ox\ max})^2$$

$$P_{fuel} = 0.00231\ (P_{avg} + 50)\ R_{ox\ avg}$$

Both Feed Systems

$$L_{nf} = 0.000013\ h\ R_{ox\ max} + 0.0063\ h$$
$$R_{ox_{max}}{}^{1/2} + 6.4\ R_{ox_{max}}{}^{1/2}$$
$$- 0.03\ h + 7.4$$

Final Correlations

Pressure Feed

2219 $W_t = (0.007 + 0.0102\ P_t)\ V_t$

        $P_t \gtrsim 366$

Graphite $W_t = (0.457 + 0.0033\ P_t)\ V_t$

Epoxy $P_t \gtrsim 569$

        $P_{syswt} = 0.001508\ P_t\ V_t$

Pump Feed

W_t $= 3.74\ V_t$

Pump wt $= 0.001641\ P_{max}\ V_t$

P_{fuel} $=$ included in pump wt equation

L_{nf} $=$ no revision for this correlation

W_t $=$ tank weight (lb)

D_t $=$ tank diameter (in.)

Pump wt $=$ pump weight (lb)

$R_{ox_{max}}$ $=$ maximum oxidizer flow rate (lb/sec)

$R_{ox_{avg}}$ $=$ average oxidizer flow rate (lb/sec)

W_o $=$ oxidizer weight lb

V_1 $=$ tank volumetric loading, 0.97 for all designs (dim)

P_{syswt} $=$ weight of pressurization system (lb)

P_{max} $=$ maximum chamber pressure (psia)

P_{avg} $=$ average chamber pressure (psia)

P_t $=$ tank design pressure

        $= P_{max} + 200$ (psia)

V_t $=$ tank volume (cf)

h $=$ pump system design pressure

        $= P_{max} + 50$ (psia)

L_{nf} $=$ weight for lines and fittings (lb)

Once a combination of discrete variables was chosen, six continuous design variables were changed within the optimization module until the best performing design was found. The continuous design variables were:

1. Fuel grain length.
2. Fuel grain port radius.
3. Fuel grain web.
4. Nozzle throat diameter.
5. Nozzle expansion ratio.
6. Fuel regression rate coefficient.

A schematic of the design process is shown in Figure 40. The operator chose a combination of discrete variables. The optimizer then varied the continuous variables until ideal velocity could not be improved while meeting the design requirements and without violating the design constraints. The operator then tested the point design to determine whether it was a local or global optimum by restarting the optimization with different values of the continuous variables. When the operator was satisfied, the optimization was considered to be complete.

Several limitations were imposed on the trade study. A fixed nozzle was simulated instead of a TVC nozzle in order to provide faster analysis. Once the trade study was completed, several point designs were run with TVC nozzles. Silica phenolic was the only nozzle throat material used. This material was chosen because of its resistance to erosion in an oxidizer-rich environment. Silica phenolic is sensitive to high temperature, so the standard nozzle erosion rate correlation was modified to include a temperature term. The erosion rate equation is as follows:

$$e = 00.00509\ (P/625)^{1.11}\ (B/1.0)^0\ (R/25)^{0.28}$$
$$(T/6143)^{3.69}$$

e = erosion rate (ips)

P = chamber pressure (psia)

B = beta (dim)

R = throat radius (in.)

T = flame temperature (°F)

The constants used in this equation apply to silica phenolic nozzles.

Motor I_{sp} efficiency for all designs was fixed at 95 percent. Motor efficiency will depend on nozzle, grain, and injector design. The assumption was that a final

```
                    ┌─────────────────────┐
                    │   Choose Concept    │
                    │ (discrete variables)│
                    └─────────────────────┘
                              │
                              ▼
  ──────────────────▶ ┌─────────────────────┐ ◀──────────────
                    │  OPTDES Preprocess  │
                    │(continuous variables)│
                    └─────────────────────┘
                              │
                              ▼
                    ┌─────────────────────┐
                    │      Hybrid         │
                    │     Ballistics      │
                    └─────────────────────┘
                              │
                              ▼
                    ┌─────────────────────┐
                    │ Component Subroutines│
                    └─────────────────────┘
                              │
                              ▼
┌──────────────┐    ┌─────────────────────┐
│   Choose     │    │    Point Design     │
│New Starting PT│    └─────────────────────┘
└──────────────┘              │
       ▲                      ▼
       │ No        Yes ┌─────────────────────┐  No
┌──────────────┐ ◀──── │  OPTDES Postprocess │ ───▶
│   Global     │       │   Constraints Met?  │
│   Optimum?   │       │    ΔV Maximum?      │
└──────────────┘       └─────────────────────┘
       │ Yes
       ▼
┌──────────────┐
│   Optimum    │
│   Design     │
└──────────────┘
```

CSA024091a
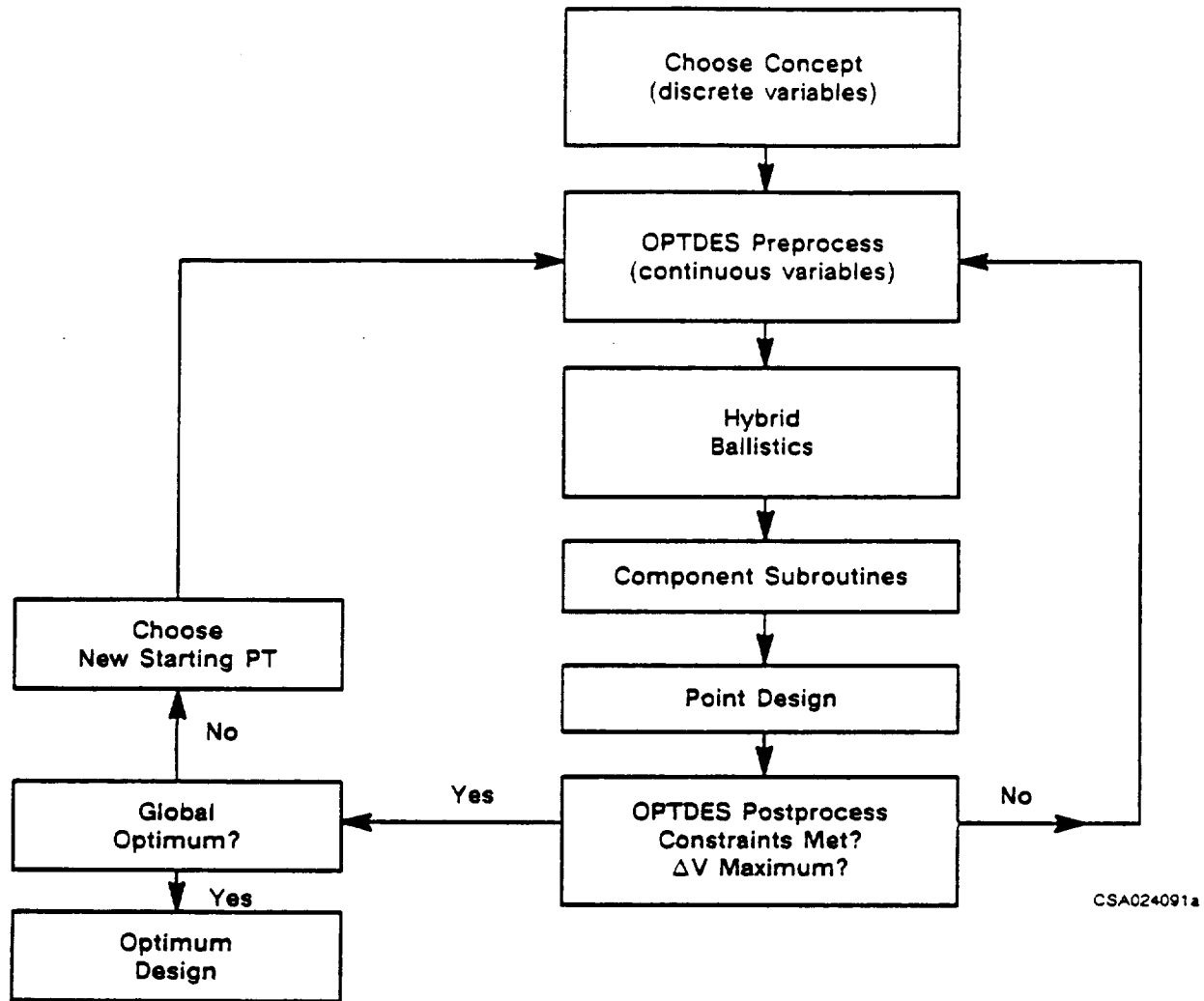
Figure 40. Design optimization process.

motor design would have features which promote good efficiency.

To simplify the trade study, the case outside diameter for the full-sized motors was fixed at 150 inches. Early work with the full-sized motors showed large changes in diameter gave large changes in length, but small changes in ideal velocity. Diameter was fixed to avoid the difficulty of comparing motors of similar ideal velocity but with dissimilar shapes. Similarly, diameter for the bulk of the quarter-sized trade studies was fixed at 75 in. (one-fourth of the cross-sectional area). The classical, pressure-fed configuration was chosen to study the effect of diameter on the quarter-sized motors.

The gas generator designs were not optimized, since the CP and wagon wheel grain designs currently available in the hybrid ballistics module are not suitable to the gas generator hybrid and the ASRM trace.

However, care was taken to produce good point designs. Point design configurations were guided by the results of previous studies.

Trade Studies

The results of each trade study are covered in separate sections. The trade studies covered are:

1. Grain design.
2. Fuel formulation.
3. Hybrid type.
4. Hybrid size.
5. Tank material.
6. Quarter-sized diameter.
7. Full-sized length.
8. Oxidizer feed system.

A general discussion on hybrid ballistics is necessary to provide an understanding of the more detailed trade studies. The discussion on hybrid ballistics is further

51

expanded in the sections on grain design and fuel formulation that follow. The remaining trade studies are primarily comparisons of optimized designs of different configurations.

Hybrid Ballistics

In this trade study, three types of hybrids were considered. The classical hybrid has a solid fuel grain, with oxidizer injection at the head end. The afterburner hybrid is like the classical hybrid, but oxidizer is also injected in an afterburning combustion chamber. The regression rate correlation for the classical and afterburning hybrids is

$$r = aP^nG^m$$

G   = mass flow of oxidizer/
       fuel grain port area

P   = chamber pressure

a   = regression coefficient

n,m = regression exponents

r   = fuel regression rate

The flux term is a key feature of the classical and afterburning hybrid regression rate correlation. Fuel mass flow rate is the product of regression rate, surface area, and fuel density. Since flux depends on port area (grain geometry), grain geometry affects fuel mass flow rate by affecting both regression rate and surface area.

The gas generator hybrid is similar to a solid rocket. It has the SRM regression rate correlation ($r = aP^n$) since no fuel is injected down the bore, and it uses live fuel. Unlike a solid rocket, the fuel grain is mixed fuel-rich; the balance of the oxidizer needed to produce near-stochiometric combustion is injected in an afterburning combustion chamber.

All three hybrids types are throttlable. Like liquid rockets, hybrid performance depends on O/F. A goal of hybrid design is to be able to throttle the oxidizer while operating at or near the optimum O/F.

For the inert fuel hybrids, increasing the oxidizer flow rate increases chamber pressure and flux, both of which increase the fuel regression rate. If the regression rate coeffecient, exponents, and fuel geometry match, the oxidizer could be throttled without deviating from the optimum O/F. Because the gas generator hybrid regression rate has no flux dependence, it is more difficult to maintain the optimum O/F while throttling.

Grain Design

Figure 41 is a schematic of the multiport wagon wheel and center-perforated (CP) grain types used in the trade studies. The multiport wagon wheel could have two or more ports. As the number of ports increases, the surface area increases and the web decreases. Low regression rate propellants require a large number of

ports. Multiport wagon wheels will have sliver or require supports in the areas shown. Additionally, they may require a more complex injection system than CP grains. Because CP grains lack sliver, they are preferable so long as the regression rate is high enough to allow good volumetric loading.
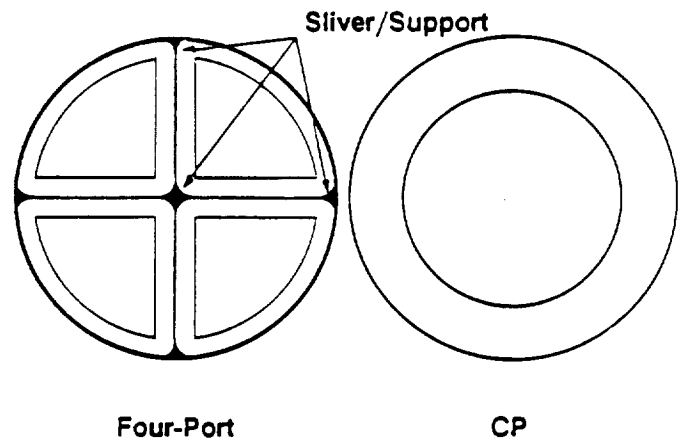
Figure 41. Fuel grain configurations.

Grain designs with several small ports and a high L/Dh may promote better mixing of fuel and oxidizer and therefore have higher combustion efficiency than grain designs have large ports and a low L/Dh. Technology areas that need improvement are: 1) prediction of combustion efficiency and 2) promotion of combustion efficiency.

Both CP and multiport grains provide progressive surface area and progressive port area traces. As will be shown, these characteristics are well suited to the classical and afterburner hybrids.

Figures 42 through 45 show detailed ballistics for the classical, pressure-fed, full-sized configuration. The fuel simulated was HTPB/Zn/GAP. Regression rate pressure exponent was 0.35; the flux exponent was 0.681. Regression rate coeffecient, grain geometry, and nozzle geometry were varied to produce optimum designs.

Figure 42a shows the surface area versus web traces for both four-port and CP designs. Both traces are progressive and linear, and for both traces the surface area approximately doubles. The CP has approximately one-half the surface area and double the web of the four-port grain.

Figure 42b is a fuel regression rate plot for the two designs. Again the shape of the curves is similar, but the magnitudes differ greatly. In order to employ a CP, the full-sized classical hybrid must deliver initial regression rates of approximately 0.6 in./sec. The four-port design
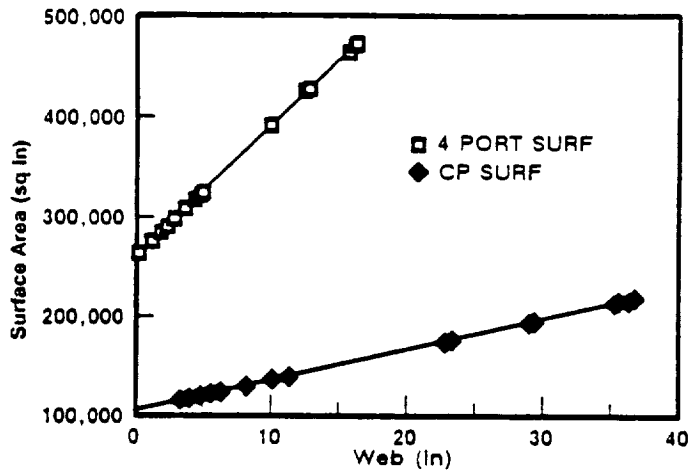
a. Surface area versus web traces.
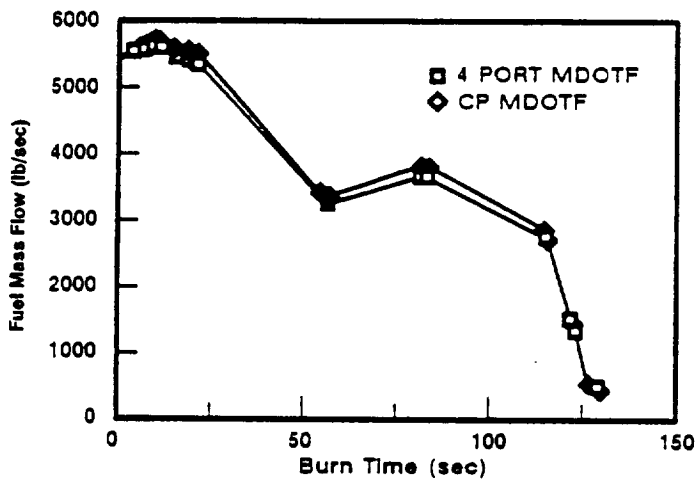
b. Fuel regression rate.
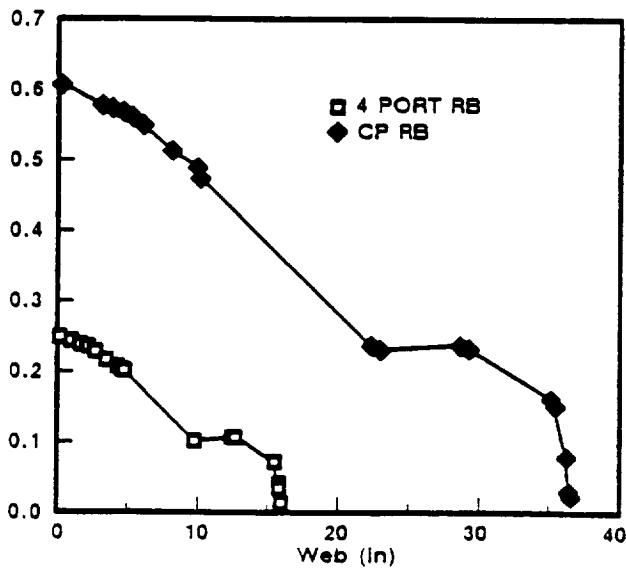
c. Fuel mass flow.

CSA024088a

Figure 42. Comparison of four-port and CP ballistics.
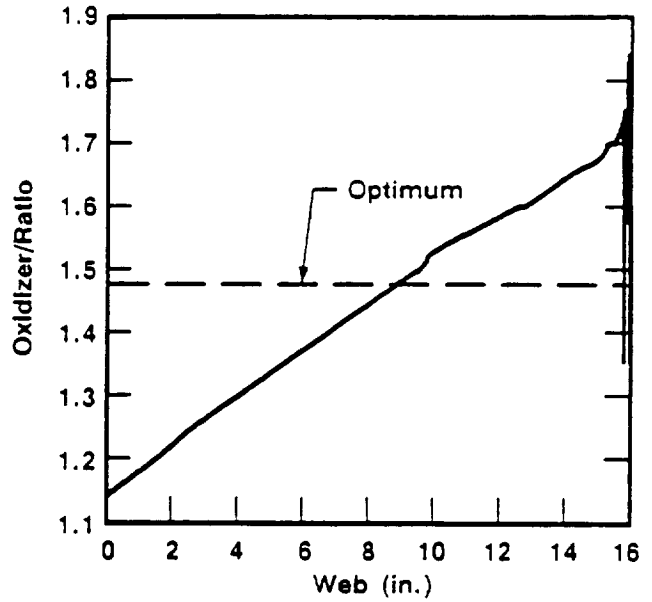
a. O/F trace.
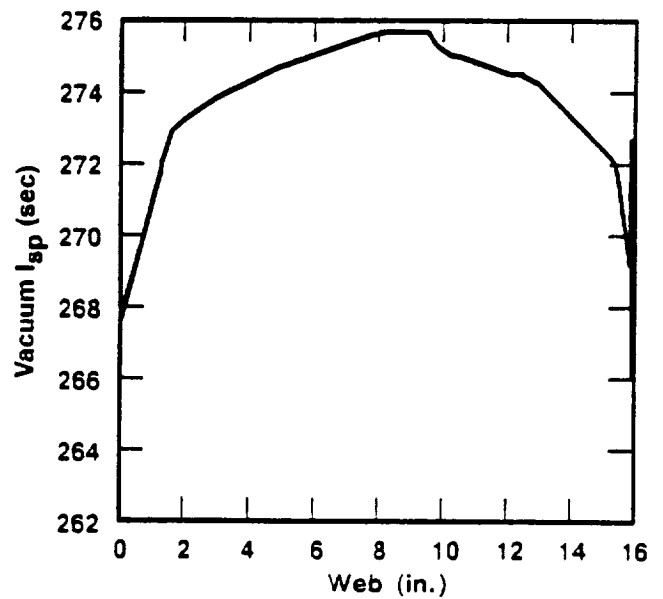
b. I_{sp} penalty from optimum O/F.

CSA024087a

Figure 43. Classical hybrid I_{sp} performance.

requires only 0.25 in./sec. Both curves show regression rates which decrease by a factor of three over the course of the simulation. The regression rates decrease because the port areas increase. The regression rate curves have the general shape as the thrust trace. This variations in regression rate track variations in the oxidizer mass flow rate.

Figure 42c shows that both grain types deliver essentially the same fuel mass flow history. The CP grain has a low surface area and requires a high regression rate. The four-port grain has more high surface area and a lower regression rate. Both motor designs combine increasing surface area and decreasing regression rate to produce fuel mass flow histories very similar to the required thrust trace.

Figure 43a is the O/F trace for the four-port design. The CP design would have a similar curve. The system optimum O/F for this configuration was just under 1.5. The classical hybrid operated fuel-rich initially, and fuel-lean at the end of burn. Figure 43b shows the I_{sp} penalty for operating away from the optimum O/F. To maintain the optimum O/F with the ASRM thrust trace, the fuel delivery needs to be more progressive. Since the surface area trace is already very progressive, the way to make the fuel delivery more progressive is to make the regression rate decrease less by reducing the value of the flux exponent.

Figure 44 shows how flux exponent affects O/F operation. As flux exponent is reduced from 0.681 to 0.5, the overall slope of the O/F curves changes from positive to negative.

Because these curves were generated with a regression rate pressure exponent of zero, they have more variation than the O/F curves for HTPB/Zn/ GAP. Because the fuel regression rate responds only to flux, the fuel mass flow rate cannot track the oxidizer flow rate as closely. The flux and pressure exponents strongly affect the ability of the motor to maintain operation near the optimum O/F.

In addition to tailoring pressure and flux exponents, an afterburning combustion chamber can maintain operation near the optimum O/F. Figure 45 includes a series of curves for a full-sized, pressure-fed, four-port hybrid with HTPB/Zn/GAP fuel. For this hybrid, the grain has the same regression rate characteristics as the classical hybrid. The grain O/F curve is similar to the classical hybrid, except that the curve begins more fuel-rich, and ends near the optimum O/F. Figure 45b shows the rate of oxidizer flow to the aft combustion chamber needed to maintain the motor optimum O/F. The I_{sp} curve (Figure 45c) shows that the afterburning hybrid maintains a high I_{sp} throughout the burn. I_{sp} is

a. Flux exponent = 0.681

b. Flux exponent = 0.60

c. Flex exponent = 0.50
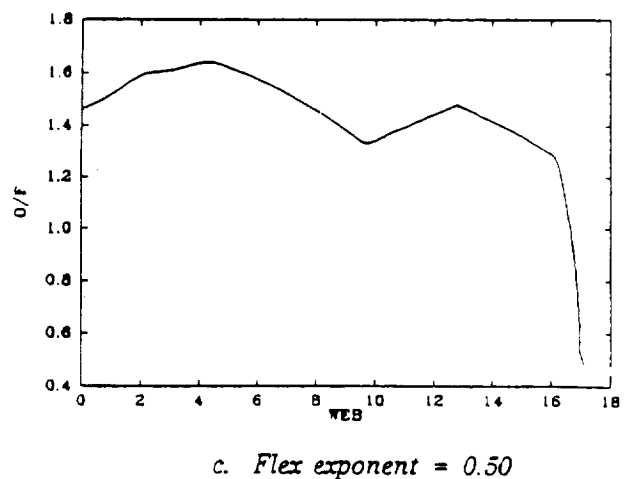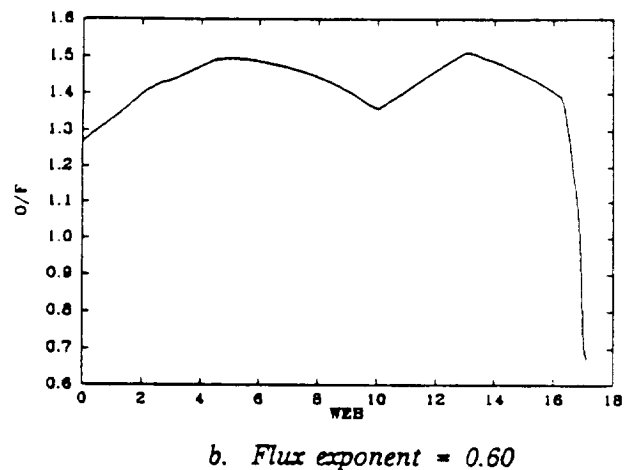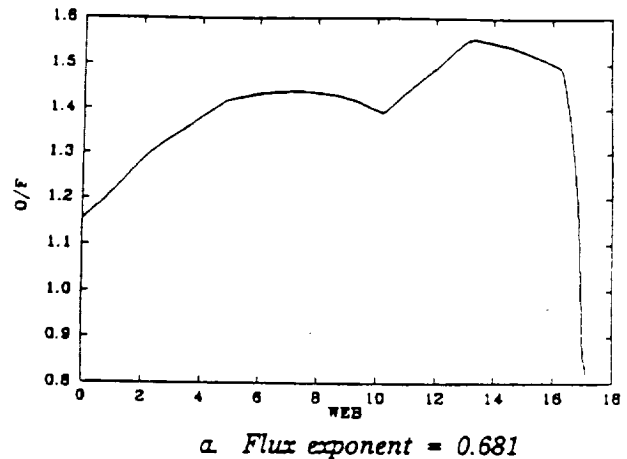
Figure 44. Effect of regression rate flux exponent on O/F.

54
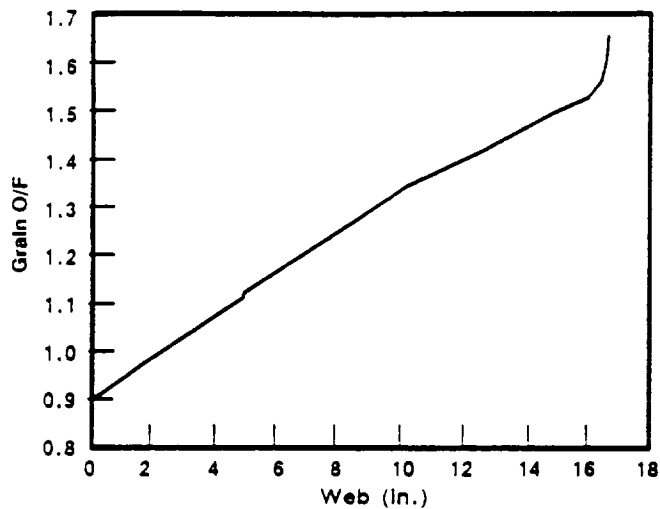
a. Optimum O/F.
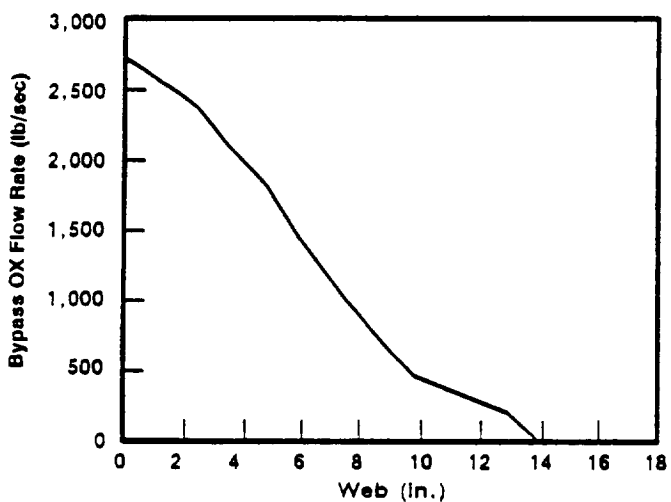
b. Oxidizer flow.
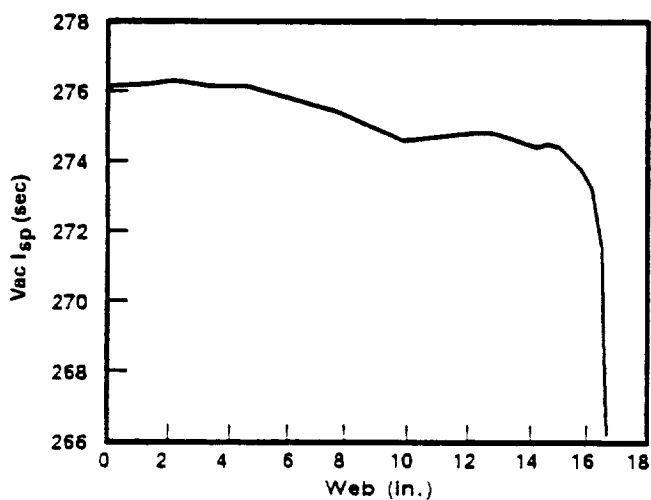
c. High I_{sp}.

CSA024086a

Figure 45. Afterburning hybrid ballistic performance.

not constant since throat erosion degrades expansion ratio, and pressure decreases through the burn.

For the afterburning hybrid, the benefit of increased I_{sp} must be weighed against the increased complexity, cost, and inert weight of the additional injection system.

Figure 46 shows a series of curves for the full-sized, pressure-fed gas generator hybrid. The surface area trace is radical compared to the inert fuel hybrids, and requires a complex grain design. This trace was necessary to maintain operation near the desired O/F (Figure 46b).

The gas generator operates at a low O/F because a large percentage of the oxidizer is contained in the fuel grain. For the gas generator hybrid, O/F was defined as the liquid oxidizer flow rate/flow rate from the solid grain.

System Fuel Trade Studies

A comprehensive fuel and oxidizer study was conducted by Thiokol's propellant lab.[9] I_{sp}, density, exhaust products, and safety were considered. Based on the results of this study, LOX was selected as the oxidizer, HTPB/AN/Al was selected as the gas generator fuel, and three inert fuels were selected for the classical and afterburning hybrids. The fuel trade studies discussed in this section were conducted at the propulsion system level.

The following discussion concerns the three inert fuels which were selected for the classical and afterburning hybrids. The fuels were HTPB, HT/Zn, and HTPB/Zn/GAP. The important fuel characteristics in the system trade studies were regression rate, I_{sp} versus O/F, and density.

Table 12 is a comparison of several fuel characteristics. Shuttle propellant and the gas generator fuel are included in the table for comparison. HTPB has the highest peak I_{sp}, and operates at the highest O/F. It has the lowest density, the lowest achievable regression rate, and no regression rate pressure dependence. HTPB/Zn/GAP has the lowest I_{sp} at the lowest O/F, but it has the highest density and the highest achievable regression rate. The HTPB/Zn characteristics are intermediate to those for HTPB and HTPB/Zn/GAP.

The inert fuel regression rate characteristics are based on laboratory-scale (2-in.-diameter) test firings. The regression rate for the gas generator propellant was estimated based on regression rates of similar AN propellants.

The metalized fuels have nonzero regression rate pressure exponents. The metalized fuels also hold the promise of low flux exponents compared to HTPB. The flux exponent for HTPB was experimentally determined to be 0.681. In the trade studies, this was the value of

55
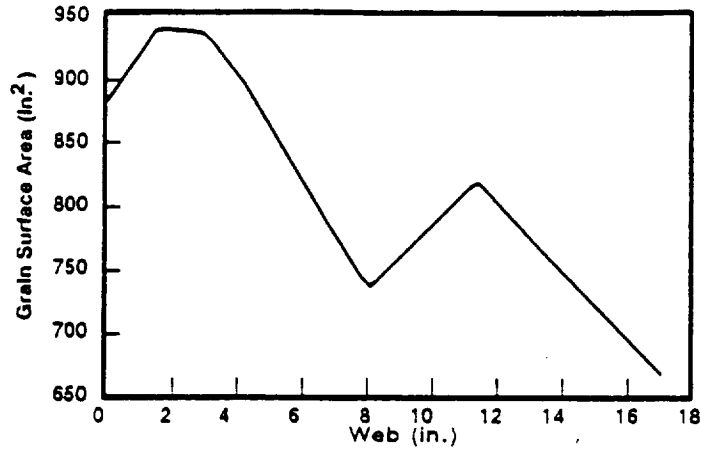
a. Surface area trace.
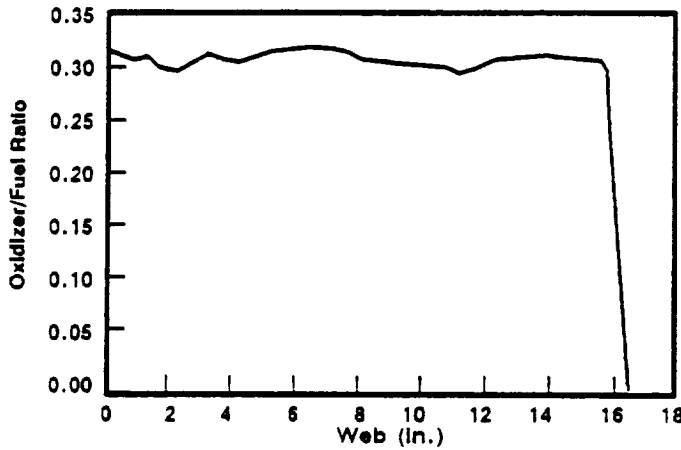
b. Low O/F
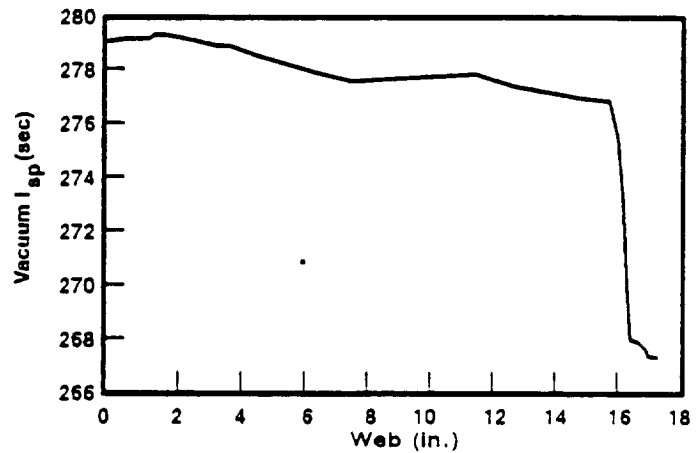
c. I_{sp}.

CSA024085a

Figure 46. Gas generator hybrid ballistic performance.

Table 12. Comparison of fuel characteristics.

Fuel	I_{sp} at* STOCHIO O/F	Density (lbm/in.^{3})	Achievable** Rate (in./sec)	Regression Pressure	Rate*** Exponents Flux
HTPB	304.4/2.15	0.0331	0.035	0	0.681
HT/Zn	294.1/1.9	0.0780	--	0.35	0.5?
HT/Zn/GAP	290.1/1.5	0.0814	0.25	0.35	0.4
HT/AN/Al (gas generator)	276.5/0.3	0.0650	0.2	0.4	0
TPH-1148 (Shuttle)	265.9	0.0641	0.435	0.35	0

• HTPB has highest I_{sp}, lowest density, highest O/F, no pressure dependance

• HT/Zn/GAP has lowest I_{sp}, highest density, highest regression rate capability, and lowest O/F

• HT/Zn has high density but lower regression rate than HT/Zn/GAP

• Gas generator fuel — Very low O/F (already oxidizer in fuel)

• Metalized fuels promise low flux exponent

---

* Vacuum theroetical at 1,000 psia and 5:1 expansion ratio
** 1,000 psi and 0.5 lbm/sec in.^{2}
*** Flux emponent of 0.681 used in trades for ineret fuel hybrids

56

flux exponent used for all the inert fuels since better information was not available when the trade studies were conducted.

Figure 47 shows how I_{sp} varies with O/F for the three fuels. All curves have the same general shape. The curves rise steeply to approximately 80 percent of the maximum I_{sp}, roll gently to the maximum value, then fall off gradually as the mixture gets increasingly oxidizer-rich.

It is significant that the peak I_{sp} for each fuel occurs at a different O/F. The stoichiometric O/F is important from a system standpoint because it indicates the relative sizes of the fuel and oxidizer portions of the motor.

Figure 48 plots temperature, beta, and I_{sp} with O/F for HTPB/Zn/GAP. These characteristics are similar for the other two inert fuels. The general shape of the I_{sp} curve has already been discussed. The temperature curve is similar in shape to the I_{sp} curve, but it drops off steeper on the fuel-rich side of stoichiometric and peaks at a higher O/F than the I_{sp} curve. Beta is essentially zero for O/F ratios below 0.7, and increases quadratically thereafter. The shuttle propellant has a beta of 0.107 and a flame temperature of 5640°F. Beta and temperature can be related to nozzle and insulation erosion. Since shuttle values are lower than those for HTPB/Zn/GAP at useful O/F ratios, the hybrid environment may be more severe than the solid rocket environment. Nozzle and insulation erosion in the hybrid environment needs to be characterized.

Operating fuel-rich has advantages. Less erosion would mean that less case and nozzle insulation is necessary. Less nozzle erosion would result in less I_{sp} degradation.

Figure 49 shows how O/F affects theoretical I_{sp} and average I_{sp}. These curves were generated assuming silica phenolic nozzle throat material and the erosion rate equation given previously. The calculations were done assuming an initial expansion ratio of 7.5, a constant pressure of 750 psia, and a constant O/F. Silica phenolic is not sensitive to beta erosion, but is sensitive to temperature. Therefore, the increased loss of I_{sp} at higher O/F ratios is due to higher flame temperatures. These curves show little increase in I_{sp} loss as O/F increases; however, the trend is to operate fuel-rich.

To compare the fuels at the system level, motors were optimized with each fuel. The motor designs are compared in Table 13. All motors were of the full-sized, classical, pressure-fed configuration, with 2219 aluminum tanks and D6AC steel cases. Case diameter for all motors was fixed at 147.9 inches. The HTPB motor optimized to this diameter. All the motors used the four-port wagon wheel grain design. Regression rate

coeffecient, grain geometry, and nozzle parameters were varied until optimum designs were found.

All designs have equivalent ideal velocity performance, therefore the baseline fuel selection was based on other criteria. The HTPB grain is nearly twice as long as the metalized grains, and the motors having metalized propellants were about 500 in. shorter. Although length is excessive, the HTPB motor is the lightest. The HTPB motor has the highest I_{sp} and requires the least propellant. Because HTPB has low density, long grains are required to achieve the needed mass flow. The HTPB grain was optimized to the port L/Dh constraint. The grains featuring the high-density metalized fuels were not L/Dh constrained.

Pressure-fed hybrids operate at lower pressures than are typical for solid rockets. The oxygen tank was designed to 200 psi more than the case, so pressure-fed hybrids carry a significant inert weight penalty. Therefore, all designs optimized to maximum pressures lower than 700 psi. The HTPB design has the longest tank and the longest case. Therefore, it optimized to the lowest pressure. For all the designs, the liquid tanks are more than twice as heavy as the fuel cases.

The HTPB motor operated at the highest average O/F, and required the most oxidizer. The HTPB motor operated fuel-lean, while the metalized fuel motors operated fuel-rich. The HTPB design would have operated fuel-rich if the port L/Dh constraint had not been reached.

The fuel mass fraction is defined as the weight of the fuel/weight of the fuel plus fuel inert weight. The oxidizer mass fraction is similarly defined. The average O/F will tend to optimize from stoichiometric to rich in the propellant which has the higher mass fraction. For the metalized fuels, the fuel mass fraction was much higher than the oxidizer mass fraction. For HTPB, the fuel mass fraction was slightly higher than the oxidizer mass fraction. Since the oxidizer tank is mounted above the fuel tank, fuel-rich operation allows a lighter intertank structure.

Apparent density is a means of comparing the loading of the oxidizer tank and the fuel case. Apparent density is the product of density and volumetric loading. LOX has a density of 0.0413 and a volumetric loading of 0.97, for an apparent density of 0.0401. Volumetric loading of the fuel will depend on the grain design. A very good volumetric loading for perforated grains is 0.88. The density of HTPB is 0.0331, so it cannot equal the apparent density of LOX. Because the metalized fuels are over twice as dense as LOX, they can have poor volumetric loading and still equal the apparent density of LOX. If the apparent density of fuel and oxidizer are equal, and, if the case and tank are of the same diameter and if the case and tank operate at the
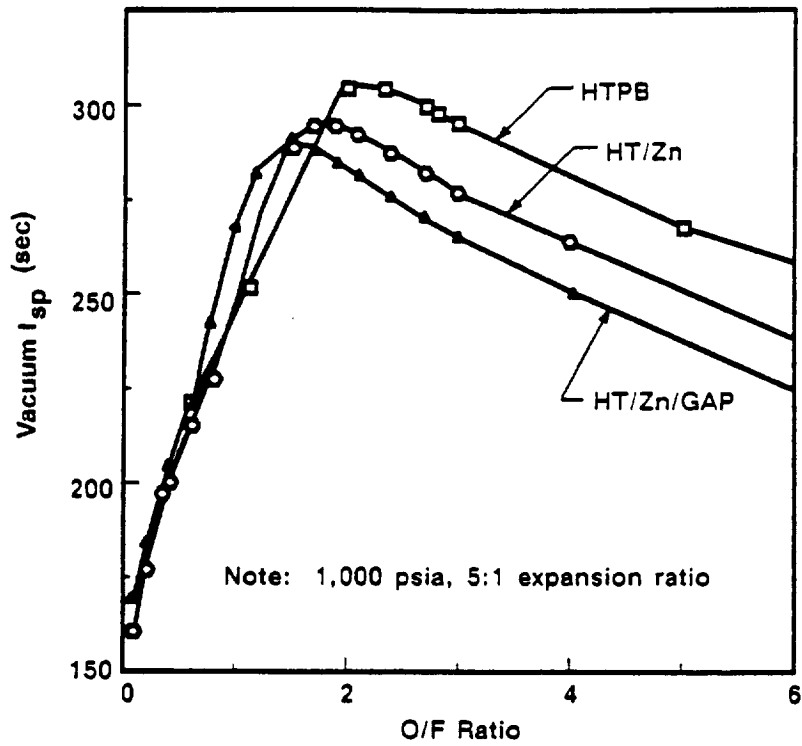
Figure 47. Theoretical I_{sp} versus O/F for inert fuels.

CSA023903a
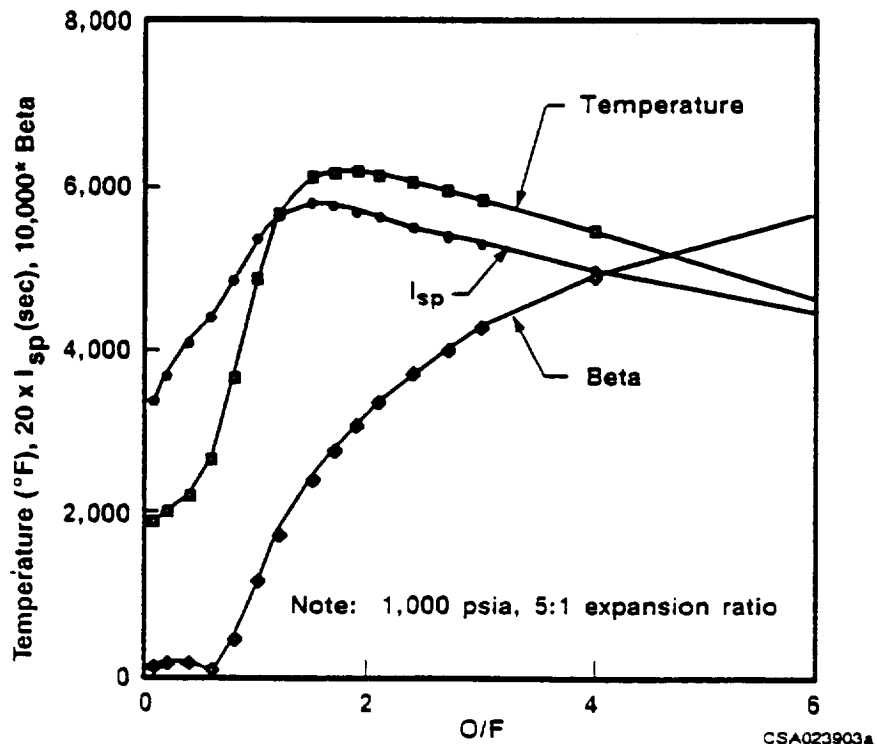
Figure 48. Important fuel characteristics of HTPB/Zn/GAP

58
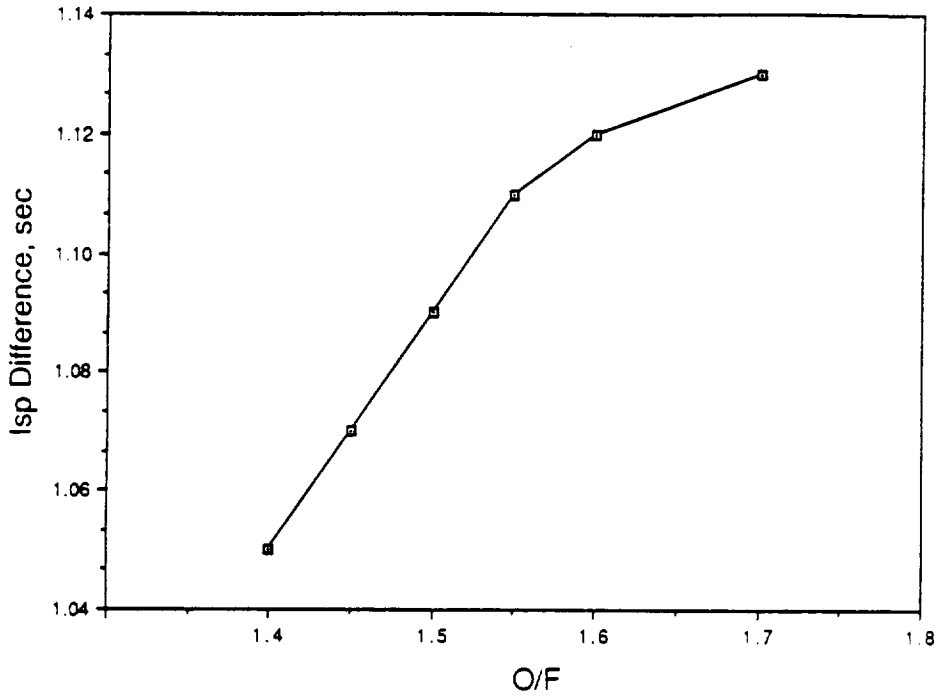
NOTE: Ht/Zn/Gap, Ei=7.5, Pc=750 psia, Dt=50 in.

Figure 49. Effect of O/F on average I_{sp}

Table 13. Effects of fuel formulation on motor design.

Fuel	HTPB	HT/Zn	HT/Zn/GAP
ΔV (f/s)	8,729	8,724	8,710
Booster Weight (lbm)	1,317,265	1,321,700	1,340,900
Total Booster Length (in.)	2,583	2,137	2,049
Grain Length (in.)	952	524	513
Vac I_{sp} average (s)	280.7	279.4	273.1
L/Dh Grain Port	30.0*	13.9	16.8
P_{max} (psia)	531	688	672
Weight Case (lbm)	34,390	26,850	25,940
Weight Liquid Tank (lbm)	72,300	80,900	74,340
Weight Oxidizer (lbm)	786,900	739,800	690,800
O/F Average	2.16	1.77	1.40
STOCHIO O/F	2.15	1.90	1.50
Fuel Density (lbm/in.^{3})	0.0331	0.0780	0.0814
Volume Loading	0.737	0.634	0.756
Apparent Density (lbm/in.^{3})	0.0244	0.0495	0.0615
Apparent Density Fuel/OX	0.61	1.24	1.54
Mass Fraction Fuel	0.9087	0.9279	0.944
Mass Fraction OX	0.9071	0.8966	0.8923
Average Regression Rate (in./s)	0.118	0.112	0.122

• Baseline configuration, 4-port

• Metalized fuels allow more compact motors

   • Metalized fuels approximately twice as dense as LOX

• Metalized fuels allow higher operating pressure

• For metalized fuels, fuel mass fraction is better than oxidizer mass fraction — Operate fuel rich

• HT booster length is excessive but offers lightest booster

---

* Constraint

same pressure, then case and tank will have nearly the same weight-per-unit length.

All the motors had four-port grain designs; therefore, all optimized to relatively high regression rates. GAP is the only ingredient tested to date which yields relatively high regression rates and allows regression rate tailorability. For this reason, the HTPB/Zn/GAP fuel was used as a baseline. HTPB/Zn and HTPB would require fuel grains with more ports if regression rates were constrained to currently achievable values.

GAP has disadvantages. It is expensive and availability is limited. GAP is a Class B explosive. However, HTPB/Zn/GAP fuel is inert. Ingredients similar to GAP may enhance regression rate without having GAP's disadvantages. This is a technology area that requires further investigation.

Hybrid Type

Table 14 is a comparison of full-sized, pressure-fed designs. Classical, afterburner, and gas generator hybrids are compared. The afterburner hybrid has minimal performance gain compared to the classical hybrid. The classical hybrid operated well enough to have an average I_{sp} only 1.1 sec lower than that for the afterburner. If the thrust trace and fuel characteristics were different, the afterburner might prove more effective. For this case, the I_{sp} increase offered by the afterburner is almost entirely offset by the additional inert weight. The afterburner also requires additional combustion chamber length, which results in an overall longer booster even though the afterburner fuel grain is shorter.

The gas generator hybrid has considerably less ideal velocity than either of the inert fuel hybrids. However, the gas generator hybrid was not optimized to the same extent as the other concepts. Complex grain optimization is not currently available for the gas generator hybrid in the hybrid design program. However, care was taken to provide a good point design. A formal grain design was not done; instead a surface-web table was input (Figure 46a) which allows the gas generator to stay near the optimum O/F of 0.3. Formal grain design would be an intensive process, beyond the scope of the Phase I effort. A grain design which approaches the desired surface-web history would be designed. The surface-web history would then be input to the hybrid design code, and the performance analyzed. Initial results indicated that grains with good volumetric loading (low inert weight) would not be able to follow the surface-web trace very well, and therefore suffer an I_{sp} penalty. Several grain design iterations would be necessary to determine the best performing design. Because the gas generator fuel is 65% AN, it requires relatively little additional oxidizer and has a relatively long grain. Grain length was estimated based on fuel weight, volumetric loading, and final surface area. Because the gas generator has a small LOX tank and, therefore, a small tank inert weight penalty, a relatively high operating pressure was chosen.

Table 14. Comparison of hybrid types.

	Classical	After Burner	Gas Generator
Ideal Velocity (fps)	8,702	8,718	8,581
Booster Weight (lb)	1,338,000	1,334,000	1,349,000
Booster Length (in.)	2,012	2,049	2,331
Fuel	HT/Zn/GAP	HT/Zn/GAP	AN/Al/HT
Grain Length (in.)	487	470	1,400
Vac I_{sp} Average (sec)	274.0	275.1	277.8
P_{max} (psia)	674	652	1,045

- Fullsize, pressure fed
- Afterburner and classical have equivalent performance
- Gas generator performance good — Not optimized

Hybrid Size

Table 15 is a comparison of full- and quarter-sized designs. Both were classical, pressure-fed designs with HTPB/Zn/GAP fuel. These designs employed revised liquid tank weight correlations and TVC nozzles. The full-sized booster has a slight ideal velocity advantage, due primarily to its higher expansion ratio and resultant higher I_{sp}. The full-sized motor has a diameter of 150 inches. The quarter-sized motor diameter was set at 75 in. (one-fourth of the cross-sectional area). For both motors, the nozzle exit outside diameter was constrained to the case outside diameter, and for both motors this limited performance. The chief advantage of the quarter-sized motor was it could employ a CP grain design instead of the four-port wagon wheel required of the full-sized motor. The quarter-sized motor was shorter than the full-sized motor, but has an unattractive booster L/D of almost 24.

Quarter-Sized Diameter Study

The bulk of the quarter-sized trade studies was done with the diameter fixed at 75 inches. The decision to fix diameter was based on early work with the full-sized motors, which showed performance to be insensitive to diameter. This trade was done to determine if the trends differed with the quarter-sized motors. Table 16 is a comparison of two quarter-sized motors. These motors are both classical, pressure-fed designs with HTPB/Zn/GAP fuel. These motors were designed with the revised liquid tank correlations and have TVC nozzles. The motor diameters considered were 75 and 90 inches.

The 90-in. motor has nearly a 100-fps advantage over the 75-in. motor. This performance advantage is due primarily to the nozzle exit outside diameter constraint. The 90-in. motor enjoys the I_{sp} advantage which the 6.6 expansion ratio provides, while the 75-in. motor only has an expansion ratio of 4.5. The 90-in. motor has a conventional booster L/D, while the 75-in. motor has a high L/D. However, with currently achievable regression rates, the 90-in. diameter is too large for a CP grain, and therefore requires a multiport grain configuration.

Length-Constrained Design

The hybrids discussed in this study were evaluated based on performance in applications to shuttle and Shuttle C. The full-sized designs previously discussed have been longer than the shuttle solid rocket booster (SRB) length of 1790 inches. A designed constrained to SRB length was done to determine how much performance would be lost by shortening the motor. The full-sized, classical, pressure-fed configuration, with 2219 aluminum tank, D6AC case, and HTPB/Zn/GAP fuel was the point of departure. These designs were done with the

Table 15. Comparison of full- and quarter-sized designs.

	Full	Quarter
No. boosters	2	8
Ideal Velocity (fps)	8,584	8,525
Grain Length (in.)	491	526
Booster Length (in.)	1,909	1,774
Booster L/D	12.7	23.7
Diameter (in.)	150	75
Grain Type	4/port	CP
Max Pressure (psia)	585	580
Vac I_{sp} Average (sec)	268.8	268.2
Initial Expansion Ratio	4.75	4.53

- Classical, pressure fed, Al tank
- Updated liquid exchanges, flex bearing nozzle
- Full and quarter provide similar performance
- Quartersize quarter CSA = > allows CP

Table 16. Quarter-sized diameter study.

Case Diameter (in.)	75	90
Ideal Velocity (fps)	8,525	8,623
Booster Length	1,774	1,248
Motor L/D	23.7	13.9
P_{max}	580.0	600.0
Vac Average I_{sp} (s)	268.2	274.7
Total Booster Weight	346,000	337,500
G/F Average	1.42	1.29
Web	16.3	14.6
Grain Design	CP	2 port
Initial Expansion Ratio	4.5	6.6

- Classical, pressure fed
- New liquid exchanges, flex bearing nozzle
- 90 in. motor requires two ports, offers good L/D, good performance
- Nozzle OD constraint hurts 75 in. motor

revised liquid system weight correlations, and employ TVC nozzles. For both designs, motor diameter was fixed at 150 inches. The length-constrained motor was not required to meet the ASRM total I_{sp}. The length-constrained motor followed the ASRM thrust trace until the propellant was consumed. It did meet all other requirements and constraints. Table 17 is a comparison of the constrained and unconstrained designs. The constrained motor met SRB length by removing fuel and oxidizer, thereby shortening case and tank. The length-constrained design reduced total I_{sp} and ideal velocity. The ideal velocity penalty for shortening the motor was 2.1 fps/inch.

The length-constrained motor operated more fuel-rich than the unconstrained design since HTPB/Zn/GAP loads more compactly than LOX. Fuel-rich operation resulted in a relatively larger fuel tank and relatively smaller oxidizer tank. Since the oxidizer tank operates 200 psi higher than the case, the optimizer took advantage of the shift in case and tank size by operating at higher pressure. Even though the length-constrained design operates farther from the stoichiometric I_{sp} than the unconstrained design, operation at higher pressure allowed the constrained motor to deliver higher I_{sp} than the unconstrained motor.

Tank Material

This comparison shows how lightweight oxidizer tanks affect the system. The tank materials traded were lightweight graphite epoxy and 2219 aluminum. The full-sized, pressure-fed configuration was used to compare the designs. The fuel used was HTPB/Zn/GAP and D6AC steel was the case material.

Table 18 shows the lightweight graphite epoxy tank results in a significantly different design. The graphite epoxy tank design combines inert weight savings and an I_{sp} increase to provide an ideal velocity increase of 284 fps. The I_{sp} increase is a result of the decreased tank inert weight, which allowed chamber pressure and expansion ratio to be higher. This ideal velocity difference is equivalent to a payload increase of 12,350 lb.

With the aluminum tank booster, the tank weighs almost three times as much as the case. With the graphite epoxy tank, case and tank weigh essentially the same. With the graphite epoxy tank, the oxidizer mass fraction is slightly better than the fuel mass fraction. The graphite epoxy design still operated fuel-rich, since fuel-rich products are less damaging to the nozzle throat and to the case insulation.

For the pressure-fed configuration, the graphite epoxy tank produces a lighter, more compact motor, with enhanced payload capability. Pump-fed configurations have low-pressure, low-weight oxidizer tanks, and will not realize as much benefit. Fuels which operate at a higher O/F would show more benefit from a graphite epoxy tank since these fuels require larger oxidizer tanks. While the performance increase from the lightweight tank is attractive, it is not required to make a full-sized hybrid booster feasible. However, for the

Table 17. Length constrained design.

	Unconstrained	Constrained
Booster Total Length (in.)	1,909	1,792
Indeal Velocity (fps)	8,584	8,343
Total Impulse (Mlbf/sec)	323.2	307.3
Max Pressure (psia)	585	747
Vac I_{sp} (sec)	268.8	272.5
Total Booster Weight (lb)	1,374,000	1,310,000
O/F Average	1.42	1.27
Initial Expansion Ratio	4.8	5.9
Burn Time	129.8	114.7

- 150 in. diameter, classical, pressure fed, revised tank weight correlations, TVC nozzle

- Constrained to RSRM length

- Performance penalty – 2.1 fps/inch

90030-12A

62

Table 18. *Tank material study.*

	2219	GRE
ΔV (fps)	8,702	8,986
Weight Case (lb)	25,745	32,394
Weight Tank (lb)	76,580	32,670
P_{max} (psia)	674	919
Vac I_{sp} (sec)	274.0	280.7
Total Booster Weight (lb)	1,338,000	1,276,000
Total Booster Length (in.)	2,012	1,969

- Fullsize, classical, pressure fed
- OX tank single largest inert weight
- GRE allows more compact, lighter motor, higher I_{sp}
  Result: Large payload increase
- Major benefit with pressure feed system
- Not critical hybrid technology

pressure-fed system, the graphite epoxy tank offers the highest performance payoff of the technologies considered in this study.

A trade study not conducted was the use of graphite epoxy instead of D6AC for the case. However, the results of that trade study can be predicted based on the results of the tank material trade. The results would be similar to, but not as dramatic as, using graphite epoxy for the LOX tank since the case is much smaller and has a lower design pressure than the LOX tank. It is not recommended to use graphite epoxy for the case unless graphite epoxy were used for the tank, since the aluminum tank is the single largest inert weight and limits operating pressure. Without graphite epoxy for the tank material, the inert weight and I_{sp} benefits would be small. Graphite epoxy for the case would provide more benefit for low-density fuels like HTPB, which require a relatively long case. Graphite epoxy for the case and tank would allow higher pressure and higher I_{sp} than graphite epoxy for just the tank.

Feed System

In this trade study pressure- and pump-fed oxidizer delivery systems were compared. The trade study was conducted on the fullsized, classical configuration using HTPB/Zn/GAP fuel and 2219 aluminum tanks. The pump-fed system offers a lightweight tank since the tank needs to hold only enough pressure to prime the pump and to provide adequate stiffness for structural stability.

The trends seen in this trade study are similar to those seen in the tank material trade study; however, the pump offers the greatest performance increase seen in this study. Table 19 shows the comparison of the pump- and pressure-fed designs. The ideal velocity increase is equivalent to a payload increase of 18,700 lb. The reduction in tank pressure reduces tank weight by 55,000 lb. This allows the motor to operate at higher pressure and achieve a higher I_{sp}. The higher pressure does result in a heavier fuel case, but allows the use of a lower regression rate fuel. Because regression rate is a function of pressure, the higher pressure pump-fed design delivered a higher average regression rate even though it optimized to a lower regression rate coeffecient.

Combining pump feed with a graphite epoxy tank would not provide significantly more performance than just the pump-feed system since the graphite epoxy tank would not be able to provide much additional weight savings. The pump-feed system would show more advantage for HTPB or similar designs, since these fuels operate at a higher O/F and require larger oxygen tanks.

Design Summaries

This section includes summaries of twelve designs which were presented to General Dynamics. General Dynamics used this information to select one full-sized and one quarter-sized concept for detailed design. Six designs are included for each size. Pump- and pressure-fed system designs are summarized for each hybrid type

Table 19. Feed system study.

	Pressure	Pump
Ideal Velocity (fps)	8,702	9,132
Total Booster Weight (lb)	1,338,000	1,260,000
Tank Weight (lb)	76,580	20,940
Case Weight (lb)	25,750	34,410
Max Pressure (psia)	674	947
Expansion Ratio	5.6	7.3
Average O/F	1.47	1.44
Vac Avg I_{sp}	274.0	281.7
Total Booster Length (in.)	2,012	1,982

- Full-size, classical, HT/Zn/GAP, 150 in. diameter

- Pump offers greatest performance increase
    - Liquid tank has high inert weight
    - Liquid tank forces low operating pressure

- Ideal velocity difference ≅ 18,700 lb payload

- Greater performance difference with HTPB and HT/Zn

- GD trade: performance versus complexity and cost

(classical, afterburner, and gas generator). All the designs employ 2219 aluminum tanks and D6AC steel cases. The designs are summarized in Tables 20 through 23.

The classical and afterburner designs were optimized to a greater extent than the gas generator designs. The difference in performance for the pump- and pressure-fed gas generator designs is due to the difference in inert weight. Gas generator operation was not tailored to the feed system; however, the gas generator designs would show little difference in performance since the gas generator designs have small oxidizer systems.

The tank weights shown for the quarter-sized designs were initially scaled with diameter. For the pressure-fed designs, the liquid tank weight is approximately one-half of what it should be, and operating pressure is higher than it would be if the tank weight were correct. Were the tank weight correlation correctly scaled, there would be more ideal velocity difference between the quarter-sized, pump- and pressure-fed designs. The quarter-sized, pressure-fed motors should have approximately the same ideal velocity and operate at approximately the same pressure as the corresponding full-sized motors. The tank weights are correct for the fullsized motors. Because of the different treatment of tank weights, designs of different diameter cannot be directly compared.

However, these designs can be used to select the best full- and quarter-sized concepts.

Point Designs

After review of the design summaries presented above, General Dynamics rated the classical, pressure-fed configuration as best overall. General Dynamics revised LOX tank weight correlations and asked Thiokol for several point designs. The requested designs were:

- Full-sized, 150-in.-diameter (Figure 50)
- Length-constrained, 150-in.-diameter (Figure 51)
- Quarter-sized, 75-in.-diameter (Figure 52)
- Quarter-sized, 90-in.-diameter (Figure 53)

All the designs employ 2219 aluminum for the oxidizer tank, D6AC steel for the case, HTPB/Zn/GAP fuel, and LOX. These designs also use submerged Flexseal nozzles, rather than fixed external nozzles which were used in the trade studies. These designs were also included in revised oxidizer system weight correlations.

Although these designs have different nozzles and oxidizer system weight correlations, the trends noted in the trade studies still hold. The designs optimized to low pressure and fuel-rich operation. The quarter- and full-sized designs had essentially the same performance. The length- constrained design operated very fuel-rich in order to take advantage of the compact loading afforded by the high-density fuel. The 90-in., quarter-sized motor had the best performance since it

Table 20. Full-sized pump-fed design summaries.

	Classical	Afterburner	Gas Generator
PERFORMANCE PARAMETERS			
AVERAGE PRESSURE,PSIA	607.8	693.3	741.1
MEOP,PSIA	1041.7	1072.1	1150.0
BURNTIME,SEC	129.5	129.6	129.8
AVERAGE THRUST,LBF	2494821.	2492917.	2490309.
AVG VAC SPECIFIC IMPULSE,LBF-SEC/LBM	281.69	288.06	277.78
TOTAL VAC IMPULSE,LBF-SEC	3.23051E+08	3.23067E+08	3.23196E+08
DELTA VELOCITY, FT/SEC	9.13242E+03	9.17945E+03	8.79428E+03
GRAIN GEOMETRY DATA			
WEB THICKNESS,IN	15.95	16.14	17.20
GRAIN LENGTH,IN	478.23	456.37	1400.00
NUMBER OF PORTS	4	4	1
PORT OUTSIDE RADIUS,IN	56.79	56.59	26.61
PORT HEIGHT-TO-RADIUS RATIO	0.57786	0.57158	9.58680
INITIAL PORT BURNBACK DISTANCE,IN	1.00	1.00	1.00
RESERVE DISTANCE BETWEEN PORTS,IN	0.00	0.00	0.00
PORT LENGTH-TO-HYDRAULIC DIA RATIO	15.38	14.87	0.00
GRAIN VOLUMETRIC LOADING	0.7526	0.7588	1.0000
AVERAGE OXIDIZER FLOW RATE	5232.6910	5179.8616	1993.4254
MAXIMUM OXIDIZER FLOW RATE	6824.2252	7039.5759	2897.0205
NOZZLE DATA			
INITIAL THROAT DIAMETER,IN	54.394	50.282	48.200
AVERAGE THROAT AREA,SQ IN	2376.78	2044.24	1881.19
INITIAL EXPANSION RATIO	7.31	8.56	9.31
AVERAGE EXPANSION RATIO	7.15	8.31	9.03
EXIT DIAMETER,IN	147.054	147.085	147.069
CASE DATA			
MOTOR OUTSIDE DIAMETER,IN	150.02	150.01	150.07
CASE LENGTH (BOSS-TO-BOSS),IN	579.41	608.52	1552.90
CASE LENGTH (TAN-TO-TAN),IN	478.23	506.37	1450.00
CASE LENGTH (SKIRT-TO-SKIRT),IN	521.26	549.36	1492.90
FORWARD OPENING DIA,IN	17.58	17.58	15.33
AFT OPENING DIA,IN	78.93	74.37	71.76
CASE CYLINDER THICKNESS,IN	0.4006	0.4120	0.4413
WEIGHTS			
CASE,LBM	34414.	36907.	95982.
INSULATION & LINER,LBM	3867.	4082.	12031.
NOZZLE, LBM	9449.	9378.	9263.
TVC SYSTEM, LBM	2393.	2045.	1879.
MISCELLANEOUS,LBM	344.	333.	582.
IGNITER,LBM	497.	498.	493.
LIQUID TANK,LBM	20935.	20741.	7992.
PRESSURIZATION SYSTEM,LBM	0.	0.	0.
LIQUID FEED SYSTEM,LBM	1113.	1149.	731.
PUMP MASS,LBM	1649.	1668.	1415.
TURBINE FUEL,LBM	7945.	8888.	3640.
FUEL CONSUMED,LBM	469230.	450246.	904799.
SLIVER,LBM	3133.	3118.	-1.
TOTAL OXIDIZER CONSUMED,LBM	677573.	671279.	258709.
OX. INJECTED THROUGH GRAIN,LBM	677573.	585539.	258709.
OX. BYPASSED TO MIXING CHAMBER,LBM	0.	85740.	0.
OXIDIZER RESERVE LEFT IN TANK,LBM	6776.	6713.	2587.
INTERSTAGE INERTS,LBM	4592.	4622.	2098.
TOTAL MOTOR INERTS,LBM	89163.	91254.	135053.
TOTAL PROPELLANT CONSUMED,LBM	1146803.	1121525.	1163508.
TOTAL MOTOR,LBM	1235966.	1212779.	1298561.
MOTOR MASS FRACTION	0.9279	0.9248	0.8960
INPUT PAYLOAD WEIGHT	16291.0000	16291.0000	16291.0000
GROSS LIFT OFF WEIGHT (GLOW)	1260202.	1237957.	1318492.

Table 21. *Full-sized pressure-fed design summaries.*

	Classical	Afterburner	Gas Generator
PERFORMANCE PARAMETERS			
AVERAGE PRESSURE, PSIA	480.3	468.5	741.1
MEOP, PSIA	741.7	717.0	1150.0
BURNTIME, SEC	129.1	129.8	129.8
AVERAGE THRUST, LBF	2501077.	2489515.	2490309.
AVG VAC SPECIFIC IMPULSE, LBF-SEC/LBM	274.04	275.09	277.78
TOTAL VAC IMPULSE, LBF-SEC	3.22929E+08	3.23129E+08	3.23196E+08
DELTA VELOCITY, FT/SEC	8.70293E+03	8.71827E+03	8.58140E+03
GRAIN GEOMETRY DATA			
WEB THICKNESS, IN	15.90	16.63	17.20
GRAIN LENGTH, IN	486.94	470.43	1400.00
NUMBER OF PORTS	4	4	1
PORT OUTSIDE RADIUS, IN	56.96	56.25	26.61
PORT HEIGHT-TO-RADIUS RATIO	0.58052	0.55679	9.58680
INITIAL PORT BURNBACK DISTANCE, IN	1.00	1.00	1.00
RESERVE DISTANCE BETWEEN PORTS, IN	0.00	0.00	0.00
PORT LENGTH-TO-HYDRAULIC DIA RATIO	15.55	15.79	0.00
GRAIN VOLUMETRIC LOADING	0.7500	0.7730	1.0000
AVERAGE OXIDIZER FLOW RATE	5424.2430	5412.7027	1993.4254
MAXIMUM OXIDIZER FLOW RATE	7054.3542	7377.3342	2897.0205
NOZZLE DATA			
INITIAL THROAT DIAMETER, IN	62.270	62.897	48.200
AVERAGE THROAT AREA, SQ IN	3094.42	3157.11	1881.19
INITIAL EXPANSION RATIO	5.57	5.46	9.31
AVERAGE EXPANSION RATIO	5.48	5.37	9.03
EXIT DIAMETER, IN	146.957	146.951	147.069
CASE DATA			
MOTOR OUTSIDE DIAMETER, IN	150.01	150.04	150.07
CASE LENGTH (BOSS-TO-BOSS), IN	585.54	618.79	1552.90
CASE LENGTH (TAN-TO-TAN), IN	486.94	520.43	1450.00
CASE LENGTH (SKIRT-TO-SKIRT), IN	530.36	563.89	1492.90
FORWARD OPENING DIA, IN	17.58	17.58	15.33
AFT OPENING DIA, IN	88.23	89.08	71.76
CASE CYLINDER THICKNESS, IN	0.2880	0.2788	0.4413
WEIGHTS			
CASE, LBM	25745.	26270.	95982.
INSULATION & LINER, LBM	3855.	4076.	12031.
NOZZLE, LBM	9297.	9336.	9263.
TVC SYSTEM, LBM	3136.	3199.	1879.
MISCELLANEOUS, LBM	350.	346.	582.
IGNITER, LBM	494.	494.	493.
LIQUID TANK, LBM	76584.	75057.	39158.
PRESSURIZATION SYSTEM, LBM	8145.	7899.	4665.
LIQUID FEED SYSTEM, LBM	1061.	1074.	783.
PUMP MASS, LBM	0.	0.	0.
TURBINE FUEL, LBM	0.	0.	0.
FUEL CONSUMED, LBM	478055.	472096.	904799.
SLIVER, LBM	3144.	3549.	-1.
TOTAL OXIDIZER CONSUMED, LBM	700356.	702547.	258709.
OX. INJECTED THROUGH GRAIN, LBM	700356.	607186.	258709.
OX. BYPASSED TO MIXING CHAMBER, LBM	0.	95361.	0.
OXIDIZER RESERVE LEFT IN TANK, LBM	7004.	7025.	2587.
INTERSTAGE INERTS, LBM	4617.	4656.	2098.
TOTAL MOTOR INERTS, LBM	143431.	142983.	169520.
TOTAL PROPELLANT CONSUMED, LBM	1178411.	1174643.	1163508.
TOTAL MOTOR, LBM	1321842.	1317626.	1333028.
MOTOR MASS FRACTION	0.8915	0.8915	0.8728
INPUT PAYLOAD WEIGHT	16291.0000	16291.0000	16291.0000
GROSS LIFT OFF WEIGHT (GLOW)	1338133.	1333917.	1349319.

Table 22. Quarter-sized pump-fed design summaries.

	<u>Classical</u>	<u>Afterburner</u>	<u>Gas Generator</u>
PERFORMANCE PARAMETERS			
AVERAGE PRESSURE,PSIA	808.6	756.7	776.9
MEOP,PSIA	1305.5	1199.8	1231.7
BURNTIME,SEC	129.7	129.8	129.8
AVERAGE THRUST,LBF	622860.	622359.	622633.
AVG VAC SPECIFIC IMPULSE,LBF-SEC/LBM	290.18	289.66	278.06
TOTAL VAC IMPULSE,LBF-SEC	8.07827E+07	8.07807E+07	8.07874E+07
DELTA VELOCITY, FT/SEC	9.13592E+03	9.11925E+03	8.88702E+03
GRAIN GEOMETRY DATA			
WEB THICKNESS,IN	17.41	16.90	17.50
GRAIN LENGTH,IN	457.83	461.62	940.00
NUMBER OF PORTS	1	1	1
PORT OUTSIDE RADIUS,IN	18.99	19.50	26.61
PORT HEIGHT-TO-RADIUS RATIO	17.41340	16.89952	9.58680
INITIAL PORT BURNBACK DISTANCE,IN	1.00	1.00	1.00
RESERVE DISTANCE BETWEEN PORTS,IN	0.00	0.00	0.00
PORT LENGTH-TO-HYDRAULIC DIA RATIO	12.05	11.84	0.00
GRAIN VOLUMETRIC LOADING	0.7278	0.7130	1.0000
AVERAGE OXIDIZER FLOW RATE	1275.5638	1289.3942	497.7216
MAXIMUM OXIDIZER FLOW RATE	1676.5499	1746.2855	732.6467
NOZZLE DATA			
INITIAL THROAT DIAMETER,IN	22.779	23.620	23.200
AVERAGE THROAT AREA,SQ IN	432.51	463.25	446.39
INITIAL EXPANSION RATIO	10.06	9.29	9.63
AVERAGE EXPANSION RATIO	9.48	8.79	9.12
EXIT DIAMETER,IN	72.243	71.989	71.995
CASE DATA			
MOTOR OUTSIDE DIAMETER,IN	75.05	74.99	75.00
CASE LENGTH (BOSS-TO-BOSS),IN	510.15	563.58	1042.14
CASE LENGTH (TAN-TO-TAN),IN	457.83	511.62	990.00
CASE LENGTH (SKIRT-TO-SKIRT),IN	479.17	533.02	1011.38
FORWARD OPENING DIA,IN	15.33	15.33	15.33
AFT OPENING DIA,IN	39.01	39.98	39.30
CASE CYLINDER THICKNESS,IN	0.2511	0.2311	0.2371
WEIGHTS			
CASE,LBM	9551.	9660.	17603.
INSULATION & LINER,LBM	1766.	1986.	4453.
NOZZLE, LBM	2078.	2070.	2041.
TVC SYSTEM, LBM	420.	451.	435.
MISCELLANEOUS,LBM	110.	109.	192.
IGNITER,LBM	492.	492.	492.
LIQUID TANK,LBM	6578.	6655.	2568.
PRESSURIZATION SYSTEM,LBM	0.	0.	0.
LIQUID FEED SYSTEM,LBM	578.	566.	356.
PUMP MASS,LBM	1300.	1290.	1089.
TURBINE FUEL,LBM	2528.	2401.	950.
FUEL CONSUMED,LBM	112951.	111516.	225961.
SLIVER,LBM	0.	0.	-3.
TOTAL OXIDIZER CONSUMED,LBM	165436.	167360.	64580.
OX. INJECTED THROUGH GRAIN,LBM	165436.	154119.	64580.
OX. BYPASSED TO MIXING CHAMBER,LBM	0.	13242.	0.
OXIDIZER RESERVE LEFT IN TANK,LBM	1654.	1674.	646.
INTERSTAGE INERTS,LBM	623.	627.	353.
TOTAL MOTOR INERTS,LBM	25149.	25580.	30226.
TOTAL PROPELLANT CONSUMED,LBM	278387.	278877.	290541.
TOTAL MOTOR,LBM	303536.	304457.	320767.
MOTOR MASS FRACTION	0.9171	0.9160	0.9058
INPUT PAYLOAD WEIGHT	4072.0000	4072.0000	4072.0000
GROSS LIFT OFF WEIGHT (GLOW)	310136.	310930.	325789.

Table 23. *Quarter-sized pressure-fed design summaries.*

	Classical	Afterburner	Gas Generator
PERFORMANCE PARAMETERS			
AVERAGE PRESSURE,PSIA	748.7	556.2	776.9
MEOP,PSIA	1223.4	868.1	1231.7
BURNTIME,SEC	130.1	130.3	129.8
AVERAGE THRUST,LBF	621096.	620571.	622633.
AVG VAC SPECIFIC IMPULSE,LBF-SEC/LBM	287.03	279.88	278.06
TOTAL VAC IMPULSE,LBF-SEC	8.08235E+07	8.08326E+07	8.07874E+07
DELTA VELOCITY, FT/SEC	8.89479E+03	8.94898E+03	8.81584E+03
GRAIN GEOMETRY DATA			
WEB THICKNESS,IN	17.47	16.71	17.50
GRAIN LENGTH,IN	479.31	480.13	940.00
NUMBER OF PORTS	1	1	1
PORT OUTSIDE RADIUS,IN	18.93	19.77	26.61
PORT HEIGHT-TO-RADIUS RATIO	17.46813	16.71271	9.58680
INITIAL PORT BURNBACK DISTANCE,IN	1.00	1.00	1.00
RESERVE DISTANCE BETWEEN PORTS,IN	0.00	0.00	0.00
PORT LENGTH-TO-HYDRAULIC DIA RATIO	12.66	12.14	0.00
GRAIN VOLUMETRIC LOADING	0.7295	0.7063	1.0000
AVERAGE OXIDIZER FLOW RATE	1253.4289	1331.0249	497.7216
MAXIMUM OXIDIZER FLOW RATE	1655.0406	1809.3185	732.6467
NOZZLE DATA			
INITIAL THROAT DIAMETER,IN	23.898	28.282	23.200
AVERAGE THROAT AREA,SQ IN	471.53	650.47	446.39
INITIAL EXPANSION RATIO	9.08	6.50	9.63
AVERAGE EXPANSION RATIO	8.64	6.28	9.12
EXIT DIAMETER,IN	72.009	72.095	71.995
CASE DATA			
MOTOR OUTSIDE DIAMETER,IN	75.01	75.03	75.00
CASE LENGTH (BOSS-TO-BOSS),IN	531.31	580.59	1042.14
CASE LENGTH (TAN-TO-TAN),IN	479.31	530.13	990.00
CASE LENGTH (SKIRT-TO-SKIRT),IN	500.70	551.76	1011.38
FORWARD OPENING DIA,IN	15.33	15.33	15.33
AFT OPENING DIA,IN	40.03	45.05	39.30
CASE CYLINDER THICKNESS,IN	0.2356	0.1690	0.2371
WEIGHTS			
CASE,LBM	9325.	7395.	17603.
INSULATION & LINER,LBM	1852.	2045.	4453.
NOZZLE, LBM	2046.	2051.	2041.
TVC SYSTEM, LBM	462.	647.	435.
MISCELLANEOUS,LBM	115.	112.	192.
IGNITER,LBM	492.	490.	492.
LIQUID TANK,LBM	12954.	10608.	5156.
PRESSURIZATION SYSTEM,LBM	3129.	2360.	1247.
LIQUID FEED SYSTEM,LBM	593.	538.	378.
PUMP MASS,LBM	0.	0.	0.
TURBINE FUEL,LBM	0.	0.	0.
FUEL CONSUMED,LBM	118477.	115434.	225961.
SLIVER,LBM	0.	0.	-3.
TOTAL OXIDIZER CONSUMED,LBM	163109.	173373.	64580.
OX. INJECTED THROUGH GRAIN,LBM	163109.	161078.	64580.
OX. BYPASSED TO MIXING CHAMBER,LBM	0.	12295.	0.
OXIDIZER RESERVE LEFT IN TANK,LBM	1631.	1734.	646.
INTERSTAGE INERTS,LBM	614.	631.	353.
TOTAL MOTOR INERTS,LBM	33212.	28611.	32994.
TOTAL PROPELLANT CONSUMED,LBM	281586.	288807.	290541.
TOTAL MOTOR,LBM	314798.	317418.	323536.
MOTOR MASS FRACTION	0.8945	0.9099	0.8980
INPUT PAYLOAD WEIGHT	4072.0000	4072.0000	4072.0000
GROSS LIFT OFF WEIGHT (GLOW)	318870.	321490.	327608.

Configuration	Classical	Ideal Velocity	8584 fps
Feed System	Pressure	Total Booster Weight	1,374,000 lb
Oxidizer Tank	2219 Al	Vacuum Average I_{sp}	268.8 sec
Fuel Case	D6 AC	Maximum Pressure	585.0 psia
Fuel	HT/Zn/GAP	Fuel Weight	497,700 lb
Oxidizer	LOX	OX Weight	704,600 lb
Grain Design	4-port wagon wheel	Tank Weight	81,680 lb
Nozzle	Submerged flex bearing	Case Weight	27,730 lb
		Total Inert Weight	155,300 lb
		Motor Mass Fraction	0.886

0.0 in. 0.00 in.

142.5 in. 150.0 in.

1147.1 in. 150.0 in.

1909.2 in. 147.19 in.

1217.1 in.
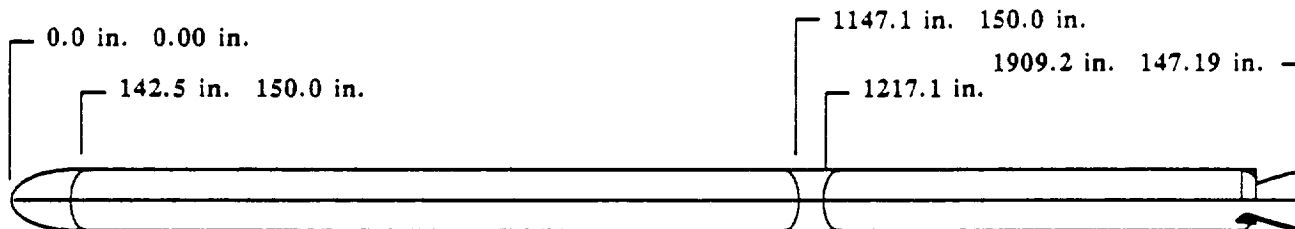
Figure 50. Full-sized design.

Configuration	Classical	Ideal Velocity	8343 fps
Feed System	Pressure	Total Booster Weight	1,310,000 lb
Oxidizer Tank	2219 Al	Vacuum Average I_{sp}	272.5 sec
Fuel Case	D6 AC	Maximum Pressure	747.0 psia
Fuel	HT/Zn/GAP	Fuel Weight	496,600 lb
Oxidizer	LOX	OX Weight	631,400 lb
Grain Design	2-port wagon wheel	Tank Weight	88,260 lb
Nozzle	Submerged flex bearing	Case Weight	26,000 lb
		Total Inert Weight	165,660 lb
		Motor Mass Fraction	0.872

0.0 in. 0.00 in.

142.5 in. 150.0 in.

1041.3 in. 150.0 in.

1791.7 in. 147.40 in.

1109.6 in.
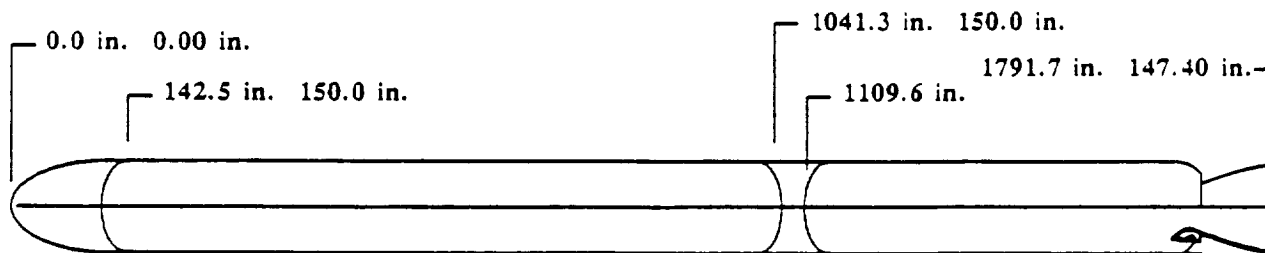
CSA023902a

Figure 51. Length-constrained design.

69

Configuration.	Classical	Ideal Velocity	8525 fps
Feed System	Pressure	Total Booster Weight	345,970 lb
Oxidizer Tank	2219 Al	Vacuum Average I_{sp}	268.2 sec
Fuel Case	D6 AC	Maximum Pressure	580.0 psia
Fuel	HT/Zn/GAP	Fuel Weight	124,600 lb
Oxidizer	LOX	OX Weight	176,400 lb
Grain Design	CP	Tank Weight	20,300 lb
Nozzle	Submerged flex bearing	Case Weight	5,300 lb
		Total Inert Weight	40,850 lb
		Motor Mass Fraction	0.881

0.0 in. 0.00 in.

71.3 in. 75.0 in.

1114.5 in. 75.0 in.

1149.8 in.

1774.0 in. 72.26 in.
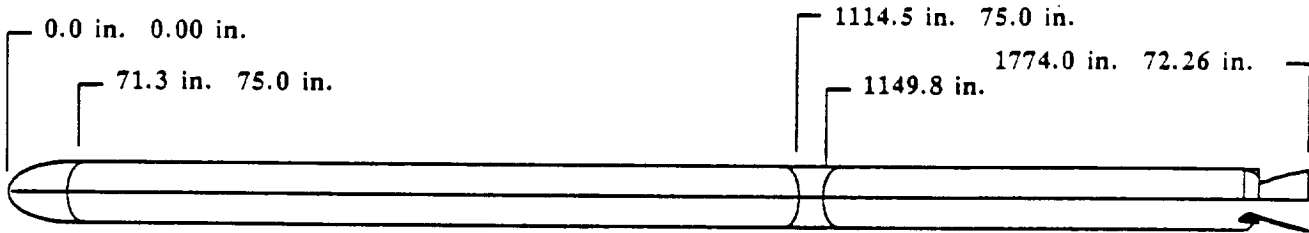
Figure 52. Quarter-sized 75-in.-diameter design.

Configuration	Classical	Ideal Velocity	8623 fps
Feed System	Pressure	Total Booster Weight	337,500 lb
Oxidizer Tank	2219 Al	Vacuum Average I_{sp}	274.7 sec
Fuel Case	D6 AC	Maximum Pressure	600.0 psia
Fuel	HT/Zn/GAP	Fuel Weight	128,500 lb
Oxidizer	LOX	OX Weight	165,500 lb
Grain Design	2-Port Wagon Wheel	Tank Weight	19,550 lb
Nozzle	Submerged Flex Bearing	Case Weight	5,440 lb
		Total Inert Weight	39,380 lb
		Motor Mass Fraction	0.882

0.0 in. 0.00 in.

85.6 in. 90.0 in.

753.3 in. 90.0 in.

787.3 in.

1247.67 in. 87.61 in.
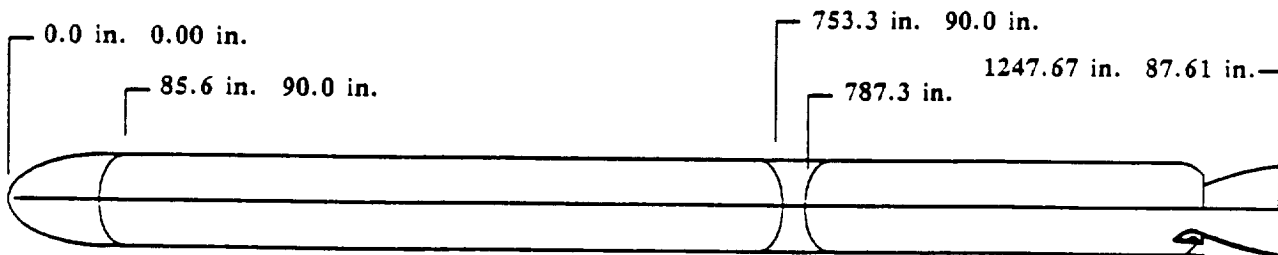
CSA023901a

Figure 53. Quarter-sized 90-in.-diameter design

was the least affected by the nozzle exit diameter constraint. However, the 90-in. motor required a two-port grain while the 75-in. motor offered a single-port grain configuration.

The figures indicate the general shape of the motors and show the relative sizes of the fuel and oxidizer portions. The L/D for all the motors is in the conventional range, except for the 75-in. design which has an L/D of 24. This design would tend to have structural stability problems. For all the designs, the case represents less than one-half of the overall length. These cases have a one-segment joint, but may be short enough that joints are not required. Storing the oxidizer in a stretched external tank would produce very short boosters.

4.0 TECHNOLOGY ACQUISITION PLANS

Trade studies and analyses were conducted to identify the optimum hybrid booster concept. The trade studies also served to identify deficiencies in the existing technology base. The technology deficiencies identified for the classical hybrid concept are summarized as follows:

- Nozzle
  - Optimum materials for the hybrid environment have not been identified
  - Engineering data do not exist over the wide range of hybrid operating conditions
- Propellant
  - Low-cost scalable approaches for regression rate tailorability have not been demonstrated
- Insulation
  - Engineering data for candidate materials in adequate for hybrid aerothermal environment and range of operating conditions
- Ignition
  - Low-cost, innocuous ignition systems specifically for hybrid applications have not been developed
- Flow and Combustion Modeling
  - Scale-up of hybrid test data has historically been unsuccessful without the capability to model fundamental flow/combustion phenomena
  - Limiting parameters such as L/D, maximum flux level, etc., have not been established for GOX injection

A technology acquisition plan was prepared to address each of these deficiencies. Each of the technology acquisition plans is then integrated into an overall program plan for Phase II. The recommended Phase II program builds on output from Phase I to further refine and incorporate any additional NASA requirements or design definition; technology acquisition activities can then be focused at the development of a specific design concept rather than broad-based technology development. The overall Phase II program culminates with the testing of a 160,000-lb thrust motor to provide for verification of developed technology. The overall approach for Phase II is illustrated in Figure 54.

Each of the technology acquisition plans has been structured to fit within an overall 2-year program as illustrated in Figure 55. As an integrated program, overall cost is significantly less than if each of the technology acquisition plans was performed separately. Thiokol developed overall costs for an integrated Phase II program rather than the cost for individual technology acquisition plans. Each of the technology acquisition plans will utilize common motor tests to generate relevant data. Four sizes of motors are anticipated: laboratory scale (2-in.), test bed (10-in.), subscale (24-in.), and technology verification (48-in.). A preliminary test matrix was developed to establish the minimum number of tests required to satisfy the requirements of each technology acquisition plan. A total of 100 laboratory scale, 32 test bed, 12 subscale, and 1 verification motors was estimated. The laboratory-scale motor provides for economical development and comparative assessment of fuel formulations and ignition systems. The test bed motor (same as the preburner for subscale motor) provides for evaluation of key operating parameters such as O/F ratios, aft mixing, and uniform grain recession. It also provides a vehicle for economical evaluation of nozzle and insulation materials. The 24-in. subscale motor provides for preliminary evaluation of the overall motor concept and confirmation of engineering predictions. The 48-in. motor provides for an intermediate step for scaling the hybrid concept up to large-scale booster applications. It provides for early verification technology development efforts. Predicted thrust and oxidizer requirements are illustrated in Figure 56. The technology acquisitions plans and Phase II costs are discussed in the sections that follow.

Technology Acquisition Plans

The individual Technology Acquisition plans are summarized in Figures 57 through 61. Each technology plan is categorized as enabling, engineering development, or enhancing. Enabling technology is required for development of a hybrid propulsion system. Engineering development is necessary to generate engineering data for design of hybrid booster. Enhancing technology are those efforts that make the hybrid more attractive but are not essential for its development.

Nozzle and insulation materials Technology Acquisition plans are categorized as engineering development. The operating environment of a hybrid is substantially

Technology

- Nozzle Materials
- Insulation Materials
- Propellant Development
- Flow and Combustion Modeling
- Hybrid Ignition

Test/Design Verification

- Analysis
- Subscale Testing

- Oxy/Acetelyne Tests
- Subscale Tests
- Analysis

- Labscale
- Subscale Tests
- Analysis

- Code Development
- Global Combustion Model
- Geometric Constraints

- Alternate Approaches
- Subscale Tests

Phase I →

→ Technology Acquisition Motor

CSA024101a

- Integrated test program
  - 10-in. motor
  - 24-in. motor

Figure 54. Phase II Flow Diagram.

different from that of an SRM, and the performance of materials within this environment has not been adequately characterized. These technology acquisition plans are designed to identify optimum materials and characterize their char, erosion, and structural integrity in the hybrid environment.

Propellant development and flow and combustion field modeling technology acquisition plans are categorized as enabling. The development of tailorable regression rate fuels and the ability to analyze internal areothermal/combustion processes in multiport fuel grains is essential for hybrid development.

Fuels with a low regression rate dictate grain designs with an unreasonable amount of port surface area. Typically, a multiport wagon wheel grain configuration is employed to achieve the necessary surface area. For example, a low regression rate fuel, such as HTPB, would require a 12-port grain configuration for a shuttle booster application, whereas the performance analysis using a high regression rate fuel, HTPB/GAP/Zn, indicated that four-port grain design is feasible. The greater number of ports results in a lower volumetric loading and, consequently, a larger overall booster. A four-port grain design with a high regression rate fuel

results in a much smaller booster design. A four-port grain design can be shown to fit within current shuttle SRM envelope and still offer a performance advantage.

Historically, high regression rates have not been demonstrated as illustrated in Figure 62. The desired operating capability, in terms of regression rate, has not been achieved using conventional approaches. However, fuel additives identified in laboratory-scale testing at Thiokol offer the potential of achieving the desired operating capability. Fuels decomposing to short-lived reactive intermediates, such as a CN radical, are the key.

In addition to requiring a high regression rate, tailorability of regression rate is necessary to optimize grain design. In its simplest form, regression follows the relationship

$$R = AG^m P^n$$

where A is a constant, G is port flux, P is motor pressure, and m and n are experimentally determined exponents. The ability to dictate the flux exponent m by fuel formulation additives allows simple progressive grain designs. The ability to dictate the pressure exponent n allows for fuel regression to follow motor throttling and operate more efficiently.

72
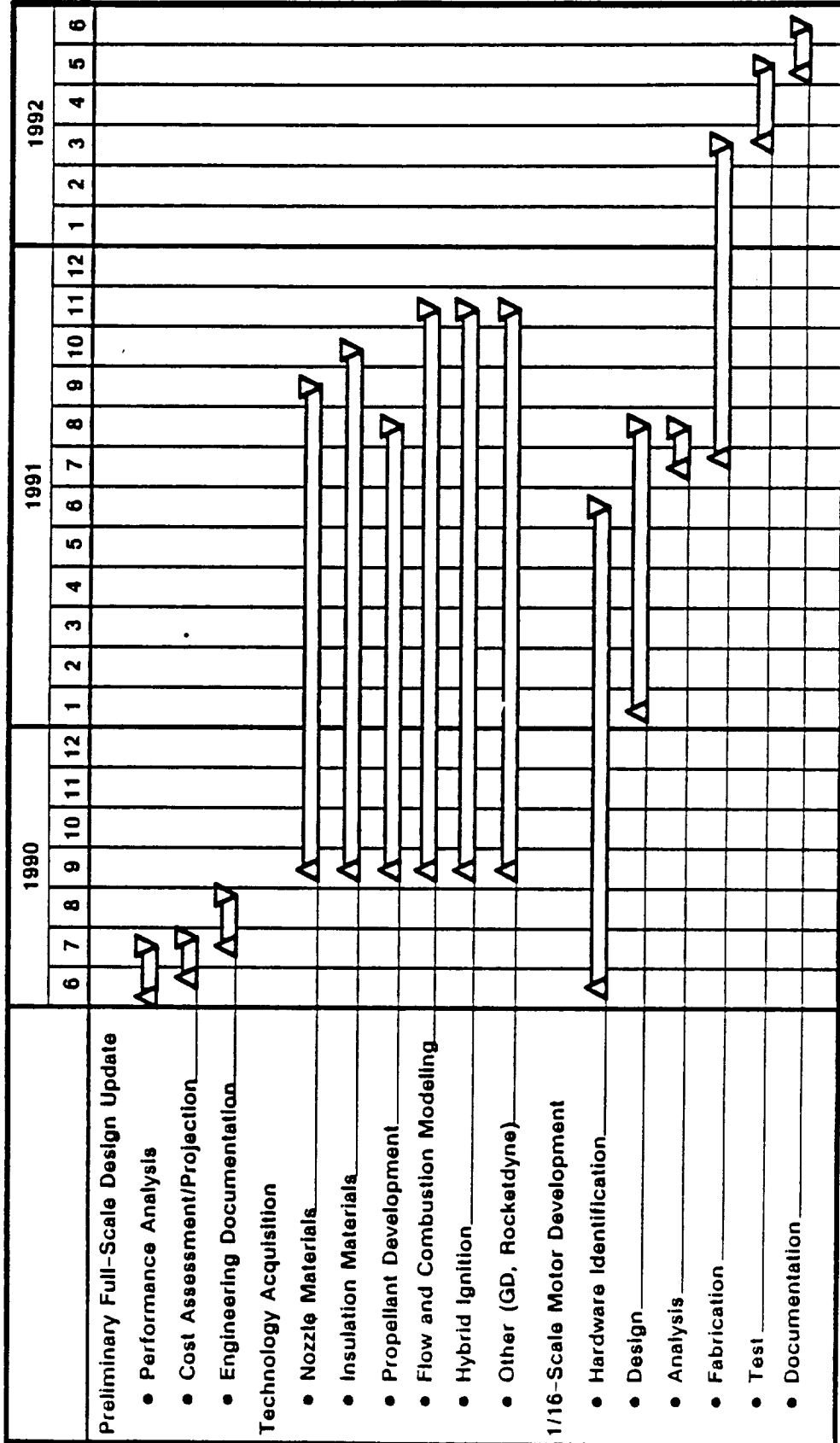
Figure 55. Overall Phase II Schedule.

CSA024099a

73
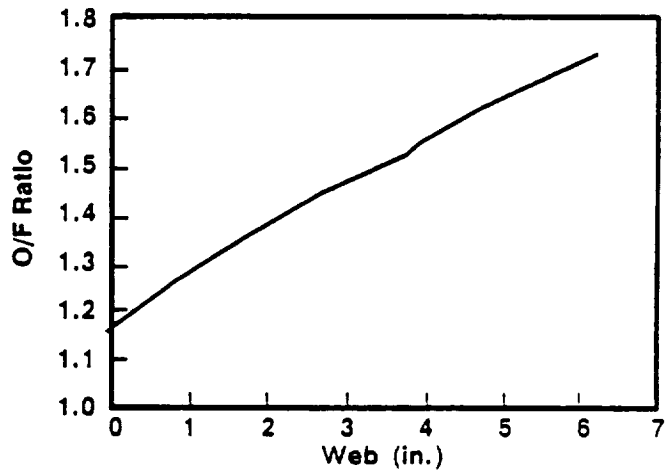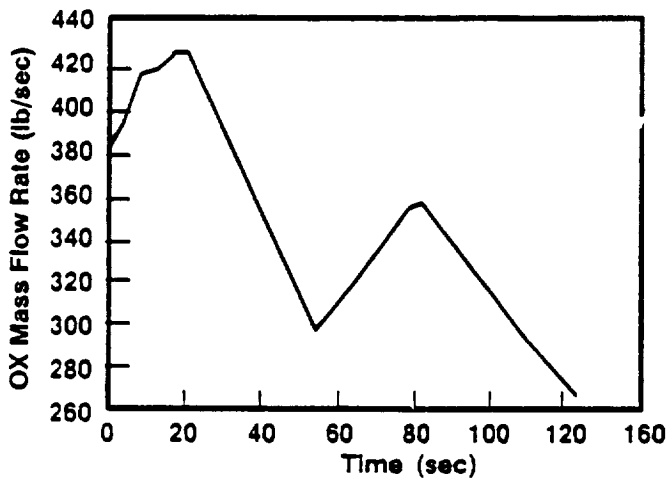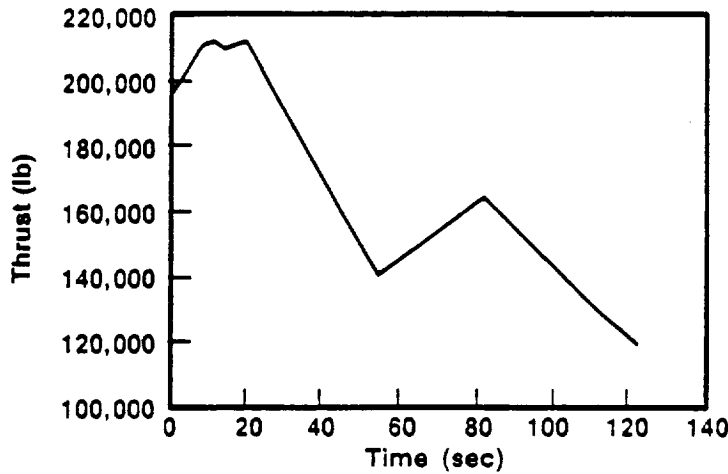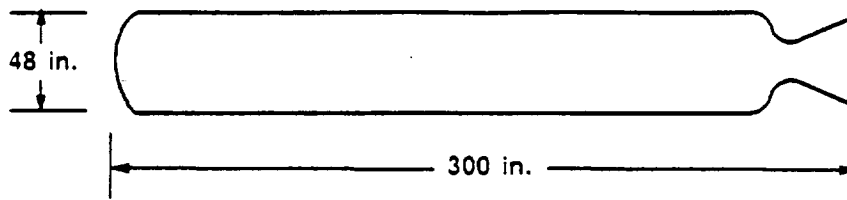
Figure 56. Technology acquisition motor.

The flow and combustion modeling technology acquisition plan is also categorized as enabling. Currently, the combination of unique aerodynamics/combustion and time-dependent processes within a hybrid have no analogies to either solid or liquid motor analyses. Development of analytical methodologies is required to address grain regression as a function of port flux and pressure, predict fuel/oxidizer mixing and after-burning, and minimize pressure oscillations associated with the liquid oxidizer phase transition and the solid phase combustion. A computational fluid dynamics (CFD) approach is required to pursue studies of fundamental phenomena in combustion and mixing and provide the essential vehicle for design scale-up. Additionally, a ballistics analysis code is required to provide for economical grain design and motor performance prediction.

Development of a hybrid ignition system is considered an enhancing technology. Historically, it has been shown that hybrid ignition and flame speed is a function of initial oxidizer flow rate. Ignition of a hybrid can be accomplished with any of the conventional, off-the-shelf pyrotechnic or hypergolic ignition systems. However, the nature of a hybrid motor readily lends itself to simpler, safer, less expensive systems.

74

Plan Title: Nozzle Materials	Technology Importance:

☐ Enabling
☒ Engineering Development
☐ Enhancing

Objective:

Overall—Develop/identify a nozzle/nozzle materials that can operate satisfactorily in a large-scale hybrid motor

Specific

Identify optimum materials for selected hybrid concepts

Generate engineering data over the wide range of hybrid operating conditions to facilitate design of large-scale nozzles

Performance data	Manufacturing data
—Erosion rate	—Materials
—Char depth	—Scrappage
—Temperature distribution	—Tooling
—Weight	—Inspection
—Uniform/reproducible erosion/char	
—Structural integrity	

Technical Approach:

Input

Requirements/Configuration
- Geometry/size
- Material
- Operating parameters
  - Pressure
  - Time
  - Exhaust species, temperature
  - Flow
- Cost
- Reliability
- NDE
- Manufacturing
- Performance
  - I_{sp}
  - Throat erosion rate

Task 1

Analytical Evaluation of Candidate

Materials
- Environment
  - Flame temperatures
  - Oxidation/reduction
  - Flow reaction conditions
  - Beta
- Performance
  - Erosion rate
  - Char depth
  - Temperature distributions

Task 2

Static Test
Selected Materials in 10-in. Motor
- Thermocouples
- Erosion/char
- Integrity

Task 3
- Correlate data
- Modify predictive techniques

Additional Data as Needed
- Thermal conductivity
- Thermal expansion
- Density/char

Task 4
- Finalize material selection for entrance, throat, and exit
- Verify in 24-in.-dia motor tests
- Assess scale-up

Task 5

Selected Material Characterization Tests
- Thermal/mechanical

160-K Thrust Motor Firing

CSA02407ia-1

Figure 57. Nozzle materials technology acquisition plan.

Task Summary:

- Task 1—Analytical Material Evaluation

    - Evaluate erosion, char, and temperature distributions in key nozzle regions:

        —Entrance
        —Throat
        —Exit

    - Analytically evaluate candidate materials

        —CCP   —ATJ   —C-C
        —SCP   —PG   —C-C with tungsten boron
        —Quartz CP   —Aluminum oxide/   —Silicon carbide/
        —K–615   aluminum oxide   metalized resin
        (high–density PAN)

    - Determine effectiveness of design approaches

        —Boundary layer control
        —Heat sink
        —Shroud

- Task 2—Material Testing/Evaluation

    - Conduct 10-in. motor tests to evaluate selected materials and the effect of motor operating conditions

- Task 3—Data Correlation

    - Evaluate test data and modify predictive techniques as necessary

- Task 4—Design/Material Selection Verification

    - Conduct 24-in. motor tests to evaluate inlet material, throat material, exit material, and advanced design concept(s)

    - Scale-up evaluation

- Task 5—Material Characterization

    - Obtain thermomechanical properties for analysis, as necessary

Figure 57. Nozzle materials technology acquisition plan (cont).

Months	1	2	3	4	5	6	7	8	9	10	11	12	13	14
Task 1—Analytical Material Evaluation	△						▽							
Task 2—Material Testing 10-in. Motor Tests				△			▽							
Task 3—Predictive Techniques				△			▽							
Task 4—Design Concept Evaluation								△			▽			
Task 5—Selected Characterization												△	▽	
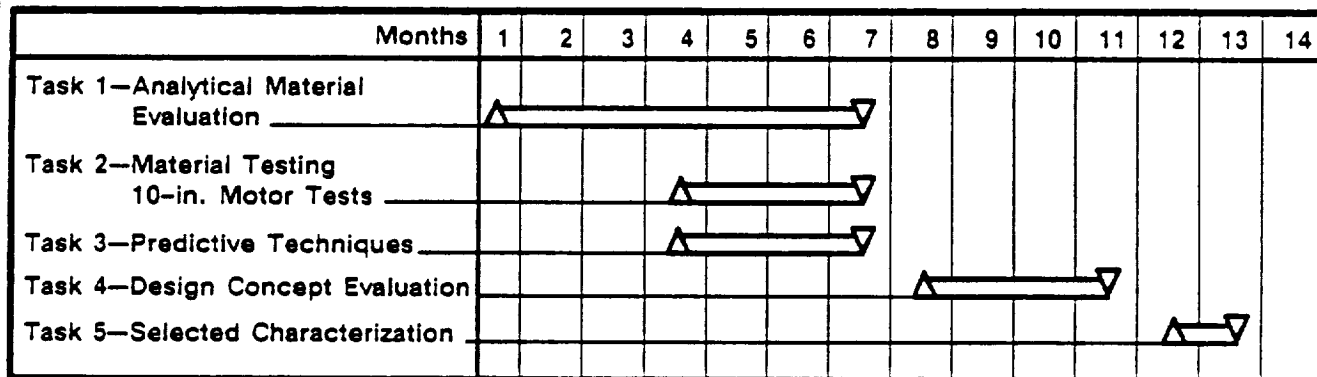
CSA024071a-3

Figure 57. Nozzle materials technology acquisition plan (cont).

77

Plan Title: Propellant Development	Technology Importance:
	☒ Enabling
	☐ Engineering Development
	☐ Enhancing

Objective:

- Overall—Identify and develop optimum fuel formulation for full-scale hybird booster

- Specific

    - Identify fuels and additives which allow regression rate tailoring of up to 0.2 to 0.5 at 1000 psi with 02 mass flux of 0.2 to 1.0 lb/sec/in.^{2}

    - Optimum approach based on cost, ballistics, and performance

    - Conduct laboratory-scale analysis and development

    - Identify full-scale cost and availability potential

    - Demonstrate selected fuel and oxidizer at 24-in. motor-scale level

Technical Approach:

CSA024072a

Figure 58. Technology acquisition plan for insulation material development.

78

Task Summary:

- **Task 1—Initial Development**

  - Conduct laboratory-scale motor (100-lb thrust)

    —P_c 200 to 1,000 psi
    —Mass flux 0.1 to 0.5 lb/sec/in.^{2}

  - Evaluate effectiveness of metals—Zn, W, Al

  - Evaluate accelerators—Gap and analogs

  - Provide initial assessment of oxidizer enhancement—Ozone

  - Determine preliminary acoustic/geometry effects (L/D, configuration)

  - Select fuels for 10-in. evaluation

- **Task 2—Cost/Performance Analysis**

  - Identify additive, fuel component availability/cost

    —Manufacturer (vendor) coordination
    —Criteria for LCC analysis

- **Task 3—10-in. Motor Evaluation**

  - Select three candidate formulations—Base on performance/cost analysis

  - Conduct six tests on each formulation—Three flux levels, three pressures

- **Task 4—24-in. Motor Evaluation**

  - Select fuel for 24-in. motor test

    —Primary candidate
    —Backup

  - Verify regression rate assumptions at high flux levels and variety of pressures

CSA024072a-2

Figure 58. Technology acquisition plan for insulation material development (cont).

79

Figure 58. Technology acquisition plan for
insulation material development (cont).

Plan Title: Ignition System Development	Technology Importance:
	☐ Enabling
	☐ Engineering Development
	☒ Enhancing

Objective:

- Overall—Evaluate ignition system concepts to determine the optimum characteristics required to safely induce steady-state combustion in a shuttle-sized hybrid rocket motor

- Specific

    - Evaluate the following ignition system concepts through laboratory testing, subscale motor tests, and analytical studies

        - Hypergolic ignition systems

            —Liquid charge hypergolic with fuel grain
            —Liquid charge hypergolic with the oxidizer

        - Grain heating techniques

            —Resistive wires embedded or bonded to fuel grain
            —Localized heat source(s)

                —Laser
                —Heat lamp
                —Resistive wires attached to grain ports

    - Pyrogen ignition system

Task Summary:

- **Task 1—Concept Screening and Requirements Definition**

    - Establish feasibility and screen candidates for further study. Determine ignition system requirements based on NASA requirements, input from primes, tests, and analytical data

- **Task 2—Design Ignition System for 10-in. Subscale Motor Tests**

    - Create preliminary design of ignition system(s) for 10-in. motor tests. Perform analysis, laboratory, and ignition system bench tests to verrify design(s)

- **Task 3—10-in. Subscale Motor Tests**

    - Fabricate ignition systems for 10-in. motor tests, evaluate ignition data and hardware performance. Correlate ignition model with data from motor tests

- **Task 4—Design Ignition System for 24-in. Subscale Tests**

    - Select ignition system design for 24-in. motor tests. Scale up selected design. Perform tests and analysis to support design

CSA024073a-1

Figure 59. Technology acquisition plan for
ignition system development.

81

- **Task 5—24-in. Subscale Motor Tests**

  - Fabricate ignition systems for 24-in. motor tests; evaluate ignition data and hardware performance

- **Task 6—Recommend Baseline Ignition System Design**

  - Establish baseline ignition system designs for shuttle sized and 1/4-scale motors

Month	1	2	3	4	5	6	7	8	9	10	11	12	13	14	15
Task 1															
Requirements Definition and Concept Screening	▭	▭													
Task 2															
Preliminary Ignition System Design for 10-in. Motors			▭	▭											
Ignition Bench Tests					▭										
Task 3															
Fabricate Ignition Components for 10-in. Subscale Tests							▭								
10-in. Subscale Tests and Data Evaluation									▭						
Task 4															
Design Ignition System for 24-in. Subscale Tests											▭				
Ignition Bench Tests												▭			
Task 5															
Fabricate Ignition System for 24-in. Subscale Tests and Data Evaluation													▭		
25-in. Subscale Tests and Data Evaluation														▭	
Task 6															
Design Ignition System for Full-Scale and 1/4 Scale Motor														▭	▭

CSA024073a

Figure 59. Technology acquisition plan for ignition system development (cont).

82

Plan Title: Flowfield and Combustion Modeling	Technology Importance:
	☒ Enabling
	☐ Engineering Development
	☐ Enhancing

Objective:

- Overall—Develop/analytical methodologies to predict hybrid grain regression and afterburning in motors of any scale

- Specific

    - Develop CFD code to pursue studies of fundamental phenomena in combustion, mixing, etc.

    - Begin development of a ballistic analysis code for industry use, capable of economical grain design and motor performance prediction

Technical Approach:

- Develop CFD capabilities for combined flow and combustion phenomena in a hybrid motor and develop an economical ballistics code. Iterate code improvements with evaluation of motor test data. Verify code development through prediction of ballistic data for subscale motor tests.

CSA024074a

Figure 60. Technology acquisition plan for flowfield and combustion model development.

PRECEDING PAGE BLANK NOT FILMED

Task Summary:

- **Task 1—CFD Development**

    - Develop combustion model

        - Identify key reactions

        - Determine reaction data (rates, heats, etc.)

        - Allow for condensed phase reactions (if oxidizer is condensed or fuel is metalized)

    - Identify turbulence model

        - Eddy viscosity

        - Effect on mixing/combustion

    - Develop body-fitted grid (especially for aft-dome region)

    - Solve Navier-Stokes equations (more general than boundary layer equations)

    - Solve particle trajectory equations (if oxidizer is condensed or fuel is metalized)

- **Task 2—Economical Ballistics Code Development**

    - Regression rate

        - Simplified turbulent boundary layer equations

            —Schvab/Zeldovich form—Energy and species solutions same as momentum
            —Solve momentum equation in transformed space
            —Define turbulence model
            —Invert transformation to identify solution in physical space

    - Afterburning

        - Steady-state mass/energy conservation in aft-dome region

            —Unburned fuel/oxidizer enters in known mass ratio
            —Assume complete combustion and heat release
            —Energy conservation determines mixture properties (temperature, viscosity, etc.)
            —Mixture properties determine nozzle flow rate
            —Mass conservation determines chamber pressure

CSA024074a

Figure 60. Technology acquisition plan for flowfield and combustion model development (cont).

Task Summary: (Cont)

- Task 3—Motor Testing
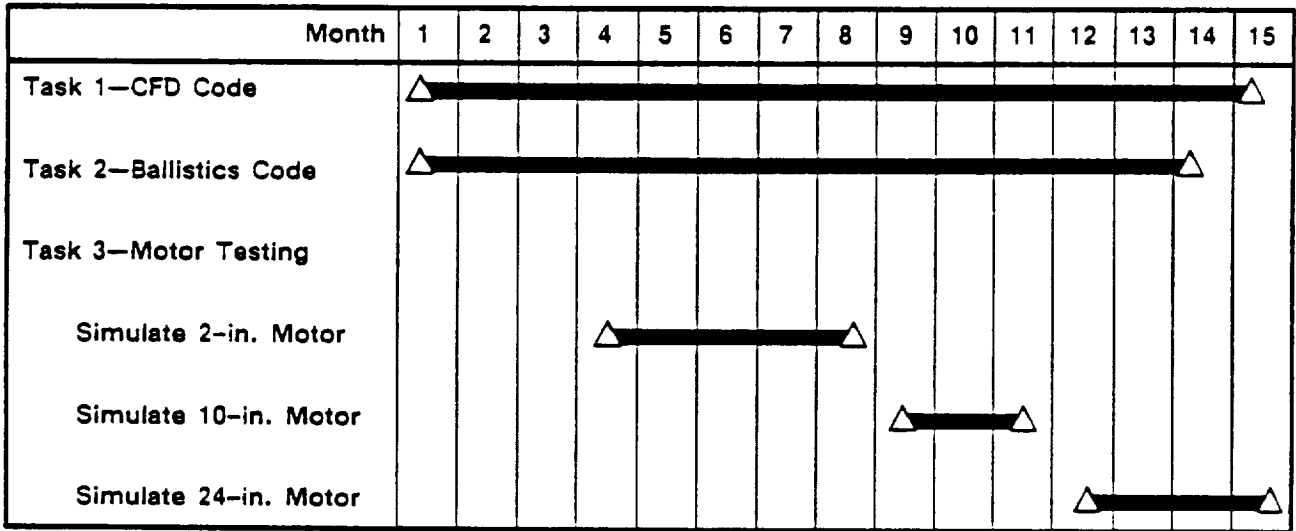
  - Evaluation test results and correlate to analytical predictions

    - Thermochemical data

      —Fuel decomposition
      —Fuel/oxidizer combustion

    - Internal flowfield data

    - Motor performance data

      —Pressure-time and thrust-time
      —Regression history via probes
      —Plume IR measurement for temperature
      —Plume sampling to determine composition
      —Verification of scale effects—Fire three motors of different size (e.g., 2-, 10-, and 24-in. diameter)

Month	1	2	3	4	5	6	7	8	9	10	11	12	13	14	15
Task 1—CFD Code	△														△
Task 2—Ballistics Code	△													△	
Task 3—Motor Testing															
Simulate 2-in. Motor				△			△								
Simulate 10-in. Motor									△		△				
Simulate 24-in. Motor												△		△	

CSA024074a

Figure 60. Technology acquisition plan for flowfield and combustion model development (cont).

36

Plan Title: Insulation Materials	Technology Importance:

Objective:

- Overall—Characterize the thermochemical and mechanical response of candidate insulation materials for use in the hybrid motor combustion environment

- Specific

  - Define insulator aerothermochemical environment for baseline hybrid motor concept

  - Define insulator test bed configuration and standard test conditions

  - Develop design data for candidate insulator materials in baseline propellant combustion environment

    —Erosion rate and char depth versus mixture ratio and pressure
    —Insulator thermochemical and physical properties data

  - Identify manufacturing processes for low cost, high reliability

  - Evaluate effects of insulator unbonds and defects in motor environment

Technology Importance:

- ☐ Enabling
- ☒ Engineering Development
- ☐ Enhancing

Technical Approach:

CSA024075a

Figure 61. Technology acquisition plan for insulation material development.

87

Task Summary:

- Task 1—Identify Material Candidates for Specific Motor Flow Regimes

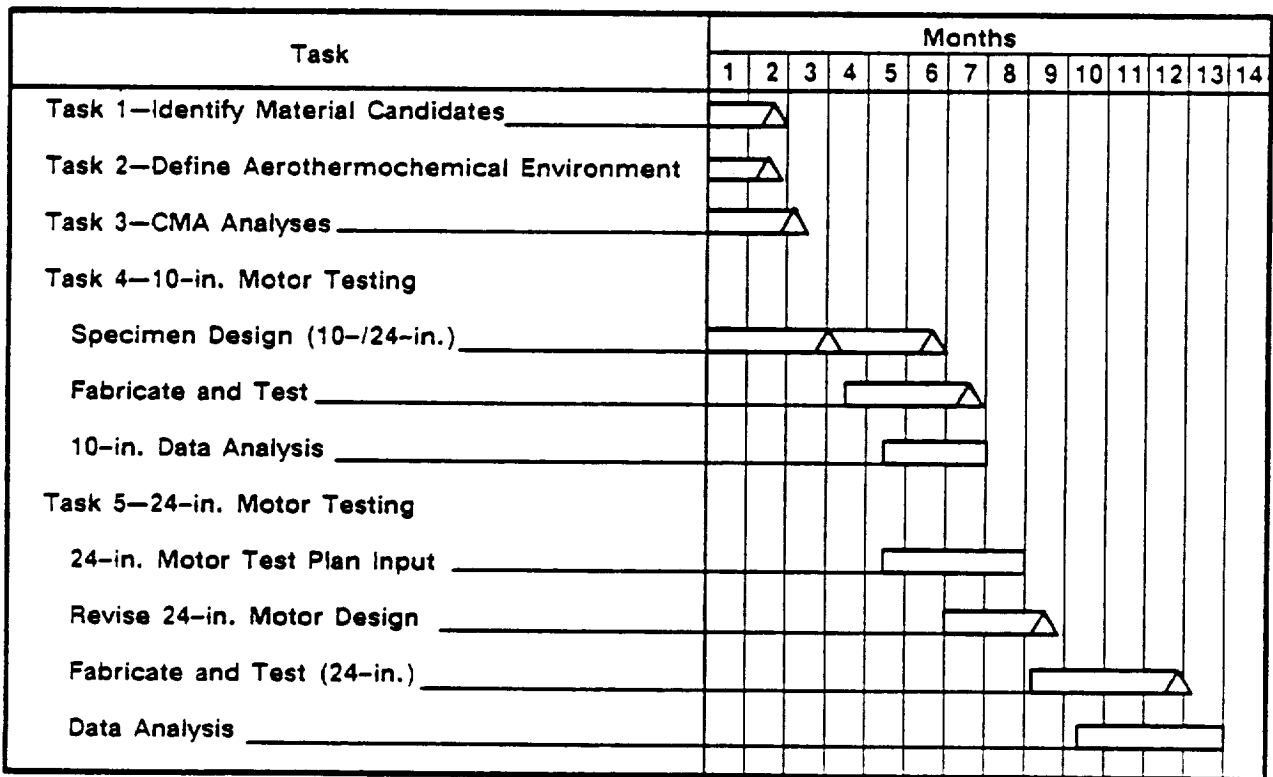- Task 2—Define Motor Aerothermochemical Environment (subscale versus full-scale)

- Task 3—Define Analytical Response of Candidate Materials to Motor Environment

- Task 4—Characterize Materials in 10-in. Motor Tests

- Task 5—Verify Selected Candidates in 24-in. Motor Tests

Schedule:

Task	Months													
	1	2	3	4	5	6	7	8	9	10	11	12	13	14
Task 1—Identify Material Candidates														
Task 2—Define Aerothermochemical Environment														
Task 3—CMA Analyses														
Task 4—10-in. Motor Testing														
Specimen Design (10–/24–in.)														
Fabricate and Test														
10-in. Data Analysis														
Task 5—24-in. Motor Testing														
24-in. Motor Test Plan Input														
Revise 24-in. Motor Design														
Fabricate and Test (24-in.)														
Data Analysis														

CSA024075a

Figure 61. Technology acquisition plan for insulation material development (cont).

88
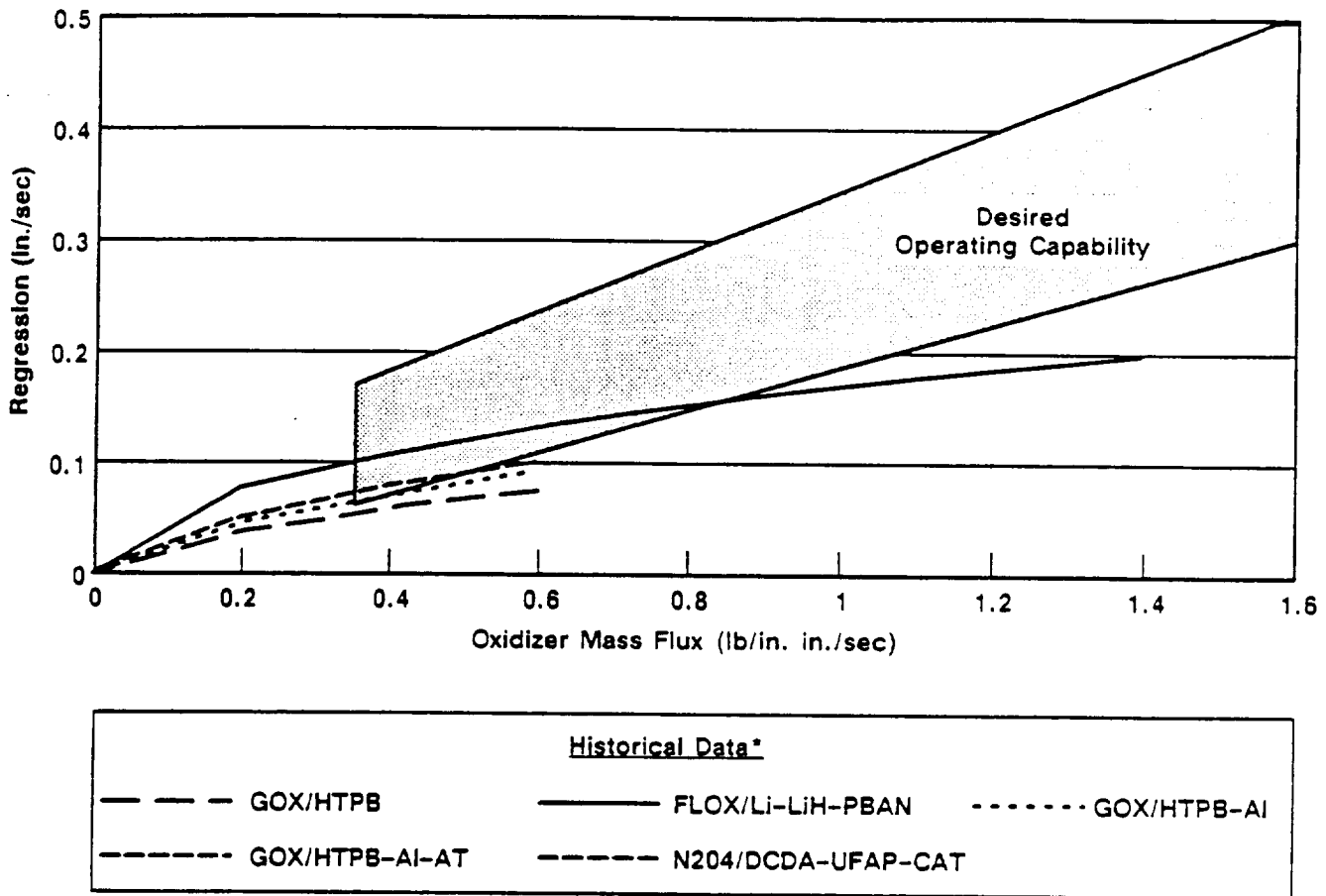
Figure 62. Regression rate requirements.

Resistive wire or laser heating of the grain prior to the introduction of oxidizer into the motor will theoretically provide motor ignition. This simple grain-heating ignition approach for hybrids has not been developed. Technology development through testing is necessary to demonstrate concept feasibility and characterize its operation. Development of a grain-heating hybrid ignition system will enhance the overall attractiveness of the hybrid.

Phase II Program Costs

Costs for Phase II, which constitute only the Thiokol activities, are calculated based on projected number of tests, estimated cost for each type of test, and estimated support required. The costs evolved from engineering estimates rather than detailed pricing exercises but should provide sufficient accuracy for planning. Additionally, since costs were developed on a per-motor basis, the program can be expanded to provide for additional technology development or reduced to meet budgetary constraints.

Costs were developed for four sizes of motors: 2-in. laboratory scale, 10-in. test bed, 24-in. subscale, and 48-in. technology verification. The 2-in. laboratory-scale motor exists at Thiokol and provides for economical screening of candidate fuel formulations and ignition concepts. The 10-in. test bed motor hardware is currently being fabricated for a preburner application and will be available for Phase II. The 24-in. motor is also being fabricated using discretionary funds and will be available for Phase II. The 48-in. motor will maximize use of existing design documentation for the MNASA motor, but hardware for this motor will be fabricated in Phase II.

Estimated costs include engineering, data reduction, instrumentation, materials, fabrication analysis, fuel grain casting, etc., and assume that all of the technology acquisition plans are implemented. Only the Thiokol costs are included. Operation of the LOX supply system, the LOX itself, and injector hardware is not included.

A factor of 1.30 is applied to account for supporting organizations such as finance, contracts, procurement, and program management. The factor of 1.30 is based on typical support requirements for a program of this type. The estimated cost for each test is summarized as follows:

Motor	Nonrecurring Tooling/Hardware Costs	Cost per Test	No. of Tests	Total
Lab Scale (2-in.)		$ 728	100	$ 72,800
Test Bed (10-in.)		44,298	32	1,417,536
Subscale (24-in.)		133,328	12	1,599,936
Verification (48-in.)	$1,430,000	917,800	1	2,347,800

5.0 TECHNOLOGY DEMONSTRATION

A large-scale technology demonstration motor was defined and costs estimated for its fabrication and test. This information was provided to General Dynamics to assist in the formulation of the overall technology demonstration plan. The motor defined is essentially equivalent in size and thrust to the quarter-scale booster defined in Section 3.5.3. LOX supply requirements defined for the quarter-scale requirements are illustrated in Figure 63. Test facility capability will be compatible with this flow schedule. Motor pressure, O/F ratio, and all other data defined for the quarter-scale motor apply to the demonstration motor.

Estimated costs were developed using the General Electric price model supplemented by data peculiar to hybrids. It was assumed that existing facilities and handling tooling could be used for fabrication. Estimated costs assume that fabrication and test would be as if it were an SRM. LOX, LOX supply system, injector hardware, and specific assembly costs were not addressed.

The costs are not a result of formal prices exercises but, when integrated with General Dynamics and Rocketdyne, costs should be adequate for long-range planning. The costs for the initial and two subsequent motors are $8.8, $6.6, and $5.3 million, respectively. These costs include all fabrication, engineering, and support costs. The duration of the program was estimated based on lead times required for hardware. Minimum program duration is estimated to be 38 months assuming business as usual for procurement, fabrication, and test times.
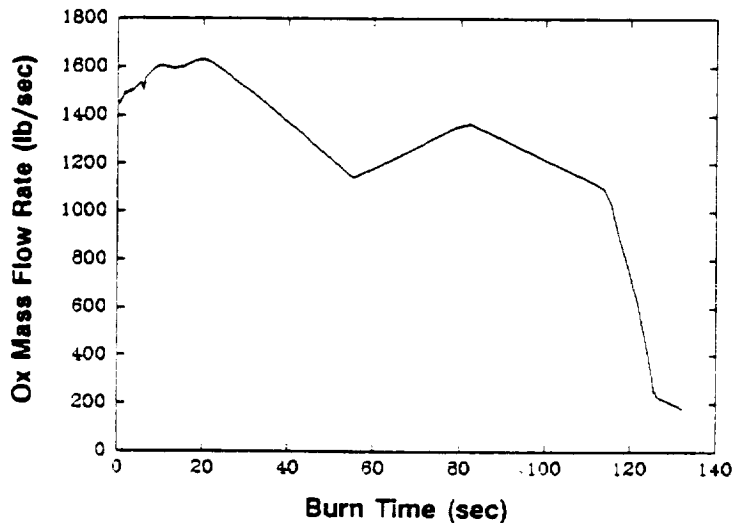

Figure 63. Oxidizer requirements for Phase III large subscale demonstration motor.

6.0 REFERENCES

1. R. B. Stewart and R. I. Gomberg, The Production of Nitric Oxide in the Troposphere as a Result of Solid Rocket Motor Afterburning, NASA Technical Note TN-D-8137, 1976.

2. Feasibility of Hybrid Propulsion Systems, Army Guided Missile Agency Report, ARGMA TR 2E3R.

3. F. A. Cotton and G. Wilkinson, Advanced Inorganic Chemistry, 3rd Edition, J. Wiley & Sons, New York, 1972.

4. "Ozone Chemistry and Technology," Advances in Chemistry Series No. 21, American Chemical Society, Washington, D. C., 1959.

5. D. B. Stickler and K. N. R. Ramoballi, Polymer Degradation Rate Control of Hybrid Rocket Combustion, NSA Report N72-13735.

6. Investigation of Fundamental Phenomena in Hybrid Propulsion, Final Report for Contract NOW64-0659, C. UTC report for Contract N00-123-62-C.

7. P. G. Butts, A. L. Wahlquist, and C. F. Price, Low Hazard Hybrid Fuel Development Program, NWC TP5617, Final Report for Contract N001-23-72-C-161, 1974.

8. The Merck Index, 10th Edition, p. 457, Merck and Co. Inc., 1983.

9. G. K. Lunk, Hybrid Propulsion Technology Fuel/Oxidizer Trades, TWR-40195.

10. C. E. Wooldridge and R. J. Muzzy, Internal Ballistic Considerations in Hybrid Rocket Design, AIAA Second Propulsion Joint Specialist Conference, Colorado Springs, Colorado, Preprint 66-628.